STATIC AND PSEUDO-STATIC STABILITY ANALYSIS OF TAILINGS STORAGE FACILITIES USING DETERMINISTIC AND PROBABILISTIC METHODS

Jenyfer Mosquera

Department of Mining and Materials Engineering

McGill University, Montreal

April, 2013

A Thesis submitted to McGill University in partial fulfillment of the requirements of the degree of Master of Engineering in Mining Engineering

ABSTRACT

Tailings facilities are vast man-made structures designed and built for the storage and management of mill effluents throughout the life of a mining project. There are different types of tailings storage facilities (TSF) classified in accordance with the method of construction of the embankment and the mechanical properties of the tailings to be stored. The composition of tailings is determined by the mineral processing technique used to obtain the concentrate as well as the physical and chemical properties of the ore body.

As a common denominator, TSFs are vulnerable to failure due to design or operational deficiencies, site-specific features, or due to random variables such as material properties, seismic events or unusual precipitation. As a result, long-term risk based stability assessment of mine wastes storage facilities is necessary.

The stability analyses of TSFs are traditionally conducted using the Limit Equilibrium Method (LEM). However, it has been demonstrated that relying exclusively on this approach may not warrant full understanding of the behaviour of the TSF because the LEM neglects the stress-deformation constitutive relationships that ensure displacement compatibility. Furthermore, the intrinsic variability of tailings properties is not taken into account either because it is basically a deterministic method.

In order to overcome these limitations of the LEM, new methods and techniques have been proposed for slope stability assessment. The Strength Reduction Technique (SRT) based on the Finite Element Method (FEM), for instance, has been successfully applied for this purpose. Likewise, stability assessment with the probabilistic approach has gained more and more popularity in mining engineering because it offers a comprehensive and more realistic estimation of TSFs performance.

In the light of the advances in numerical modelling and geotechnical engineering applied to the mining industry, this thesis presents a stability analysis comparison between an upstream tailings storage facility (UTSF), and a water retention tailings dam (WRTD).

First, the effect of embankment/tailings height increase on the overall stability is evaluated under static and pseudo-static states. Second, the effect of the phreatic surface location in the UTSF, and the embankment to core permeability ratio in the WRTD are investigated. The analyses are conducted using rigorous and simplified LEMs and the FEM - SRT.

In order to take into consideration the effect of the intrinsic variability of tailings properties on stability, parametric analyses are conducted to identify the critical random variables of each TSF. Finally, the Monte Carlo Simulation (MCS), and the Point Estimate Method (PEM) are applied to recalculate the FOS and to estimate the probability of failure and reliability indices of each analysis. The results are compared against the minimum static and pseudo-static stability requirements and design guidelines applicable to mining operations in the Province of Quebec, Canada.

Keywords: Tailings storage facilities (TSF), Limit Equilibrium Method (LEM), Shear Reduction Technique (SST), pseudo-static seismic coefficient, probability of failure, Point Estimate Method (PEM), Reliability Index.

RÉSUMÉ

Les parcs à résidus miniers (PRMs) sont de vastes structures utilisées pour le stockage et la gestion des déchets pendant l'opération et après la clôture d'un site minier. Différentes techniques d'entreposage existent, dépendant principalement de la méthode de construction de la digue et des propriétés physiques, chimiques et mécaniques des résidus à stocker. La composition des résidus est déterminée par la technique utilisée pour extraire le minerai du gisement ainsi que par les propriétés physico-chimiques du gisement.

De manière générale, les installations de stockage de résidus miniers sont dans une certaine mesure, sujettes à des ruptures. Celles-ci sont associées à des défauts de conception et d'exploitation, des conditions spécifiques au site, des facteurs environnementaux, ainsi que des variables aléatoires telles que les propriétés des matériaux, les événements sismiques, ou les précipitations inhabituelles. Par conséquent, la stabilité des PRMs à long terme est nécessaire sur la base de l'évaluation de risques.

Les analyses de stabilité sont généralement effectuées à l'aide de la méthode d'équilibre limite (MEL), cependant, il a été prouvé que s'appuyer exclusivement sur les MELs n'est pas exact car la relation entre déformation et contrainte est négligée dans cette approche, tout comme le déplacement ayant lieu au pendant la construction et l'opération des PRMs. En outre, la variabilité spatiale intrinsèque des propriétés des résidus et autres matériaux utilisés pour la construction des PRMs n'est pas prise en compte.

En conséquence, de nouvelles méthodes et techniques ont été développées pour surmonter les limites de la MEL. La méthode des éléments finis (MEF) et la Technique de réduction de cisaillement (TRC), par exemple, ont été appliquées avec succès pour l'analyse de la stabilité des PRMs. De même, l'approche probabiliste pour l'analyse de la stabilité des pentes a gagné en popularité car elle offre une simulation complète et plus réaliste de la performance des PRMs.

À la lumière des progrès réalisés dans le domaine de la modélisation numérique et de la géotechnique pour l'industrie minière, cette thèse présente une comparaison entre une installation d'entreposage des résidus en amont et un barrage de stériles et d'eaux de décantation.

En premier lieu, l'effet de l'augmentation de la hauteur des résidus sur la stabilité globale est évalué en vertu des états statiques et pseudo-statiques. En deuxième lieu, l'effet de l'emplacement de la nappe phréatique dans installation d'entreposage des résidus en amont et le rapport de perméabilité de remblai dans le barrage de stériles et d'eaux de décantation sont étudiés. Les analyses sont conduites en utilisant la modélisation numérique des MELs et la MEF – TRC.

Des analyses paramétriques sont effectuées pour identifier les variables aléatoires critiques de chaque parc à résidus miniers. Finalement, pour évaluer, la simulation de Monte Carlo (MCS) et la méthode d'estimation ponctuelle (MEP) sont appliquées pour recalculer les facteurs de stabilité et pour estimer la probabilité de défaillance et les indices de fiabilité qui leur sont associées. Les résultats de chaque analyse sont comparés aux exigences minimales de stabilité des pentes applicables aux opérations minières dans la province de Québec, Canada.

Mots-clés: Parcs à résidus miniers (PRMs), coefficient sismique, Technique de Réduction de Cisaillement (TRC), probabilité de défaillance, Méthode d'Estimation Ponctuelle (MEP), indice de fiabilité.

ACKNOWLEDGEMENTS

I would like to devote my ultimate gratitude to Almighty God for being an endless source of love, strength, and support to me, and for the opportunity to complete this work. Likewise, I would like to express my deepest gratitude to the following persons:

Dr. Hani Mitri, my thesis supervisor. I am profoundly grateful to him for his technical guidance, his professional advice, strategic planning skills, and his thoughtful encouragement which allowed me to achieve my academic goals and to complete this degree. Special thanks to him as well for having given me the opportunity of being part of the Mine Design Lab group. The financial support provided by the National Sciences and Engineering Research Council of Canada (NSERC) fund that I was beneficiary of under his supervision is equally highly appreciated.

Dr. Tarek Hamade. I would like to thank him for his support, guidance, and technical advice at every stage of my thesis. For the time he spent reviewing my work and making valuable suggestions that helped me improve and give direction to my research.

Special thanks to all and each one of my fellow graduate students at the Mine Design Lab: Shahe, Wael, Zaka, Atsushi, Luc, Nick, Raju, Isaac, and Guillaume for their help, technical advice, and friendship. You are all very kind human beings and very talented professionals. You have all my respect and admiration.

Professor Kristian Waters, my former academic supervisor for his support while enrolled in the Graduate Diploma in Mining at McGill. Special thanks to Ms. Barbara Hanley for her kind help since my first day at McGill.

Last but not least, I would like to thank and dedicate this thesis to my parents, Wilbor and Paulina; to my siblings Albert and Winny, and my niece Isabella; to my grandparents Dirla, Victor Hugo, and Antonina for their unconditional love, trust, prayers, and support each and every day of my life. I love you all very much. This belongs to you!

TABLE OF CONTENTS

LIST OF FIGURES

LIST OF TABLES

LIST OF SYMBOLS AND ABBREVIATIONS

CDF: Cumulative Distribution Function

ESA: Effective Stress Analysis

FEM: Finite Element Models

FOS: Factor of Safety

LEM: Limit Equilibrium Method

MCS: Monte Carlo Simulation

M-P: Morgenstern-Price Method

O-F: Ordinary Fellenius Method

PDF: Probability Density Function

PEM: Point Estimate Method

SRT: Shear Reduction Technique

TSA: Total Stress Analysis

TSF: Tailings Storage Facility

USA: Undrained Strength Analysis

UTSF: Upstream Tailings Storage Facility

WRTD: Water Retention Tailings Dam

L/H= beach width ratio for phreatic surface location

K_h: Horizontal seismic coefficient

ks/kc: embankment permeability (ks) to core permeability (kc) ratio

ϕ: Friction Angle – ϕ' effective friction angle

c: Cohesion – c': effective cohesion

C_c: Compression Index

C_v: Coefficient of Consolidation

G_s: Specific gravity

PI: Plasticity Index

LL; Liquid Limit

PL: Plastic Limit

σ: Total stress

σ': Effective Stress

u: Pore water pressure

ρ: Mass Density or Correlation Coefficient

k: Permeability

g: Gravity (9.81 m/s^2)

S: Degree of saturation

e: Void ratio

E: Young's Modulus

γ: Unit weight (with subscripts dry, sat for saturated, and w for water)

ε: Strain

ν: Poisson's ratio

τ: Shear strength

COV: Coefficient of Variation

pf: Probability of Failure

μ: Mean value

σ: Standard deviation in probabilistic analysis

β: Reliability Index

R.V; Random variable

Cov(X, Y): Covariance

PGA: Peak Ground acceleration

CHAPTER 1: INTRODUCTION

1.1 Tailings Storage Facilities in mining operations

The mining industry has a key role in the development of all civilizations because it provides the raw materials required to produce most of the existing goods that sustain life. However, the increased demand of these materials has proportionally increased mining production rates and the volume of mine wastes generation. Mine wastes, or tailings, are the materials left over after extracting, milling, and chemically treating an ore body to remove its valuable mineral portion. Tailings require large disposal areas called Tailings Storage Facilities (TSFs). Due to the complex processes that take place within tailings impoundments, TSFs bear the most significant environmental, economical and safety impacts of all mining operations. TSFs are classified into two categories according to the constitutive materials and construction technique of the retaining embankment. One category is the Water Retention Tailings Dams (WRTDs), and the other one is a broader category that consists of various types of raised embankment tailings storage facilities.

In the case of WRTDs, the embankment is built to its full height prior to the beginning of milling and/or processing operations, and native borrow material is used as construction material. Generally, WRTDs have an internally zoned structure, have an impervious core, and are good for sites where co-disposal of tailings and storage of high volumes of residual water is required (ICOLD, 2001; Vick, 1983). According to Martin and Morrison (2012), despite of being costly, WRTDs are considered an asset for the mine owners because steady state is achieved at an early stage of construction and have a finite life.

In raised embankment TSFs, the retaining embankment is built in stages as the mining operation progresses, and generally, they have poor water storage capacity (Julien and Kissiova, 2011; Priscu, 1999; Qiu and Sego, 1998a; Vick, 1983). Raised embankment TSFs are sub-classified into Centerline, Downstream, and Upstream Tailings Storage Facilities depending on the direction in which the embankment crest is constructed (Mittal, 1974; Vick, 1983). In Upstream Tailings Storage Facilities (UTSFs), e.g., a borrow starter dyke is initially constructed and the subsequent raising of the embankment is done using hydraulically deposited or cycloned tailings in the upstream slope direction.

Martin and Morrison (2012) concluded that, despite of being the most economical type of TSFs, UTSFs are the least favourable raised embankment option because steady state is reached only after closure. This implies perpetual maintenance and liabilities for the mining company. According to Vick (1983) and Saad and Mitri (2010), raised embankments TSFs are the single most common type of TSFs used for mine wastes storage, and the upstream method is the construction technique most often adopted.

Accordingly, the design and performance of TSFs is governed by site-specific variables, mining operation techniques, and the regulations applicable to the mining project. These variables will determine the operating requirements, the availability of construction materials, and the physical and mechanical properties of the deposited tailings. Other criteria such as site seismicity and environmental/climate conditions also play a key role in TSFs stability assessment. The stability and adequate functioning of TSFs portrays the technical expertise of mine managers, engineers, and operators. Therefore, detailed and comprehensive investigation of probable causes and consequences of TSFs unsatisfactory performance is required.

1.2 Problem definition

The variability in construction methods and the unique geotechnical properties of tailings make of TSFs highly complex structures to manage. Additionally, since there are no standardized guidelines for the design and operation of such large structures, there are also multiples methods to assess the stability of TSFs in the short and long-term. Generally, TSFs stability analyses are conducted with deterministic LEM methods. However multiple authors have highlighted the limitations of this for evaluating essential variables that govern the overall stability of the impoundment. In fact, TSFs failure and/or events of unsatisfactory performance are topics of growing concern in mining engineering due to the fast rate of mine wastes production, the rigorousness of regulatory stability, safety and environmental requirements, and increased social awareness. This thesis looks at three points of concern in TSFs stability assessment: slope instability, limitations of the analytical methods used to conduct stability analyses, and the effect of material properties variability on stability analyses.

TSFs failure due to slope instability

The USCOLD (1994), the ICOLD (2001), and the UNEP (1996) reports on tailings dam's incidents in the world concluded that the most common failure mechanism of TSFs is slope instability (Figure 1-1).

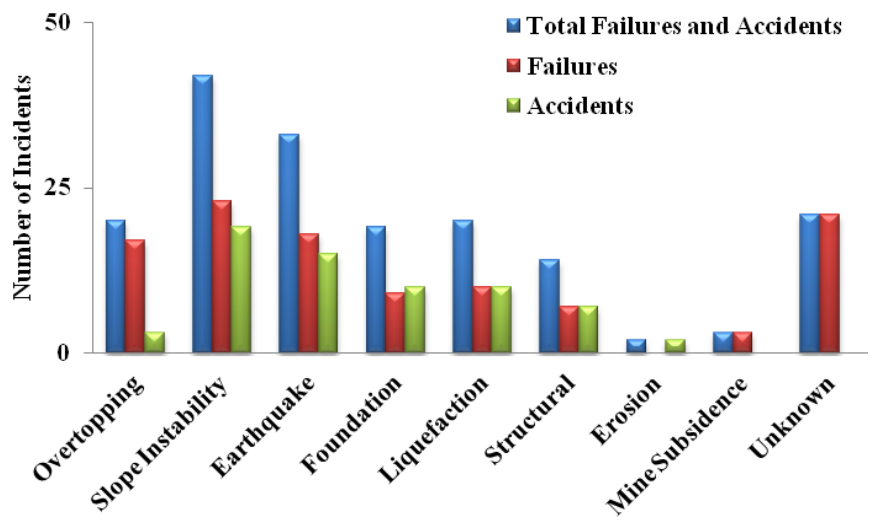

Figure 1-1 Tailings storage facilities incident causes according after (ICOLD, 2001; Strachan, 2001)

Upstream Tailings Storage Facilities (UTSFs) have incurred the higest number incidents compared to Water Retention Tailings Dams and other types of raised embankment TSFs. The number of recorded incidents by type of TSF is prsented in Figure 1-2.

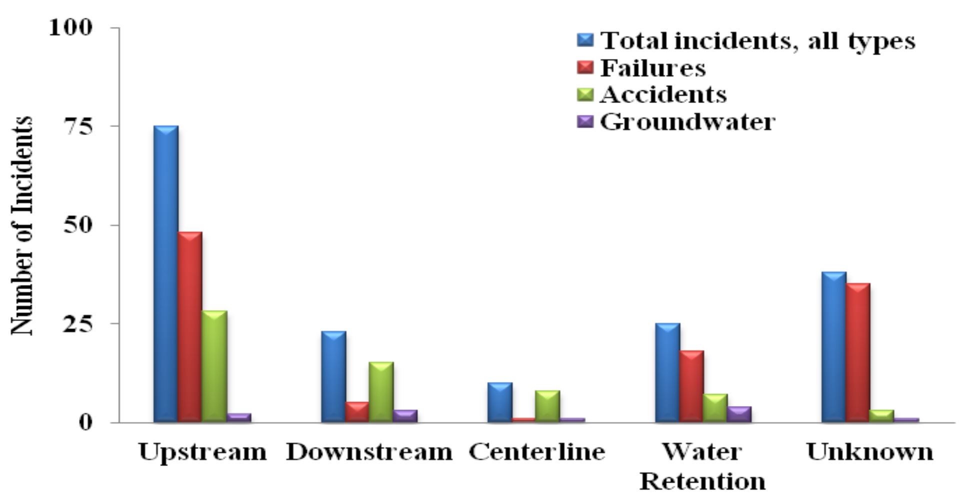

Figure 1-2 Failure incidents by type of Tailings Storage Facility (ICOLD, 2001)

Some of the causes that were attributed to UTSFs higher failure vulnerability are related to the mechanical properties of tailings used as construction materials, excessive loading rates practices, and poor consolidation and settlement processes before a new stage is raised. High embankment raising rates contribute to pore pressure increase and significant reduction of the shear strength of materials (Vick, 1983, Azam, 2010; ICOLD, 2001; Saad, 2008 and Hamade et al., 2011). Reduction in shear strength breaks equilibrium and the safety factor reduces. Poor site investigation and operational practice paired up with unusual events, seismic episodes, and changes in materials strength properties over time and/or stage of construction are other factors that contribute to slope instability and TSFs failure potential.

- ***Limitations of the methods used for TSFs stability analyses***

In traditional geotechnical practice, TSFs stability analyses are conducted by calculating a deterministic FOS using Limit Equilibrium Methods (LEMs). This approach is commonly adopted due to the few input parameters required for obtaining reasonable safety factors. However, the reappearance of failure cases and the complexity of the geotechnical processes intrinsic to these structures have shown that relying exclusively on this approach may not warrant full understanding of the behaviour of TSFs. Essentially, the LEM neglects the stress-deformation constitutive relationships that ensure displacement compatibility (Hamade et al., 2011; Krahn, 2003; Lade and Yamamuro, 2011; Saad and Mitri, 2010). Additionally, many assumptions about the location, shape, and possible failure mechanisms of the sliding mass are required for the LEM. The shortcomings of the LEM have been the topic of multiple publications and geotechnical engineering research in recent years (Cheng and Lau, 2008; Duncan, 1996; Fredlund, 1984; Hammanh et al., 2009; ICOLD, 1986; Krahn, 2003).

The rapid development of computer technology has allowed for an increased use of numerical methods of analysis, a better understanding of the LEM, and has contributed to the development of more sophisticated slope stability analysis methods. One method that has been successfully used for slope stability analyses is the Finite Element Method (FEM) - Shear Reduction Technique (SRT).

The FEM-SRT satisfies the stress-strain and displacement limitations of the LEM and eliminates the assumptions about interslice forces and shape of the sliding mass. Nonetheless, the FEM-SRT approach has shown limitations associated with the need of additional material properties and computation time for routine stability analyses. Besides, the SRT is also a deterministic method.

- ***Deterministic stability analyses neglect uncertainty of material properties***

The LEMs and the FEM-SRT are deterministic methods that produce a single FOS that does not take into consideration the intrinsic variability of the materials mechanical properties. In contrast, stability analyses with the probabilistic approach use random variables and the principles of common probabilistic methods to obtain a mean FOS and to estimate the probability of failure (*pf*) and reliability index (β) of the system. These important pieces of information counterweight the deterministic approach because they describe the most probable level performance of the TSFs.

1.3 Scope and Objectives

In light of the abovementioned concerns and limitation about TSFs stability analyses, and taking into cosideration that effective stability analyses require the use of advanced and comprehensive analytical tools, this thesis has three objectives:

First, to conduct a comparative stability analysis of two typical tailings storage facilities under static and pseudo-static states to determine which of the two delivers the highest level of performance when subjected to embankment/tailings height increase, changes in the phreatic surface location, and/or change in the embankment to core permeability ratio.

Second, to analyze the effect of conducting TSF stability analyses with LEMs of variable rigorousness or the FEM-Shear Reduction Technique to determine how each approach could affect the compliance of minimum stability requirements in the province of Quebec.

Third, to calculate the mean FOS, probability of failure, and reliability indices of the two TSFs by applying sensitivity analyses, Monte Carlo Simulation, and the Point Estimate Method using the same loading and analytical conditions of the deterministic approach.

1.4 Thesis outline

This thesis consists of seven chapters organized according to the following description:

Chapter 1 outlines the importance of tailings storage facilities in mining operations. The problem definition, scope, and objectives of the thesis are described.

Chapter 2 presents a literature review on tailings production, mechanical properties and the parameters for tailings storage facilities design. A description of common types of tailings storage facilities and deposition methods is also included.

Chapter 3 presents the methods generally used in mining applications to conduct stability analyses of tailings storage facilities. The principles of the limit equilibrium method, shear strength reduction technique, static and pseudo-static analysis, deterministic and probabilistic approach are described in this chapter.

Chapter 4 presents the methodology, geometries, design parameters and analytical approaches used to conduct the stability analyses of the UTSF and the WRTD. The numerical modelling criteria and the design assumptions are presented in this section.

Chapter 5 reports the results and discussion of the static and pseudo-static stability analyses following a deterministic approach under different loading conditions.

Chapter 6 presents the results and discussion of the static and pseudo-static stability analyses using the probabilistic approach. Likewise, the description and results of the sensitivity analyses, Monte Carlo Simulation and Point Estimate probabilistic methods to obtain the probability of failure, reliability indices level of performance of each TSF are provided.

Chapter 7 presents the conclusions of the thesis and recommendations for future research. After this section, the list of the references and important data used to conduct this research is included in the bibliography and appendix sections, respectively.

CHAPTER 2: LITERATURE REVIEW ON TAILINGS PRODUCTION, MECHANICAL PROPERTIES, AND TSFs DESIGN PARAMETERS

Tailings are a mixture of diversified-grain-size-particles material formed during the processing phases of an ore body (U.S.EPA, 1994). The volume of production and intrinsic properties of tailings vary in conformity with the beneficiation techniques employed, type of mineral being exploited (e.g. base metal, precious metal, coal, or oil sands), the ore grade, and stripping ratio. Tailings Storage Facilities are structures in which tailings are stored during and after mining operations take place; their design integrates technical, operational, environmental, and safety requirements of the mine site. Tailings intrinsic properties and containment methods are concepts linked to one another. A description of these individual variables and the correlation between them is provided in following sections.

2.1 Tailings Production

Certain ore bodies can be mined without requiring any further processing techniques to produce marketable commodities (e.g. coal, quarries), however, the majority of metal mines require additional treatment before a mineral of commercial value can be produced. The upgrading techniques of metal ores include physical and chemical processes. Some of the most common used methods are depicted in Figure 2-1.

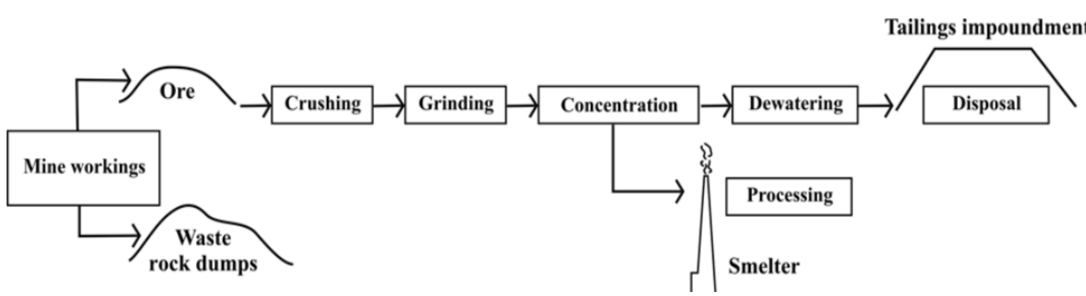

Figure 2-1 Typical mineral processing techniques by (Rademeyer, 2007)

First, crushing and grinding are performed with the purpose of breaking down the rock fragments into specific grain sizes that facilitate the extraction of the mineral. Gradation, angularity, and hardness of the tailings material, in turn, are governed by these physical transformation techniques.

Then, the grinded material is subjected to chemical upgrading processes to concentrate, separate, and remove the mineral. Concentration, gravity or magnetic separation, froth flotation, heap leaching, and heating are common chemical mineral processing methods (Vick, 1983). Two aspects of importance about the chemical processing phase of an ore body are the large quantities of process-water requirements and the ability of the chemical reagents to change the physic-chemical characteristics of the fines (Lottermoser, 2003).

Most mineral processing operations conclude with a dewatering stage. Dewatering consists on removing the excess water from the metal production using thickeners or hydro cyclones. A portion of the water recuperated during the dewatering stage can be reused in the production process; the remaining portion corresponds to the slurry (saturated tailings) sent to the tailings storage facility. The distribution and deposition of tailings depends on the physical, chemical, geotechnical, and rheology properties achieved during the milling and processing phases.

2.2 Mechanical Properties of Tailings

Tailings are different from most naturally occurring materials, however, their mechanical properties and behaviour can be associated with that of soils with the same gradation (Dimitrova and Yanful, 2012). The characterization of the tailings is a requirement for design, construction, operation, and monitoring of TSFs. Similarly, it is used as an evaluation tool that provides information on significant environmental impacts such as Acid Mine Drainage (AMD), surface/groundwater contamination, and TSFs stability in the short and long term. A brief review of the most important tailings properties and testing methods required for TSFs design is provided in the following sections.

2.2.1 Gradation – Grain Size Distribution Curve

Gradation consists on classifying the composition of tailings according to its constitutive particle sizes diameters. Gradation is the first indicator of other tailings engineering properties such as shear strength, permeability, deformability, and compressibility. Gradation governs the seepage behaviour and the design of the drainage, filter, and liners systems of a TSF.

Tailings gradation is determined by the Particle Size Distribution Curve (PSDC) obtained during the Standard Sieve Test. Tailings sieve test yields three particle size categories: clay size (for tailings particles with a diameter smaller than 0.074 mm), silt size (for particles with a diameter between 0.074 μm and 0.06 mm), and sand size (for tailings particles with a diameter greater than 0.06 mm) (Das, 2007; Bardet, 1997; Saad, 2008). Tailings sand size portion is called mill or beach tailings, and the clay and silt size portions are called slimes (Vick, 1983; Vermeulen, 2001). Tailings particles with diameters smaller than 0.074 mm, are measured using the Hydrometer test and are called fines (Saad, 2008).

Although tailings particle size distribution does not necessarily correlate with the geotechnical behaviour or mineral composition of natural soils with the same particle size, it is the first indicator of fundamental properties of tailings used to assess construction methods, hydraulic operational units, shear strength, and mechanical properties of the TSF (Vick, 1983, Vermeulen, 2001, Das, 2007; Bardet, 1997). The particle size distribution curve also allows for the calculation of the coefficient of uniformity, coefficient of curvature, and the roundness of tailings (Selvadurai, 2006; Blight, 1979). Tailings, unlike most soils, are characterized by a very angular shape acquired during milling operations. Typical particle size distribution curves for different tailings materials are presented in Figure 2-2.

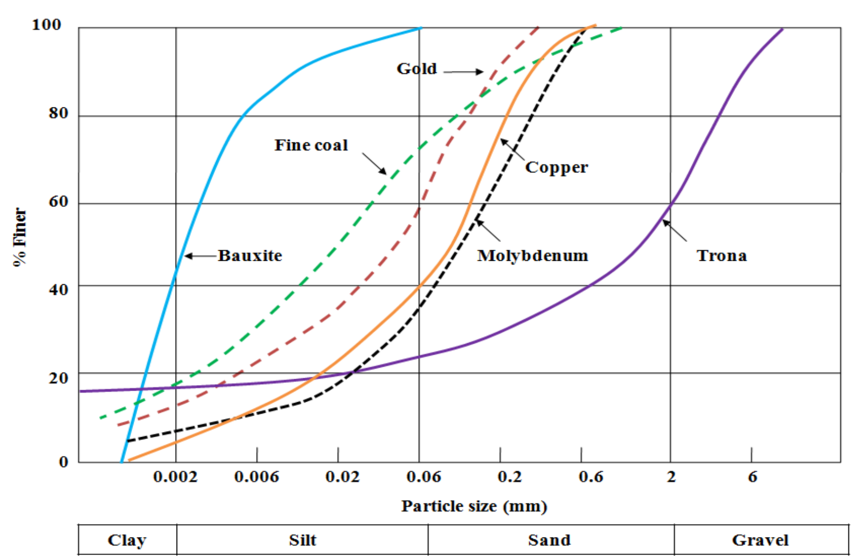

Figure 2-2 Grain size distribution curves for different tailings materials. After (Sarsby, 2000)

As shown in the Figure 2-2, gold tailings are composed primarily of sands and silts with a small fraction of clay size particles (Qiu and Sego, 1998a; Rassam and Williams, 1999; Vick, 1983, Saad, 2008, Hamade et al., 2011). Vick (1983) classified gold tailings as cohesionless non-plastic silt (ML). The segregating potential of tailings derived from the grain size distribution governs most of the tailings mechanical properties, the rate of rise of the embankment, the potential beach profile, and permeability distribution within the impoundment (Vick, 1983; Saad and Mitri, 2010; Saad, 2008).

2.2.2 Specific Gravity (G_s)

Specific gravity, defined as the ratio of the unit weight of soil solids to the unit weight of water, is used in mining applications as a comparison of the tailings density respect to that of the water (Selvadurai, 2006; Bardet, 1997; Das, 1997). The value of specific gravity is used in mass-volume relations for calculating the void ratio, degree of saturation, and density of the tailings. The specific gravity of tailings can be measured using the standard Pycnometer test (Vermeulen, 2001; Selvadurai, 2006). Table 2-1 summarizes typical values of specific gravities for different types of tailings material.

Table 2-1 Specific gravity of selected tailings materials

Tailings	Specific Gravity	Source
Ester U.S Coal	1.5 -1.8	Vick, 1983
Oil Sands	2.18 – 2.58	Jeeravipoolvarn et al., 2009
Gold	2.5-3.5	Vermeulen, 2001

2.2.3 Void Ratio (e)

Void ratio, defined as the ratio between the volume of void-space to the volume of solids, is the parameter that governs tailings consolidation, compressibility, permeability, and particles movement within the impoundment (Bardet, 1997; Das, 2007, Vick, 1983). Tailings void ratio is generally measured using the standard Odometer test (Vermeulen, 2001). According to Saad (2008), the void ratio of the tailings is assumed uniform during the TSF construction. Typical values of void ratios for different types of tailings are presented in Table 2-2.

Table 2-2 Void ratio for different types of tailings

Type of Tailings	Void Ratio	Source
Tailings Sands	0.6-0.9	Vermeulen, 2001; Vick, 1983
Low plasticity slimes	0.7-1.3	
High plasticity slimes	5-10	
Gold Tailings	1.1-1.2	Saad, 2008
Coal Wash	0.6-1.0	
Oil Sands Tailings	0.9	

Void ratio is very important in controlling the seepage through the TSFs. According to Blight (1979), the shear strength gain of tailings is the result of a decrease in pore pressure when water is expelled from interstices due to a change in void ratio. Consequently, the change in void ratio within the impoundment should be monotored throuhgout the life of the mine site using both in situ and lab experiments (Abitew, 2010; Ding et al., 2010; Shamsai et al., 2007).

2.2.4 Degree of Saturation (S)

The degree of saturation is one of the most significant properties used to determine the index properties and consistency of tailings (Vick, 1983; Saad and Mitri, 2011). Degree of saturation is defined as the ratio of the volume of water to the volume of voids. The transportation of the tailings in a slurry condition produces tailings with low initial in situ density and high water content, thus, low mechanical strength is show during this stage. Avila (2011) concluded that the degree of saturation of tailings determines shear strength of tailings and gives information about the liquefaction potential due to applied loads.

2.2.5 Porosity (n)

Fetter (2001) defines porosity as the measure of empty void space in the soil mass. According to Vick (1983), tailings have 40 % porosity upon deposition. After deposition, it becomes a function of gradation and water content. Tailings porosity can be calculated using mass-volume phase relations if the average void ratio of the tailings is known. Saad (2008) concluded that porosity decreases as tailings particle size increases due to aggregates formation of the finer portion of tailings showing higher resistance to compaction.

2.2.6 Atterberg Index Limits

Atterberg limits are an important measure of the consistency and degree of cohesion and adhesion of the fine-grained soils often used for additional classification and characterization of tailings (Selvadurai, 2006; Das, 2007; Bardet, 1997; Saad, 2008). The liquid limit, plastic limit, and plasticity index of tailings are used extensively with other geotechnical properties to estimate compressibility, settlement potential, permeability, and tailings shear strength. Vermeulen (2001), presented typical values of Atterberg limits for gold tailings as follows: liquid limit between 22 and 43; plastic limit in a range of 22-35, plasticity index between1-8, and the shrinkage limit from 2.7 to 4.7. Based on these values, gold tailings are classified as cohesionless non-plastic silts as shown in Figure 2-3

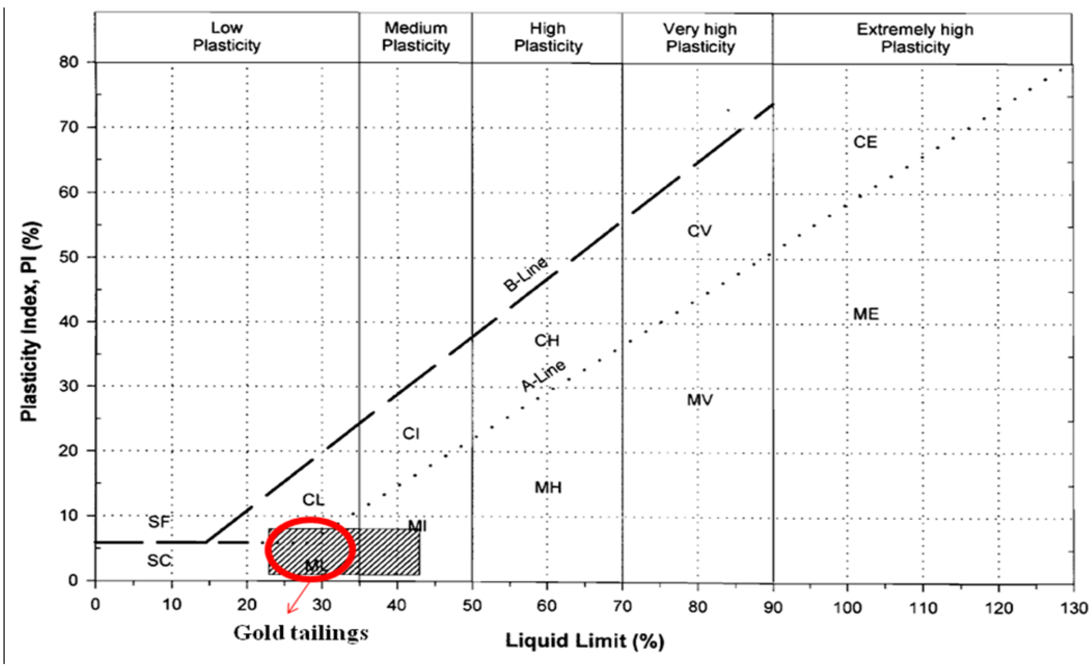

Figure 2-3 Casagrande's classification of tailings (Vermeulen, 2001)

2.2.7 Relative density

Vick (1983) defined relative density as the ratio between the loosest and the densest states that tailings may achieve in laboratory tests. It can be calculated using Equation 2-1:

$$D.r. = \frac{e_{\max} - e_0}{e_{\max} - e_{\min}} x100\% \quad \textbf{(2- 1)}$$

where e_{max} is the void ratio in its loosest state, e_{min} is the void ratio in densest state, and e_0 is the initial void ratio of tailings upon deposition (Vick,1983). According to Blight (1979), Caldwell and Stevenson (1984), and Abadjiev (1985), relative density is site-specific and should be measured *in-situ* to estimate the liquefaction potential of the impoundment. Saad (2008) and Vick (1983) explained that beach tailings usually reach average relative densities in the range of 30-50% when spigotting or similar deposition methods are used. However, for TSFs located in areas of moderate seismicity, embankment tailings should attain a minimum relative density of 60 % or greater to reduce the risk of liquefaction (Vick, 1983; Saad, 2008).

Tailings dry density is other important parameter governed by clay content and it is dependent on the void ratio and specific gravity of the deposited tailings (Saad, 2008). The average tailings dry density is usually measured over the impoundment's depth as an indicator of gain or loss of strength. It is also used to determine changes in the impoundment's volume due to settlement and consolidation processes (Vermeulen, 2001; Saad and Mitri, 2011; Vick, 1983; Mittal, 1974). A low average dry density is expected due to segregation of tailings over the beach (Ding et al., 2010). The slurry pulp density is another property of tailings defined as the weight of solids per unit weight of slurry at which tailings exit thickening or cycloning processes before deposition into the TSFs. Typical pulp density values for tailings range between 40-50% solids per unit weight of slurry (Vick, 1983). Pulp density is used in rheology analyses as a measure of the slurry viscosity, and in combination tailings particle size, and specific gravity, as an indicator of the potential settling rate of fine and coarse tailings.

2.2.8 2.2.8 Permeability (k)

Tailings permeability is primarily governed by gradation and plasticity, the deposition method, change in void ratio, and the distance from the discharge point (Blight, 1979; Clayton et al., 2004; Fetter, 2001; Priscu, 1999; Qiu and Sego, 2001; Rassam and Williams, 1999; Saad, 2008; Vermeulen, 2001; Vick, 1983). Generally, the coarser material (sand tailings) settles near the embankment forming a sloping beach. The finer portion of tailings flows into the decant tailings pond where slimes tailings deposit (Vick, 1983; Saad, 2008).

Vermeulen (2001) concluded that the spatial variation of tailings permeability from the embankment to the decant pond will determine the location of the phreatic surface within the impoundment. The coarser material with higher permeability has the important task of lowering the phreatic surface near the embankment (Saad, 2008; Vick, 1983; Qiu and Sego, 2001). According to Blight et al., (1985), Fell et al.,(2005), Mittal and Morgenstern, (1976), and Vick (1983), the permeability of whole tailings, can be calculated with Hazen's empirical method:

$$k=D_{10}^{2} \tag{2- 2}$$

where k is the average permeability in cm/s, and D_{10} is the particle diameter for 10% passing in millimetres. Fell (2005) concluded that sand tailings permeability can be in the order of 10^{-4} m/s and as low as 10^{-9}m/s for slime tailings. Typical values of tailings permeability are presented in Table 2-3.

Table 2-3 Typical values of tailings permeability

Tailings	k (m/s)	Source
Clean, coarse, or cycloned sands with less than 15% fines	10^{-4} to 10^{-5}	Fell, 2005
Peripheral-discharged beach sands with up to 30% fines	10^{-5} to 5 x10^{-6}	
Non-plastic or low plasticity slimes	10^{-7} to 5x10^{-9}	
High Plasticity slimes	10^{-6} to 5 x10^{-9}	
General	1x10^{-6}	Vermeulen, 2001
Sand Tailings under effective stress 50 to 300 kPa	1x10^{-4} to 1x10^{-8}	

Fell (2005) and Vick (1983) concluded that tailings permeability decreases with decreasing void ratio due to the higher compressibility of fine-grained materials present in the slimes tailings layers. According to Abadjiev (1976), the layered nature of tailings deposits allows for significant anisotropies in tailings permeability. Vick (1983) reported tailings anisotropies (k_h/k_v), range from 2 to 10. Vermeulen (2001) reported tailing anisotropies range from 5-10 in gold tailings. Saad (2008) reported anisotropy of 0.8 and 0.1 for embankment and slimes gold tailings, respectively.

2.2.9 Compressibility

Compressibility measures the degree to which tailings decrease in volume when supporting a vertical stress (Saad, 2008). Compressibility is lowest in coarse-grained tailings where particles are in contact with each other and increases as the proportion of fines increases (Fell, 2005). The compressibility of tailings is commonly obtained from the one dimensional consolidation test (Saad, 2008; and Vick, 1983). Sand and slime tailings appear to have higher compressibility than similar natural soils due to higher angularity and loose depositional state (Vermeulen, 2001). The amount of compression is typically determined by the consolidation state of tailings (Vick, 1983).

Vermeulen (2001) concluded that, typically, slimes tailings are in normally consolidated or even under-consolidated state upon deposition, but sub-aerial deposition and capillary effects on tailings may build up some overconsolidation states. Vick (1983) stated that there is a similar effect of stress history on the compressibility of slimes tailings and natural clays in which desiccation or capillary suction may produce some overconsolidation. Typical values of compression index (C_c) of sand and slime tailings are presented in Table 2-4.

Table 2-4 Compression index (C_c) tailings.

Tailings Type	C_c	Source
Sand tailings	0.05-0.1	Vermeulen, 2001; Vick, 1983
Slimes tailings – low plasticity	0.20-0.30	
Gold slimes	0.35	
Sand tailings	0.02-0.04	Saad, 2008
Slimes tailings – low plasticity	0.08-0.15	
Oil sands	0.06	Vick, 1983
Fine coal refuse	0.06-0.27	

2.2.10 Consolidation characteristics of tailings

The consolidation of tailings is similar to those of natural soils. A stress increase caused by augmenting the vertical stress when a new embankment is raised or new deposition of tailings occurs compresses the underlying tailings layers. Vermeulen (2001) and Vick (1983) concluded that compression of tailings occurs by deformation of the grain particles and expulsion of water and/or air from the void space.

According to Holtz and Kovacs (1981), total settlement has three components: immediate settlement, primary consolidation settlement, and the secondary consolidation settlement:

$$S_T = S_i + S_c + S_s \tag{2- 3}$$

where, S_i is the immediate settlement, which is caused by the elastic deformation without any change in the moisture content; S_c is the primary consolidation settlement, which is the result of a volume change in saturated cohesive materials when the water that occupies the void space is expulsed, and S_s the secondary consolidation settlement, which is observed in saturated cohesive fine tailings and is the result of the plastic adjustment of soil fabrics (Abadjiev, 1976; Blight et al., 1985; Mittal and Morgenstern, 1976; Priscu, 1999; Qiu and Sego, 2001; Vick, 1983).

Saad (2008) found that sand tailings release the pore pressure immediately after deposition due to their high permeability and draining capacity. Pore pressure release is accompanied by a reduction in the volume of the soil mass, which, in turn, produces strength gain. In sand tailings, settlement and consolidation occur simultaneously as a result of their immediate drainage capacity and it is difficult to measure in the laboratory (Vick, 1983).

The settlement and consolidation processes of fine-grained tailings are different from that of sand tailings. When saturated fine-grained slime tailings are subjected to a vertical stress increase, the excess pore pressure generated dissipates over a long period of time due to the low permeability and poor drainage capacity of these materials. As a result, the volume change or consolidation process extends over long periods of time and can remain saturated if the drainage system is not properly designed (Saad, 2008). Typical values of coefficients of consolidation (C_v) for different tailings are presented in Table 2-5.

Table 2-5 Coefficients of consolidation (C_v) for gold tailings

Tailings Type	C_v (m^2/yr)	Source
Sand Tailings	1.6x103 to 0.3x106	Saad 2008; Vermeulen, 2001; Vick, 1983
Slimes Tailings	0.3 to 30	
Slime Tailings	198	Vermeulen, 2001; Blight, 1981
General	300	

According to Blight (1981), the coefficient of consolidation decreases with increasing effective stress and decreasing void ratio. Vermeulen (2001) and Vick (1983) concluded that tailings consolidation is governed by permeability and compressibility. Vick (1983) indicated that the coefficient of consolidation can be calculated in one-dimensional compression using Equation 2-4:

$$C_v = \frac{k}{\gamma_w m_v} \tag{2- 4}$$

where k is the permeability, γ_w is the unit weight of water, and m_v is the coefficient of volume change $m_v = \frac{\partial \varepsilon}{\partial \sigma}$.

The total vertical deformation resulting from the loading process is called settlement (Holtz and Kovacs, 1981). Tailings, as any other geomaterial experience deformations due to compressive, tensile, or shear forces exerted by the self-weight of the material, the load of new raised embankments, and/or the water pressure (Selvadurai, 2006). Deformations in TSFs require special consideration in order to evaluate the shear strength gain and density increase that takes place during consolidation and settlement processes.

2.2.11 Shear Strength

Tailings deliver shear strength from different sources. One source is the effective friction angle (ϕ′) which is dependent on the veridical effective stress. Other source is source is the cohesive force between adjacent particles, or effective cohesion (c′) which is independent from the vertical effective stress. Shear strength is derived from the relative density of tailings (Barrera et al., 2011; Duncan and Wright, 2005; Fell et al., 2005; Mittal and Morgenstern, 1976; Qiu and Sego, 1998b; Vick, 1983).

According to Dimitrova and Yanful (2012), Vermeulen (2001), and Vick (1983), tailings are cohesionless materials with effective friction angles slightly higher than natural soils of similar gradation. This characteristic has been attributed to the angularity of tailings particles due to milling processes (Blight et al., 2005; Clayton et al., 2004).

Table 2-6 shows typical cohesion and friction angles values for gold tailings materials reported in the literature.

Table 2-6 Typical values of cohesion and friction angles of gold tailings

Tailings	c′ (kPa)	ϕ′ (deg.)	Source
Gold sands tailings		30-37	Vick, 1983
	0-3	30-33	Qiu and Sego, 2001; Saad, 2008
		29-35	Vermeulen, 2001
Gold slimes tailings		28-41	Blight, 1979
	0-5	5	Qiu and Sego, 2001; Saad, 2008
		29-35	Vermeulen, 2001
		28-40.5	Fell et al., 2005

Saad (2008) found that there is little variation between the Mohr-Coulomb effective friction angle for sand and slime tailings and that the friction angle tends to decrease by moving towards the slimes zone. According to Vermeulen (2001), tailings that undergo drying and wetting cycles result in varying shear strength properties. When moisture is added to the tailings as they reach the ponded water in the impoundment, the attraction between the surface ions on the clay mineral reduces and so does the angle of internal friction.

2.3 Tailings Containment Methods and Design

TSFs design is governed by site-specific variables, the project economics, and availability of construction materials. Equally, it is determined by water storage requirements, regional seismicity, climate conditions, and the regulations applicable to the mining project. Vick, (1983) indicated that it is important to locate the TSF downhill and as close as possible to the mill to facilitate slurry transportation and minimize pumping costs.

Vick (1983) classified TSF layouts into ring dyke (for flat terrains), cross valley, side hill and valley-bottom impoundment according to the topographic setting and quantity of embankment fill required for construction. The ultimate height and slope of the impoundment are also determined according to the topography evaluation of the site. Vick (1983) reported that TSFs with ultimate heights between 30 m to 60 m usually prove to be optimal from management, operational and safety stand points. On the other hand, embankments with ultimate heights of 123m - 152m or more, almost always cause operational and safety problems.

These conclusions are in good agreement with the reports by Azam (2010), USCOLD (1994), ICOLD (2001), Rico et al., (2008) and WISE (2012). Table 2-7 summarizes other determining factors for TSFs location.

Table 2-7 Factors influencing TSFs location (Modified from Vick, 1983)

Criteria	Effect
Location and elevation relative to the mill	Length of tailings and return-water pipelines
Topography	Capital and operational cost of pumps Embankment layouts and fill requirements
Hydrology and Groundwater	Water storage requirements, flood handling Moisture content of borrow material and foundation. Rate and direction of seepage Contamination potential
Geology	Availability of natural borrow material Foundation stability
Seismicity	Stability concerns and liquefaction trigger

2.4 Embankment construction methods

In practice, multiple methods and materials are used for TSFs embankment construction. As a general rule, the construction method is selected according to the availability and cost of the materials (Martin and Morrison, 2012 and Vick, 1983). At most mine sites using stripped waste rock, native borrow soil, and mill tailings lowers costs significantly. However, tailings may not be entirely suitable for embankment construction if they exhibit poor geotechnical properties.

In order to use tailings as construction materials certain gradation, shear strength, permeability, and stability requirements should met. Generally, mill tailings are suitable for embankment construction. However, static or seismic liquefaction continues to be a common failure mechanisms observed in TSFs containing tailings of low or no plasticity. Usually, compaction is required to improve density and sufficient mechanical performance of tailings. Likewise, spigotting or cycloning deposition techniques are required to enhance particle segregation according to the grain size distribution.

Depending on the sequence of construction of the embankment, TSFs are classified into water retention tailings dams (WRTDs) and raised embankment tailings storage facilities (Vick, 1983).

2.4.1 Water Retention Tailings Dams (WRTD)

In water retention tailings dams the embankment is built to its full height prior to the beginning of operations. WRTDs are provided with an impervious core that allows for water storage. Additionally, natural borrow is used for embankment construction (Martin and Morrison, 2012; Vick, 1983). Figure 2-4 depicts a typical cross-section of a WRTD.

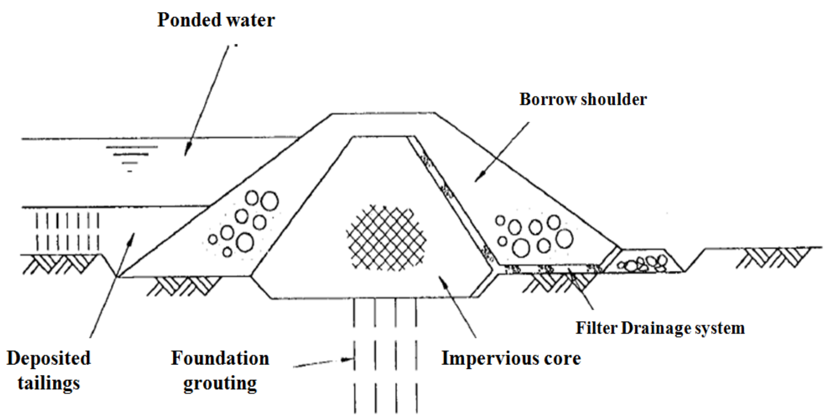

Figure 2-4 Cross-section of a typical water retention tailings dam (ICOLD, 1996)

According to Vick (1983), WRTDs are generally constructed at mine sites with high waste water storage requirements. This type of TFS is suitable for any type of tailings material and is recommended for sites with moderate to high seismic potential. Martin and Morrison (2012) concluded that despite of their high cost WRTDs are considered an asset for the mining operation because they have a finite lifespan and achieve steady-state at an early stage of production. Hamade et al.,(2011) explained that WRTD are a good option for emerging technologies such as tailings co-disposal.

2.4.2 Raised Embankment Tailings Storage Facilities

Raised embankments TSFs are built in stages as the mining operation progresses. There are three types of raised embankment TSFs named after the direction in which the retaining embankment is constructed. They are classified as downstream, centerline and upstream tailings storage facilities.

- ***Downstream raised embankment***

In the downstream technique, cycloned sand is deposited over a starter dike in the downstream slope direction for subsequent dykes construction. Downstream embankments are often designed as quasi water retaining structures and have zero reliance on tailings for stability in the short and long-term (Martin and Morrison, 2012, Vick, 1983, and U.S. EPA, 1994). The core and drainage zone allow for water storage directly against the upstream face of the embankment impoundment. Figure 2-5 displays a typical cross-section of a downstream construction method.

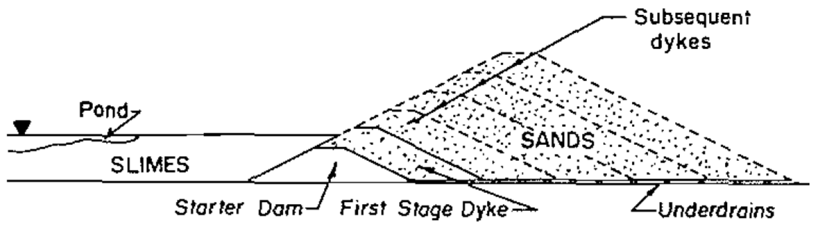

Figure 2-5 Downstream method of construction (Mittal and Morgenstern, 1976)

Downstream raised embankments require more material to build the embankment than others TSFs. The downstream method was developed to reduce the risks associated with the upstream design when subjected to earthquake shaking (ICOLD, 2001).

- ***Centerline raised embankment***

In the centerline construction method the embankment crest moves vertically during the staged raising of the embankment (Saad, 2008). The centreline method is considered an intermediate point between the upstream and downstream designs. Centerline TSFs are more stable than the upstream method but do not require as much construction material as the downstream design (U.S. EPA, 1994). Figure 2-6 shows a typical cross-section of the centerline method of construction.

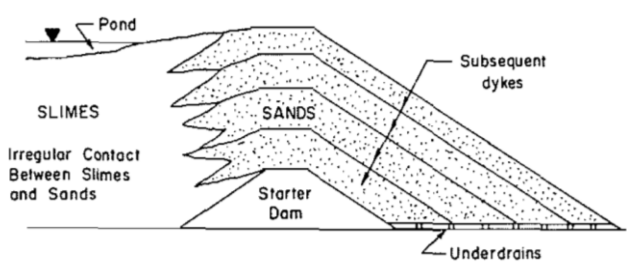

Figure 2-6 Centerline method of construction (Mittal and Morgenstern, 1976)

Mittal and Morgenstern (1976), Vick (1983) and U.S. EPA (1994) concluded that centerline raised embankment require less sand content in mill tailings, and therefore, the rate of raise is higher than in the upstream or downstream methods. Similar to the downstream method, centerline raised embankments require an under-drainage systems to avoid pore pressure increase.

Centerline raised embankments do not require a wide beach, thus, tailings with low content of sands are acceptable (U.S. EPA, 1994). Centerline TSFs are not recommended for permanent storage of water. Short-term storage of water is permitted if the embankment has been properly compacted and a good internal drainage exists. Vick (1983) indicated that theses TSFs have good seismic resistance.

- ***Upstream raised embankment***

In the upstream method a borrow starter dyke is initially constructed and the subsequent raising of the embankment is done using hydraulically deposited or cycloned tailings in the upstream direction. Figure 2-7 shows a typical cross section of an upstream raised embankment.

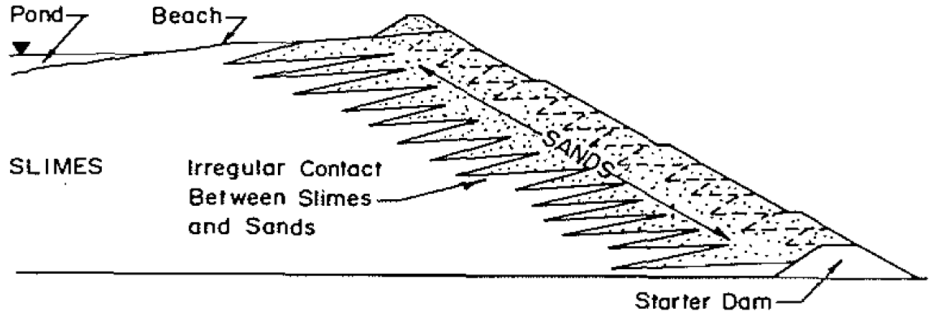

Figure 2-7 Upstream method of construction (Mittal and Morgenstern, 1976)

According to Martin and Morrison (2012) the upstream technique is the most economical but the least favourable raised embankment method. The main cause is because steady state is reached only at closure. Vick (1983) indicated that mill tailings for upstream tailings storage facilities (UTSF) require at minumum of 40-60% sand content to be suitable for further embankment raise. Furthermore, multiples researchers have concluded that Upstream TSFs have poor water storage capacity (Vick, 1983; Davies and Martin, 2000; Julien and Kissiova, 2011; Martin and Morrison, 2012; Qiu and Sego, 2006). In fact, the phreatic surface should be kept as far away from the embankment as possible.

Martin and Morrison (2012) concluded that UTSFs require wide beach for embankment stability and good segregating capacity. The permeability of the foundation and the size of decant pond are other fundamental variables to control water seepage through UTSFs.

Abadjiev et al.,(1987), ICOLD (1993), Martin (1999), Saad and Mitri (2011), and Saad et al.,(2011) concluded that for UTSFs embankment construction a slow a rate of raise is necessary to allow for dissipation of construction-induced pore pressures. Another key factor is to construct and efficiently operate an under-drainage system in the foundation-starter dyke interface to maintain low pore pressures and avoid piping from occurring (Priscu, 1999). Martin and Morrison (2012) and Vick (1983) concluded that UTSFs are not appropriate for regions of moderate to high seismicity due to the liquefaction susceptibility of the non-cohesive coarse tailings of low plasticity.

2.5 TSFs impoundment design criteria

TSFs design incorporates all the variables, properties, and materials that that govern stability and that must be kept under control to avoid unsatisfactory performance of the impoundment. There are similar design criteria for the WRTD and for the UTSF; e.g., the phreatic surface location, anisotropy, and boundary conditions. Similarly, important design differences belong to each type of TSF. Some design parameters unique to UTSF are the beach width and the lateral permeability variation of the beach. WRTD design criteria are similar to conventional water retention dams. WRTDs design includes impervious core, filters, drainage systems, and foundation grouting specifications. UTSFs, on the other hand, do not have impervious core and depend primarily on the drainage system to control de location of the phreatic surface (ANCOLD, 1999).

2.5.1 Phreatic surface location

The location of the phreatic surface is a fundamental variable that governs the overall static and pseudo-static stability of all types of TSFs. The internal water level within the impoundment will determine the vulnerability of the facility to pore pressure related failure mechanisms. The gradation and permeability of the materials near the embankment, in the zone near the embankment seepage regime of the TSF determine the distribution of tailings into the impoundment upon deposition (Vick 1983).

Vick (1983) explained that the phreatic surface location in a WRTD is primarily governed by the embankment to core permeability ratio as indicated in Figure 2-8.

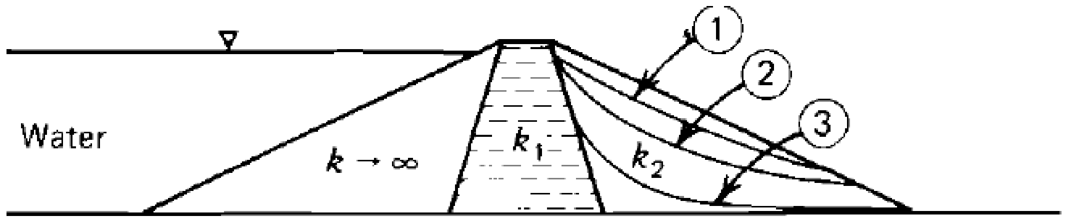

Figure 2-8 Effects of embankment-core permeability ratio on the phreatic surface location of a WRTD on an impervious foundation: (1): k2 = 10k1; (2): k2 = 20k1; (3): k2 = 100k1; kh/kv = 16 from Vick (1983).

Figure 2-8 shows that, for this specific case, an embankment to core permeability ratio of k_2/k_1=100 would yield the lowest phreatic surface and provide more stability to the WRTD. That is, the higher the permeability ratio, the lower the phreatic surface location on the downstream slope of the dam. Therefore, the embankment-core permeability ratio should be at least 100 to achieve low phreatic surface and minimize the adverse effects of anisotropy (Vick, 1983).

The location of phreatic surface location for UTSF is a more complex process that involves interactions between the beach width, the lateral variability of permeability in the beach, anisotropy of tailings permeability, and the impoundment's boundary conditions (Vick, 1983).

Abadjiev (1976), Blight et al.(1985), Saad et al., (2011), and Vick (1983) concluded that the location of the phreatic surface in UTSFs is best controllable when the permeability of the of the constitutive materials decreases in direction of the pond water and increases in the direction of the embankment and seepage flow. Figure 2-9 illustrates the desirable distribution of permeability and location of the phreatic surface for and UTSF suggested by Vick (1983).

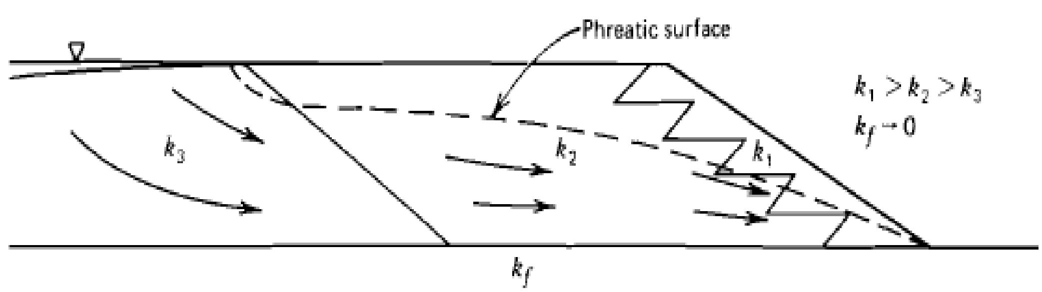

Figure 2-9 Proper internal permeability configuration for phreatic surface control in an UTSF. Arrows indicate flow direction. Modified from Vick (1983).

- ***Beach width***

The beach width corresponds to the distance from the pond to the crest of the embankment and orthogonal to the embankments ultimate height. Abadjiev (1976), Blight et al.,(1985), Saad et al.,(2011), Martin and Morris (2012), and Vick (1983), the beach width is the most important factor influencing phreatic surface location, and hence, the parameter that controls the overall stability of the UTSF. Vick (1983) proposed a method to determine the optimum location of the phreatic surface by assuming different values of beach widths ratios (measured from the toe of the embankment) normal to the height of the embankment summarized in Equation 2-5.

$$\textit{Phreatic}\text{ Surface Location} = \frac{\textit{Beach}\text{ Width (from toe of embankment)}}{\textit{Embankment Ultimate}\text{ Height}} = \frac{L}{H} \quad \textbf{(2- 5)}$$

The idealized phreatic surface location in UTSF with different values of beach width ratios are presented in Figure 2-10.

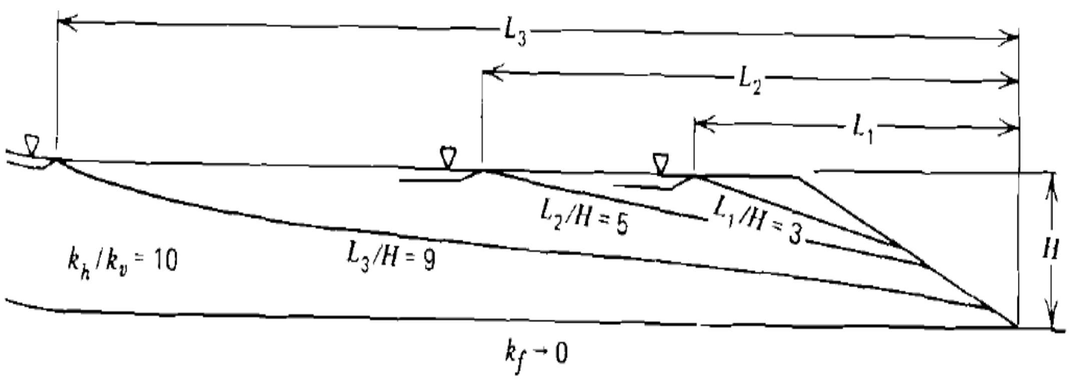

Figure 2-10 Influence of the beach width on phreatic surface for homogeneous, anisotropic UTSF on an impermeable foundation. (After Vick, 1983)

As depicted in Figure 2-10, an UTSF with an L/H ≥ 9 ratio would provide and optimal phreatic surface location for the impoundment. An L/H ratio much less than 9 would produce a troublesome phreatic surface location. The L/H ≤ 3 would be critical and undesirable for the stability of the embankment (Vick, 1983). Julien and Kissiova (2011) suggested a minimum 50 m distance from the phreatic surface to the crest of the UTSF embankment to avoid critical instability. In this thesis, the L/H ratio criterion was used to assess the effect of the phreatic surface location on the UTSF stability.

- ***Lateral permeability***

Lateral permeability variation of the beach tailings is another factor that governs the phreatic surface location in an UTSF (Abadjiev, 1976; Blight et al., 1981; Priscu, 1999; Vick, 1983). The degree of permeability variation also depends on the gradation of the deposited tailings and the slurry pulp density of the discharge. Vick (1983) stated that the variation in permeability in an UTSF is characterized by the ratio of tailings permeability at the spigot point (k_o) to the permeability at the edge of the pond water at the slimes zone (k_L) as shown in Equation 2-6:

$$\text{Variation in Permeability}_{UTSF} = \frac{k_o}{k_L} \qquad \textbf{(2- 6)}$$

Figure 2-11 shows that a low phreatic surface location is expected when the variation between the in permeability in the embankment is greater than the permeability near the slime zone. Abadjiev (1976) and Vick (1983) concluded that beach permeability variations ($k_0/k_L \geq 100$) combined with an adequate beach width (L/H> 5) can contribute to low phreatic surface location in an UTSF.

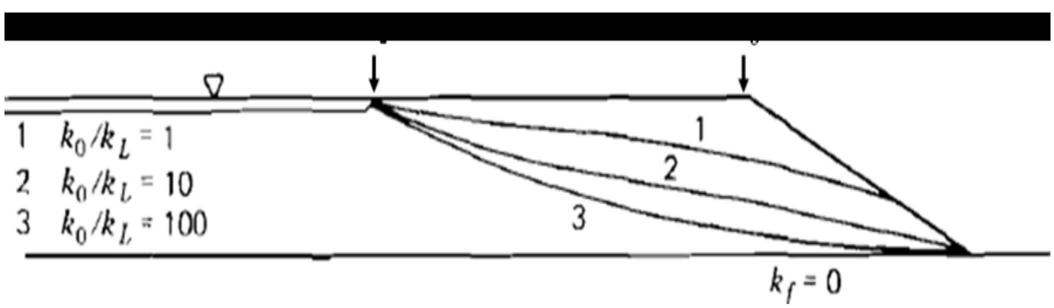

Figure 2-11 Influence of beach permeability variation on phreatic surface location for variable ko/k_L in UTSF (Modified from Vick 1983).

- ***Effect of anisotropy***

Studies on deposited tailings permeability by Abadjiev (1976), Vick (1983), Aubertin (1995), Blight et al.,(1985), and Godt et al.,(2012) concluded that anisotropy of tailings permeability has a lesser effect on the phreatic surface location in UTSF because the flow within the impoundment is predominantly in the horizontal direction and much less significant in the vertical direction due to the layered nature of the slurry upon deposition. The effect of anisotropy in the location of the phreatic surface in WRTD is characterized by the dominance of vertical flow direction within the dam.

2.5.2 Filters/ Drainage systems

Filter and drainage systems are important components of TSF design because they represent the primary means of phreatic surface control and piping and/or liquefaction induced failure prevention (Blight et al., 1981; U.S. Army Corps of Engineers, 1986). The purpose of a drain is to remove excess water from the impoundment to promote consolidation and strength gain of saturated layers. Two common types of internal drainage zones are chimney and blanket.

Chimney drains rise vertically or inclined within the embankment to capture lateral seepage. Horizontal blanket drains are located at base of the structure along the starter dyke and foundation interface (Vick, 1983, Martin and Morrison, 2012). Blanket drainages are common in UTSFs, whereas a combination of chimney and blanket drains is often seen in WRTDs (Julien and Kissiova, 2011; Martin, 1999; Mittal and Morgenstern, 1976; Saad et al., 2011).

Drainage systems are usually made of gravel materials of high permeability. Martin and Morrison (2012) recommended that the material used in drains should normally be 200 to 1000 times more permeable than the drained tailings. Filters are designed to permit the passage of fluid while preventing migration of particles into the drainage system of the TSF to avoid the occurrence of hydraulic piping or internal erosion. Filters are commonly made of clean sand or gravel and sand mixtures (Martin, 1999; Saad et al., 2011; Sarsby, 2000).

2.5.3 Foundation

The foundation is a fundamental constitutive zone of TSFs design because it determines the ultimate height and bearing capacity of the impoundment (Morsy et al., 1995). The characteristics of the foundation govern rate of raise and consolidation processes. Likewise, the foundation has an important role in regulating the seepage through the impoundment to avoid piping (Saad, 2008). The primary design criteria of TSFs foundations are shearing resistance parameters, degree of saturation, index limits, ultimate bearing capacity, pore pressure distribution, and total and differential settlement to analyze their response to vertical stress exerted by the embankment and the tailings

(Morsy et al., 1995; Saad, 2008; Vick, 1990). The deformation induced by the impoundment to the foundation is also of paramount importance in tailings design and stability analyses (Alencar et al.,1994; Morsy et al., 1995; Watts, 1981). Saad (2008) and Hamade et al., (2011) conducted transient coupled hydromechanical analyses TSFs using a glacial till clayey foundations underlain by bedrock.

2.5.4 Freeboard

Freeboard is a design criteria used to determine the maximum level of the impoundment with respect to the embankment crest that will safeguard the TSF from overtopping and/or flooding due to a surplus of water during operation or at a given moment in time (ANCOLD, 1999; DOME, 1999; Martin and Morrison, 2012; U.S. EPA, 1994). The minimum freeboard of a TSF is project-specific and is determined by the designers according to local regulations and climatic characteristics of the site (Saad, 2008). Usually, three types of impoundment levels are taken into consideration in defining the freeboard: the operational freeboard, the Probable Maximum Flood (PMF) freeboard, and the closure freeboard. Studies by Hamade et al.,(2011); PHP Billiton (2010), and Saad (2008) suggested a minimum of 2m for WRTD and USTF as a reasonable freeboard distance. This same value of freeboard adopted in this thesis.

2.5.5 Starter Dyke

The starter dyke is the first structure of all sequentially raised embankments; hence, it is a key component of TSFs design. The starter dykes is generally made of cohesionless compacted waste rock or borrow materials. The starter dyke of UTSFs should be a free draining zone of high permeability and high shear strength. In the case of downstream raised embankments, the starter dyke must be made of impervious materials to allow for permanent or temporal water storage (U.S.EPA, 1994; Vick, 1983).

2.5.6 Rate of Rise

The rate of rise in TSFs design is defined as the change in vertical height with respect to time (Martin and Morrison, 2012). The rate of rise is a fundamental variable in TSF design because it controls the velocity at which the embankment can be built without jeopardizing the stability of the impoundment due to the increase in pore pressure in zones with fine grained materials (e.g. slime tailings).

Mittal and Morgenstern (1976) and Vick (1983) indicated that the rate of rise governs the consolidation process of tailings. Martin and Morrison (2012) explained that the rate of rise can be used to determine the storage capacity at each stage of construction using TSF stage-capacity curves. Vick (1983) stated that the rate of rise is dependent on the production rate of the mill.

Reports by ANCOLD (1999), Azam (2010), Mittal and Morgenstern (1976), U.S. EPA (1994), and Vick (1983) suggested that a safe rate of raise for USTF that will allow for pore pressure dissipation and consolidation of tailings should be less than 4.5 - 9 m/year. A rate of raise greater or above 15 m/year can be unsafe for any type of TSF. Saad (2008) used 5.25 m/year rate for a gold tailings UTSF. Hamade et al., (2011) used the concept of rate of raise for the filling stages of tailings into a WRTD impoundment.

2.6 Deposition Methods

Tailings discharge into the impoundment is commonly done through subaqueous or subaerial deposition methods. The selection of a deposition method has a remarkable influence in the settlement and grain-size distribution of tailings within the impoundment. Subaqueous or below water deposition is commonly used to deposit tailings with acid mine drainage (AMD) generation potential. These types of tailings oxidize very quickly and therefore oxygen restriction is achieved by placing them underwater. Subaqueous deposition requires an impoundment capable of storing considerable volumes of water. Tailings deposited with the subaqueous method are fully saturated, and therefore, possess low shear strength.

Subaerial deposition refers to discharge above the water line, on the ground, or directly on the tailings beach. This method is more common than the subaqueous method (Saad, 2008, Priscu, 1999, Vick, 1.983; Mittal and Morgenstern, 1974). In subaerial method tailings flow onto on a sloping beach with low velocity allowing natural grain-size-based segregation upon deposition. The coarser material settles near the point of discharge forming a beach.

The finer material will deposit near the decant pond (Blight and Bentel, 1983; Qiu and Sego, 2006). Spigotting is a widely used subaerial method for delivering non-segregated tailings. Basically, single or multiple spigots are evenly distributed along the perimeter of the impoundment and are connected to a main delivery line coming from the mill (Robertson, 1987). Figure 2-12 shows a typical distribution of spigots in and UTSF.

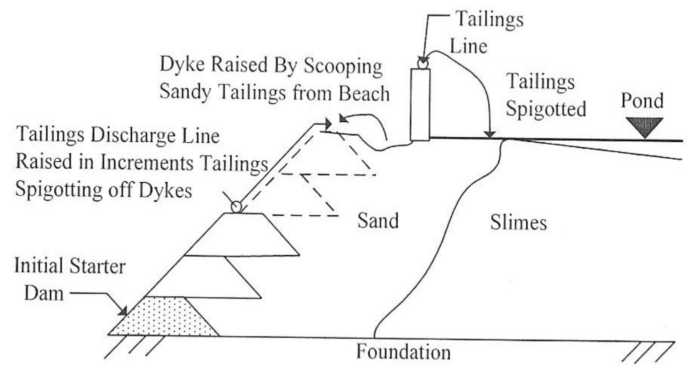

Figure 2-12 Tailings deposition using the spigotting method in an UTSF. (After Saad, 2008)

As shown in Figure 14, tailings are fed sequentially until a desired level of sands has been reached to construct the embankment and to commence the raising process (Abadjiev et al., 1987). In practice, multiple spigots are used simultaneously to reduce the discharge velocity of the tailings and promote the formation of a laminar flow and augmenting the drainage potential. Cycloning is another deposition method used for non segregating tailings with high fines content. In this method, the main tailings feeding line from the mill is directly connected to cyclones located on the embankment as depicted in Figure 2-13. The cyclones overflow, containing fine grained particles, is piped into the settling towards the decant pond.

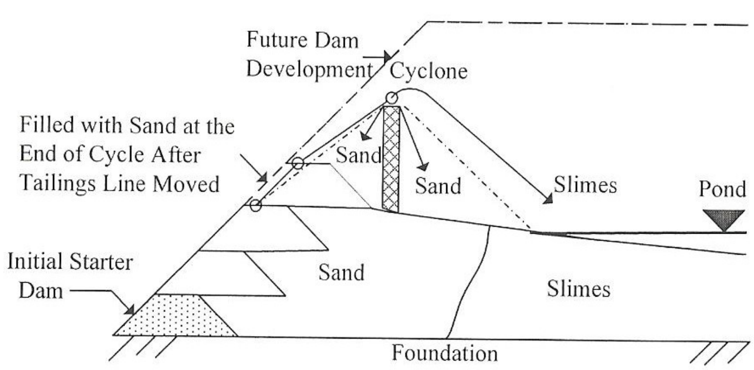

Figure 2-13 Tailings deposition using the cycloning deposition method in an UTSF (After Saad, 2008)

Figure 2-13 illustrates how the cyclone's underflow, containing coarse sands, is directly discharged of the cyclones to form the embankment through scooping and compaction (ANCOLD, 1999; Ding et al., 2010). Due to the great challenges associated with TSF water management, increased environmental awareness, and more rigorous regulations for mine wastes management, there is a tendency towards new deposition methods (Martin and Morrison, 2012). Dewatering and dry deposition of tailings in the form of thickened tailings and dry cake tailings are now being used. These methods are beyond the scope of this thesis, however, a brief summary on dry tailings deposition is provided in Figure 2-14.

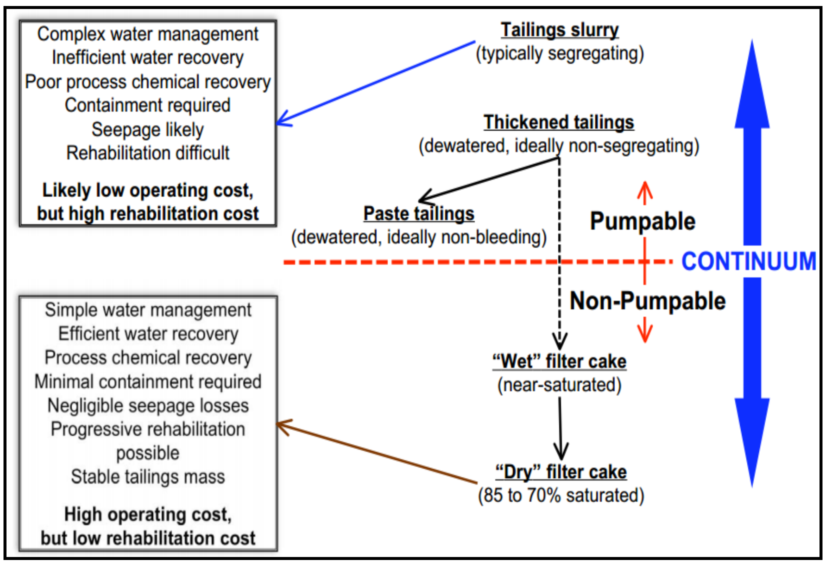

Figure 2-14 Tailings deposition methods continuum, (Martin and Morrison, 2012)

CHAPTER 3: METHODS FOR TSF STABILITY ANALYSIS

Studies by the UNEP (1996), ICOLD (2001), Azam (2010); Rico et al., (2008), and Starchan and Caldwell (2010) concluded that slope instability is the most common failure mechanism observed in TSFs, and UTSFs are considered the most vulnerable type. Refer to Figures 1-1 and 1-2 of this thesis for more details on number and types of failure incidents in the world. Slope stability analyses of TSFs must be performed under variable conditions, levels of risk, and analytical approaches applying fundamental concepts of geotechnical engineering and soil mechanics. The objective is to produce reliable results that provide realistic estimations of the processes taking place within an impoundment. TSFs stability analyses should be comprehensive enough to include the complexity and level of uncertainty associated to tailings properties and mining operations in general. According to Saad (2008) and Hamade et al., (2011), TSF's stability analyses can be divided into static, pseudo-static, and transient analyses depending on the model's boundary conditions, loading conditions, and overall configuration of the case study. In this section, these approaches are briefly discussed with emphasis on static and pseudo static stability analyses.

3.1 Static Analysis

In static stability analyses it is assumed that the performance of the TSF is independent of time. Static analyses can be performed under different loading and boundary conditions depending on the mechanical properties of the constitutive materials, the seepage conditions through the STF, and environmental/climatic characteristics of the site. The ultimate purpose is that the analyses results reflect the most probable conditions and processes taking place within the impoundment.

3.2 Seepage through TSFs

The primary governing criterion of interest in static and pseudo-static TSFs stability analyses is seepage. Seepage governs the overall hydraulic performance of the facility with regards to pore pressure distribution, location of the phreatic surface, and water supply. Pore pressure-based failure mechanisms (e.g. piping, liquefaction) and ground water contamination potential are also controlled by seepage analysis.

A seepage analysis determines the drained and undrained conditions within a TSF and defines the sources of strength available in each case. It was concluded from studies by Abadjiev (1976), Blight et al.,(1985), Das (2007), Fetter, (2001), Mittal (1974); Saad et al.(2011), and Vick (1983) that seepage through TSFs is similar to that of hydraulic structures, thus, it is governed by the following assumptions:

- Flow occurs under steady-state conditions and obeys Darcy's law.
- Laplace's equation is valid in confined flow.
- The porous media is assumed fully saturated and the flow path changes directions within the impoundment with predominant vertical direction and a small component in the horizontal direction due to the effect of the gravitational force.
- Flow is laminar and incompressible.
- Boundary conditions, permeability of the porous media, and hydraulic heads imposed by the model's geometry are known and well defined.

If a two dimensional flow (x, y direction) and isotropic permeability of the soil stratum is assumed, seepage through TSF is determined by Laplace's theory of continuity given by:

$$\frac{\partial^2 h}{\partial x^2} + \frac{\partial^2 h}{\partial y^2} = 0 \qquad \textbf{(3- 1)}$$

Laplace's equation can be solved either by the flow net method or finite element numerical methods. Seepage analyses with finite element can be applied in complex geometries (Fetter, 2001).

Numerical methods used to solve Laplace equation in complex flow conditions are usually based on finite difference or finite element methods. Both methods can be used in 1, 2-, or 3-dimensional modeling (Rocscience, 2007). In the finite element method solution, the flow region is divided into discrete elements with n number of equations with n number of unknowns. Material properties, such as permeability are specified for each element and boundary conditions. A system of equations is solved to compute heads at nodes and flows in the elements.

3.2.1 Anisotropy in seepage analyses

In practice, not all materials within a TSF are isotropic. Tailings, for instance, are characterized for being anisotropic due to layering and varying gradation during deposition (Abadjiev, 1976). This implies that the coefficient of permeability is dependent upon the direction of flow and tends to be greater in the horizontal direction (K_h) than in the vertical direction (K_v). Consequently, the 2D-steady-state equation:

$$k_x \frac{\partial^2 h}{\partial x^2} + k_y \frac{\partial^2 h}{\partial y^2} = 0 \qquad \textbf{(3- 2)}$$

In order to transform Laplace's and compensate for anisotropy, the porous media cross section has to be adjusted by the square root of the ratio of the permeability in the two directions. Assuming k_h and k_v as the horizontal and vertical permeability, respectively, the horizontal dimension of the porous media cross section is changed by a ratio of $\sqrt{k_v / k_h}$.

Holtz and Kovacs (1981), concluded that anisotropic problems can be solved using the same methods than for isotropic methods (flow-net) once the geometric transformation and scale adjusting of the permeability had been completed.

3.2.2 Drained and undrained shear strength

The drained and undrained states describe the ease with which water moves through tailings particles and its effects on the pore pressure (Duncan and Wright, 2005; Selvadurai, 2006). In TSFs stability analysis, two types of stresses are usually considered: the total stress, and the effective stress.

Total stress is the sum of all the forces (including the interparticle contacts and pore pressure) acting on the material of interest (Duncan and Wright, 2005). The effective stress includes only the forces that are transmitted to the system through the intergranular contacts when the voids spaces are empty, that is, by subtracting the pore pressure from the total stress (Das, 2007, Duncan and Wright, 2005).

Effective stress is generally calculated through Terzaghi's Equation as follows:

$$\sigma' = \sigma - u \qquad \textbf{(3- 3)}$$

where σ′ denotes the effective stress, σ denotes the total stress, and u denotes the pore water pressure or neutral pressure (Holtz and Kovacs, 1981). Equally important is to determine the shear strength (τ) of the porous media when it is slowly subjected to loading. The drained shear strength is present when no pore pressure develops and water can drain freely through the porous media. Shear strength can be calculated using the Mohr-Coulomb strength criterion as shown in Equation 3-4,

$$\tau = c' + \sigma' \tan \phi' \qquad \textbf{(3- 4)}$$

where c′ is the effective cohesion, σ′ is the effective stress on the failure plane at failure, and ϕ′ the effective angle of internal friction (Duncan and Wright, 2005). Vick (1983) found that compared to natural soils, tailings have higher drained shear strength due to their angularity and higher friction angle values. Also, for normally consolidated tailings, the effective cohesion is zero in drained shear strength tests. The most important factor influencing the drained shear strength is the effective friction angle of tailings (Vick, 1983). The undrained shear strength (S_u) is the strength that tailings display during a fast loading rate and there is few or no flow of water from the void space (Duncan and Wright, 2005).

$$S_u = \frac{(\sigma_1 - \sigma_3)_f}{2} \quad \textbf{or} \quad \begin{matrix} S_u = c \\ \phi_u = 0 \end{matrix} \qquad \textbf{(3- 5)}$$

where S_u is the radius of the Mohr's Circle of Total Stress and σ_1, and σ_3 are major and minor principal stresses respectively in the Mohr's circle of total stress; c is the total cohesion, and ϕ_u, is the total friction angle for saturated clays. The undrained shear strength is very important in TSFs stability analyses because it determines the pore pressure increase within the impoundment.

The shear strength of tailings must be measured both in-situ and laboratory tests. Same as in natural soil characterization, the shear strength of tailing is measured with the Triaxial Shear Tests in the form of the *Consolidated Drained* (CD) test, *Consolidated Undrained* (CU) test, and the Unconsolidated Undrained (UU) test when the embankment is constructed rapidly without pore pressure dissipation (Selvadurai, 2006). In-situ shear strength properties of tailings are generally measured by means of the Cone Penetration test (CPT), the Vane shear test (for fine tailings and low permeability soils), or the Standard Penetration Test (SPT).

3.3 Types of stability analysis

TSF stability analyses are generally carried out in two different ways: Total Stress Analysis (TSA) and the Effective Stress Analysis (ESA). Likewise, depending on the drainage capacity of the constitutive materials and the time required to achieve equilibrium with respect to the loading rate or stage of construction, stability analyses can be conducted for short-term, rapid-drawdown, or long-term conditions (Duncan and Wright, 2005). In the TSA, failure occurs under undrained conditions and the total shear strength (undrained) shear strength parameters (ϕ and c) are used. The TSA is typical for short-term and rapid drawdown analyses (Saad, 2008; Vick, 1983, Duncan and Wright, 2005).

In the ESA, drained conditions are assumed and the effective shear strength parameters (ϕ' and c') are used. The pore pressure regime is predicted form steady state seepage analysis. The ESA is typical for long-term stability analyses when total dissipation of pore pressure has occurred (Saad, 2008; Vick, 1983, Duncan and Wright, 2005). The Undrained Shear Analysis (USA) is an intermediate approach between the ESA and the TSA. In this type of analysis, failure occurs under undrained state, but strength gain due to consolidation is taken into consideration. The USA is typical for end of construction analyses (Saad, 2008; Vick, 1983, Duncan and Wright, 2005.

3.4 The Factor of safety (FOS)

The factor of safety (FOS) for slope stability analysis is usually defined as the ratio of the available shear strength to the mobilized shear stress as show in Equation 3-6 (Saad, 2008; Vick, 1983, Duncan and Wright, 2005; Rocscience (2006 and 2007).

$$FOS = \frac{s}{\tau} \qquad \textbf{(3- 6)}$$

where s is the available shear strength and τ is the equilibrium shear stress. The factor of safety represents the factor by which the shear strength must be reduced so that the reduced strength is just in equilibrium with the shear stress. The factor of safety can be expressed in terms of effective Mohr –Coulomb strength parameters as:

$$FOS = \frac{c' + \sigma' \tan\phi'}{\tau} \qquad \textbf{(3- 7)}$$

where c´ and ϕ´ are the effective cohesion and friction angle parameters, ϕ' and τ is the equilibrium shear stress. The first step to calculate the FOS using the limit equilibrium method is to assume a possible slip surface along which the sliding will occur. Then, one or more equations of static equilibrium are applied in order to obtain the FOS and the stresses acting on the slip surface (Saad, 2008; Vick, 1983, Duncan and Wright, 2005, Rocscience, 2006). At this stage, the calculation becomes a trial and error procedure because the objective is to identify the slip surface with the lowest FOS, thus, multiple surfaces have to be assumed (Rocscience, 2006).

The slip surface that yields the minimum FOS, also referred to as the critical slip surface, would represent the most probable sliding surface through which the slope would fail, however, this might not be the case. Additionally, the slip surface is generally assumed to be of circular shape and with constant FOS along it.

3.5 The Limit equilibrium method (LEM)

The limit equilibrium method of slices is the most common procedure used to calculate the FOS and the forces acting along the critical slip surface (Krahn, 2003). In this method, the sliding critical slip surface soil mass is divided into a finite number of vertical slices and calculations of the static equilibrium of forces (acting in the horizontal direction) and equilibrium of moments are performed for each slice (Duncan, 1996; Fredlund and Krahn, 1977; Rocscience, 2006). The forces acting on a typical slice are presented in Figure 3-1.

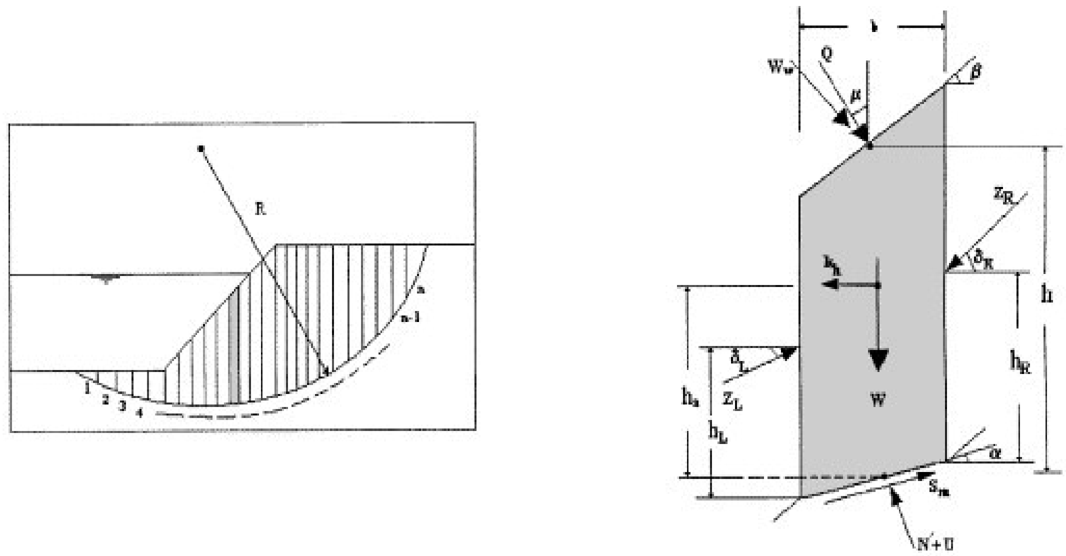

F = factor of safety.
S_m = mobilized shear strength.

$$S_m = \frac{c'.b + N'\tan\phi}{F}$$

U = pore water pressure.
W = weight of slice.
W_w = surface water force.
Q = external surcharge.
N' = effective normal force
K_h = horizontal seismic coefficient.
μ = Angle of inclination of external load.

Z_L = left inter-slice force.
Z_R = right inter-slice force.
δ_L = left inter-slice force inclination angle.
δ_R = right inter-slice force inclination angle.
H_L = height of force Z_L.
H_R = height of force Z_R.
α = Inclination of slice base.
β = Inclination of slice top.
b = width of the slice.
h = average height of the slice.
h_a = height to the center of the slice.

Figure 3-1 Forces acting on a typical slice – LEM (Malkawi et al., 2000)

Different approaches have been developed to offer solutions to the method of slices (Duncan, 1996; Fredlund and Krahn, 1977; Rocscience, 2006). Each approach makes specific assumptions about the interslice forces, the shape and location of the critical slip surface, and the equations of statics that are satisfied in the FOS formulations (Duncan and Wright, 2005).

Common limit equilibrium methods used to calculate the FOS and the static equilibrium conditions that each one of them assumes are presented in Table 3-1. The considerations about the the characteristics and relationships between normal (E) and shear (X) interslice forces adopted by each method are listed in Table 3-2.

Table 3-1 Equations of statics satisfied by different LEMs (Rocscience, 2006)

Method	Moment Equilibrium	Force Equilibrium
Ordinary or Fellenius	Yes	No
Bishop's Simplified	Yes	No
Janbu's Simplified	No	Yes
Spencer	Yes	Yes
Morgenstern-Price	Yes	Yes
Corps of Engineers -1	No	Yes
Corps of Engineers - 2	No	Yes
Lowe-Karafiath	No	Yes
Janbu Generalized	Yes (by slice)	Yes
Sarma-vertical slices	Yes	Yes

Table 3-2 Assumptions about Interslice force characteristics and relationship (Rocscience, 2006)

Method	Interslice Normal (E)	Interslice Shear (X)	Inclination of X/E resultant, and X-E relationship
Ordinary or Fellenius	No	No	No interslice forces
Bishop's Simplified	Yes	No	Horizontal
Janbu's Simplified	Yes	No	Horizontal
Spencer	Yes	Yes	Constant
Morgenstern-Price	Yes	Yes	Variable; user function
Corps of Engineers -1	Yes	Yes	Inclination of a line from crest
Corps of Engineers - 2	Yes	Yes	Inclination of ground surface at top of slice
Lowe-Karafiath	Yes	Yes	Average of ground surface and slice base inclination
Janbu Generalized	Yes	Yes	Applied line of thrust and moment equilibrium of slice
Sarma-vertical slices	Yes	Yes	$X=c+ E \tan \phi$

LEMs are generally classified into two main categories: non-rigorous and rigorous methods (Cheng and Lau, 2008). As can be concluded from Tables 3-1 and 3-2, in non rigorous methods either force or moment equilibrium is satisfied but not both at the same time, whereas in rigorous methods both force and moment equilibrium are satisfied (Rocscience, 2006). In order to better understand the implications of conducting stability analyses using simplified or rigorous LEMs on the FOS, a brief description of the governing equations of the two limit equilibrium methods used in this thesis, namely, the Ordinary-Fellenius method (simplified) and the Morgenstern-Price method (rigorous) is provided below. It is expected that the stability analysis of a TSF will yield different values due to the different assumptions and equations that each method uses.

3.5.1 The Ordinary - Fellenius (O-F) method

According Fredlund and Krahn (1977), Cheng and Lau (2008), Duncan (1996) and Krahn (2003), the Ordinary-Fellenius (O-F) method is considered the simplest of the methods of slices because is the only method that assumes a linear equation of the factor of safety. In this method, a circular slip surface is assumed and the inter-slice forces are considered parallel to the base of each slice. Furthermore, the O-F method only satisfies moment equilibrium equations of statics (Duncan and Wright, 2005; Fredlund, 1984; Hammanh et al., 2009; Rocscience, 2006). In the O-F method, the orthogonal base normal force is used to compute the available shear strength and the weight is the gravitational driving force parallel to the slice base (Rocscience, 2006). In the O-F method, the FOS is defined as the ratio of the summation of the available shear resistance along the critical slip surface to the summation of the mobilized shear as shown in Equation 3-8:

$$FOS = \frac{\sum\left[c'\beta + N\tan\phi'\right]}{\sum W\sin\alpha} \tag{3- 8}$$

where c´ the effective cohesion, β is the slice base length, N is the base normal (Wcosα), ϕ´ is the effective friction angle, W is the slice weight, and α is the slice base inclination. Chang and Duncan (1983) concluded that the O-F method of slices is less accurate than any other LEM; Fredlund and Krahn (1977) found that because the O-F method neglects interslice force, calculations of the FOS with this method can bear errors as high as 60%.

3.5.2 The Morgenstern – Price (M-P) method

The Morgenstern – Price (M-P) method is a rigorous LEM that satisfies both moment and force equilibrium. This method assumes a range of interslice shear-normal force conditions. The FOS is calculated using two equations: one with respect to moment equilibrium (F_m) and the second one with respect to horizontal force equilibrium (F_f) as shown in Equations 3-9 and 3-10:

$$F_m = \frac{\sum\left(c'\beta R + (N-u)R\tan\phi'\right)}{\sum Wx - \sum Nf \pm \sum Dd} \tag{3- 9}$$

$$F_f = \frac{\sum\left(c'\beta\cos\alpha + (N-u\beta)\tan\phi'\cos\alpha\right)}{\sum N\sin\alpha - \sum D\cos\omega} \tag{3- 10}$$

where c′ and ϕ′ are the effective cohesion and friction angle respectively; *β, R, x , f , d* and *ω* are geometric parameters; *u* is the pore water pressure, N is the base normal, W is the slice weight, and α is the slice base inclination (Rocscience, 2006). The M-P method assumes that the shear forces between slices are related to the normal forces as follows:

$$X = E\lambda f(x) \tag{3- 11}$$

where *f(x)* is an assumed function that prescribes values at each slice boundary; λ is an unknown scaling factor (a percentage) of the *f(x)* function assmumed; E is the interslice normal force, and X is the interslice shear force. Another key variable for both moment and force equilibrim FOS is the slice base normal force (N). This force is defined as:

$$N = \frac{W + \left(X_R - X_L\right) - \dfrac{c'\beta\sin\alpha + u\beta\sin\alpha\tan\phi'}{F}}{\cos\alpha + \dfrac{\sin\alpha\tan\phi'}{F}} \tag{3- 12}$$

where, F is either F_m or F_f when substituted into the corredpondent factor of safety equation, and X_R and X_L are the interslice shear forces on the right and left side of a slice (Rocscience, 2006). Krahn (2003) concluded that the rugurosity of the M-P method yield more reliable FOS.

3.5.3 Limtations of the LEM approach for slope stability analysis of TSF

The main limitation of limit equilibrium method is that it does not warrant full understanding of the behaviour of TSFs because the stress-deformation constitutive relationships that ensure displacement compatibility are neglected (Rocscience, 2006; Hamade et al., 2011; Duncan, 1996). According to Rocscience (2006), Krahn (2003), and Duncan (1996), the LEM is based purely on principles of statics, that is, sumation of moments and forces, but it does not take into consideration other fundamental phenomenena inherent to slope stability analyses. Another limitation is that LEMs rely on assumptions about the location, the shape, the failure mechanism, and the forces acting on the potential sliding mass. These assumptions require trial and error processes to ensure the calculation of a realistic minimum factor of safety.

Aditionally, the LEM, as well as any other stability analysis method based on the determinisitc approach, neglects the intrinsc variability of the material properties of the case study. This limitation adds subjetivity to the method because the practitioner's decisions are based on results that bear great uncertainy.

3.6 Finite Element Method - Shear Reduction Technique (FEM-SRT)

The Shear Reduction Technique (SRT) is a deterministic method used to conduct two-dimensional plane strain nonlinear slope stability analyses based on the Finite Element Method (Duncan, 1996; Griffiths and Lane, 1999; Matsui and San, 1992). The SRT, which according to Griffiths and Lane (1999) was first proposed by Zienkiewicz, et al., in 1975, uses the stress-strain analysis approach to identify the zones within a discrete soil mass in which the soil shear strength is unable to resist the applied stress and fails naturally (Rocscience, 2007). The prediction of the zones of critical shear strength reduction is accompanied by simultaneous estimation of displacement and deformation processes taking place within the facility. One fundamental characteristic of the stress-strain computations achieved with the SRT is that no assumptions about the probable failure mechanism, shape and/or location of the failure plane of the soil mass are required (Duncan, 1996; Griffiths and Lane, 1999).

In the SRT method, the effective shear strength parameters (c´ and ϕ´) are progressively divided by a reduction factor until a point of non convergence occurs (Duncan, 1996). The factor at which this convergence happens is called the Shear Reduction Factor (SRF). The reduced strength parameters are defined in Equations 3-13 to 3-16 (Duncan, 1996; Griffiths and Lane, 1999; Rocscience, 2007):

$$\frac{\tau}{SRF} = \frac{c'}{SRF} + \frac{\tan\phi'}{SRF} \qquad \textbf{(3- 13)}$$

$$\frac{\tau}{SRF} = c^* + \tan\phi^* \qquad \textbf{(3- 14)}$$

$$c^* = \frac{c'}{SRF} \qquad \textbf{(3- 15)}$$

$$\phi^* = \tan^{-1}\frac{(\tan\phi')}{SRF} \qquad \textbf{(3- 16)}$$

where c* and ϕ* are reduced Mohr-Coulomb shear strength parameters and SRF is the shear reduction factor equivalent to the FOS in LEM analyses. Griffiths and Lane (1999) explained that in FEM analysis using the SRT, non-convergence of the model is an indicator of slope failure. Therefore, the SRF is considered the equivalent to the factor of safety in limit equilibrium analyses. The SRT can be used both for static and pseudo-static stability analyses using the deterministic or the probabilistic approaches (Xu and Low, 2006).

3.6.1 Elastic properties of materials for the SRT analysis

Slope stability analyses with the SRT require the elastic properties of tailings, e.g., Young's modulus (E), Poisson's ratio (ν), and the dilation angle (ψ) are fundamental input parameters to conduct SRT stability analyses (Rocscience, 2007). These properties, which can be obtained from the triaxial shear tests, govern the stress-strain relations of the materials prior to or during failure (Duncan, 1996; Griffiths and Lane, 1999; Hammah et al., 2004; Rocscience, 2007). Hammah et al., (2004) concluded that the elastic properties influence the magnitudes of computed deformations; hence, right estimates of these properties are required. Furthermore, Rocscience (2007) found that for models with multiple materials the ratios of the different Young's modulus can affect the deformation patterns and produce failure mechanisms that differ from limit equilibrium solutions. This means that when comparing the LEM and the SRT, although the factor of safety can be very similar, the failure mechanisms differ if deformation analyses are included in the model (Rocscience, 2007).

The dilation angle (ψ), for example, controls the amount of plastic volumetric strain developed during plastic shearing and it is assumed constant during plastic yielding (Craig, 2004). Clayey materials are characterized by a very low amount of dilation (Rocscience 2007), and in sand materials, the angle of dilation depends on the angle of internal friction. For non-cohesive soils friction angle $\phi > 30°$, the dilation angle can be estimated as $\psi = \phi - 30°$ (Bardet, 1997; Rajapakse, 2008). According to Rocscience (2007), for materials following a Mohr-Coulomb failure criterion, dilatancy varies between zero (for materials with non-associative flow rule) and the friction angle (for materials with associative flow rule).

Griffiths and Lane (1999) found that the dilation angle does not have a significant impact in slope stability analyses. Chang and Huang (2005), concluded that the elastic properties of tailings have little influence on the prediction of safety factors calculated with SRT approach. For instance, Griffiths and Lane (1999) and Chang and Huang (2005), concluded that the shear strenght properties govern slope stability in the SRT analysis. For the purpose of this thesis, the elastic properties of the materials were taken into consideration for slope stability analyses with the SRT.

3.6.2 Displacements and deformation in the SRT

Tailings, similarly than soils, deform from its initial to final position when subjected to external loads or internal forces (Chang and Huang, 2005). Strains are defined by assuming that tailings are continuous materials. Figure 3-2 depicts the initial and final position of element OACB to O"A"C"B" due to deformation processes (Bardet, 1997).

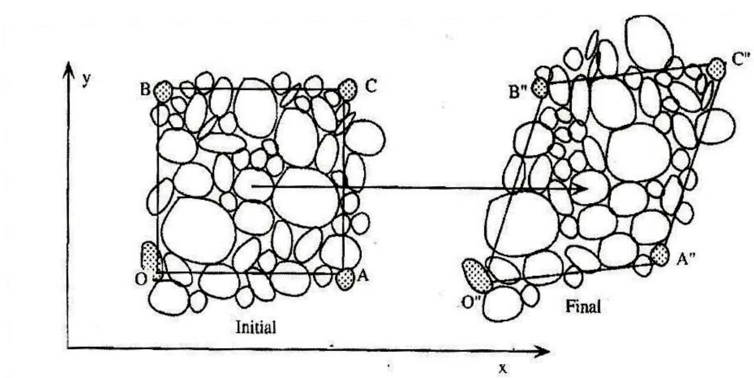

Figure 3-2 Deformation of a soil element from initial to final position (Bardet, 1997)

Bardet (1997) indicated that the displacement of point O from its initial position (x,y) is characterized by the displacement vector (u, v). The components of u and v are assumed to be continuous functions of x and y. As a result, u and v could be approximated by using Taylor expansions in the proximity of point O:

$$u(x+dx, y+dy) = u(x,y) + \frac{\partial u}{\partial x}(x,y)dx + \frac{\partial u}{\partial x}(x,t)dy + ... \quad \textbf{(3- 17)}$$

$$v(x+dx, y+dy) = v(x,y) + \frac{\partial v}{\partial x}(x,y)dx + \frac{\partial v}{\partial x}(x,t)dy + ... \quad \textbf{(3- 18)}$$

The coordinates of the displacement vectors of points A, B, and C may be calculated using the above equations and their positions relative to point O as presented in Table 3-3.

Table 3-3 Coordinates of initial positions of points O, A ,B, and C and coordinates of their displacement (Bardet, 1997).

	Initial position		Final position	Displacement	
Point	**x**	**y**	**point**	**X**	**Y**
O	**x**	**y**	**O”**	**U**	**v**
A	x + dx	y	A”	$u+\frac{\partial u}{\partial x}dx$	$v+\frac{\partial v}{\partial x}dx$
B	x	y + dy	B”	$u+\frac{\partial u}{\partial y}dy$	$v+\frac{\partial v}{\partial y}dy$
C	x + dx	y + dy	C”	$u+\frac{\partial u}{\partial x}dx+\frac{\partial u}{\partial y}dy$	$v+\frac{\partial v}{\partial x}dx+\frac{\partial v}{\partial y}dy$

The element O”A”C”B” is obtained by translating OACB without deforming or rotating it. The displacement of O, A, B and C is shown in Figure 3-3

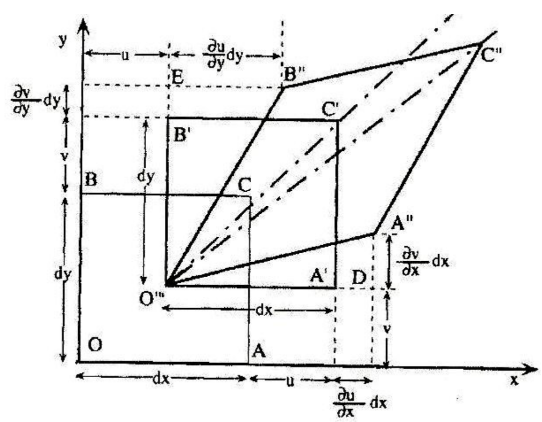

Figure 3-3 Infinitesimal displacement of points A, B, and C neighbors of O (Bardet, 1997).

3.6.3 Shear strain

As shown in Figure 19, the rotation of points OA and OB are equal to the angles $\overline{A'O''A''}$ and $\overline{B'O''B''}$, respectively. $\overline{A'O''A''}$ can be approximated by using the following equation proposed by Bardet, (1997). The shear strain is represented by the term ε_{xy}:

$$\overline{A'O''A''} \approx \tan\left(\overline{A'O''A''}\right) = \frac{\frac{\partial v}{\partial x}dx}{dx+\frac{\partial u}{\partial x}dx} \approx \frac{\partial v}{\partial x} \qquad \textbf{(3- 19)}$$

where $\left|\partial u / \partial x\right|$ is much smaller than 1

$$\overline{B'O"B"} \approx \tan\left(\overline{B'O"B"}\right) = \frac{\frac{\partial u}{\partial y}dy}{dy + \frac{\partial u}{\partial y}dy} \approx \frac{\partial u}{\partial y} \quad \textbf{(3- 20)}$$

where $\left|\partial v / \partial y\right|$ is much smaller than 1. The angular distortion of $\overline{AOB}$ is

$$\overline{AOB} - \overline{A"O"B"} = \frac{\partial u}{\partial y} + \frac{\partial v}{\partial x} = -2\varepsilon_{xy} \quad \textbf{(3- 21)}$$

Most SRT software produce displacement, stress distribution, and deformation plots contouring that allow for the visualization of plastic zones development with respect to stress levels (Rocscience, 2007; Chang and Huang, 2005). Vick (1983) reported similarity between the stress-strain behaviour of tailings and natural soils of the same gradation. Studies by Chang and Huang, (2005), Hamade et al., (2011), and Rocscience (2007) obtained good agreement between LEM and SRT stability analyses in which elastic-perfectly plastic constitutive relationship was assumed.

Figure 3-4a shows and idealized elastic-perfectly plastic constitutive relation curve versus real elastic-perfectly plastic stress-strain curves of the Merriespruit of gold tailings shown in Figure 3-4b. In Figure 3-4b, point (A) is the elastic region; point be (B) is the yield tensile strength region; point (C) is the plastic region, and point (D) is failure point (Papageorgiou et al., 1999). According to this figure, gold tailing could be approximated to an elastic-perfectly plastic stress-strain behavior (Hammah et al., 2004).

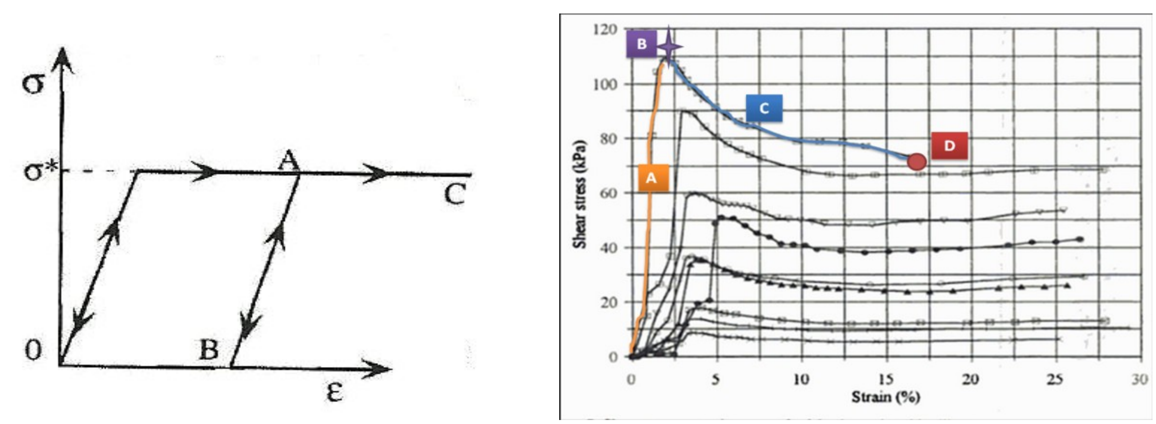

(a) Idealized **(b) Actual, Merriespruit gold tailing**

Figure 3-4 Typical elastic-perfectly plastic stress-strain curve (Bardet, 1997 and Papageorgiou et al., 1999)

A summary of the characteristic of the LEM and FEM-SRT methods for TSF stability analysis is presented in Table 3-4. These criteria were taken into consideration for the model set up and further calculations in the thesis.

Table 3-4 Summary of LEM and the SRT characteristics

Criteria	(LEMs)	(FEM- SRT)
Type of Analysis	Limit state analysis	Stress-strain analysis
Assumptions about the slip surface:		
Interslice forces	Yes	No, no slices required
Shape	Yes	No
Location	Yes	No
Failure state criterion	*Trial and error*. Multiple slip surfaces using simplified and rigorous methods. Compatible with Mohr-Coulomb failure criterion	*Natural.* Failure occurs in zones in which the shear strength is not sufficient to resist shear stress. Compatible with Mohr-Coulomb failure criterion
FOS	Ratio of the sum of resisting forces to the sum of the driving forces	Factor that reduces actual shear strength parameters until no convergence occurs
Prediction of settlement and deformation	No	Yes, depending on software used
Consolidation	No	Yes, depending on software used
Possibility of seismic analysis	Yes	Yes
Possibility of probabilistic analysis	Yes	Yes
Method - Complexity	Low, possibility of hand calculation	Intermediate, specialized software required
Computational time	Short	Significant depending on geometry complexity and mesh quality
Acceptance, use	High , widespread	Moderate, increasing
Reliability of results	Highly conservative. Reliable if more than one LEM (e.g. rigorous) is used to conduct and combined with probabilistic methods	Good. Could be higher if combined with probabilistic methods

3.6.4 Large Strain Method for deformation analyses

The compressibility and permeability of TSFs usually exhibit significant changes when subjected to stress increases due to continuous tailings deposition (Geier et al., 2011). Therefore, the conventional small strain deformation analysis proposed by Terzaghi in 1950 does not completely apply for all tailings stability analyses. Although Darcy's Law is valid for all hydraulic gradients, the soil particles are considered incompressible and compression and flow are considered one-dimensional, the permeability and compressibility do not remain constant throughout the raising process. Geier et al., (2011) presented a large strain analysis based on the Gibson's consolidation method which removes the constraints imposed on the compressibility and permeability relationships by the small strain method. Large strain analysis is beyond the scope of this thesis due to the scope and type of software used for the stability analyses.

3.7 Pseudo-static Analysis

Pseudo-static stability analyses of TSFs are necessary to estimate the effect of seismic forces on the impoundment's factor of safety when all dynamic properties of the system are neglected (James et al., 2011; Liu et al., 2012; Lopez-Caballero et al.,2010). In the pseudo-static analysis the peak ground acceleration is transformed into a pseudo-static inertia force as a horizontal gravity load multiplied by the weight of the sliding mass (Rocscience, 2007). The effect of this load is analyzed instantaneously, hence, time is neglected. In dynamic analyses, on the other hand, the actual earthquake acceleration time history is applied to the system in the form of the peak ground acceleration (Woodward and Griffiths, 1996).

Studies by Baker et al., (2006), Day (2002), Melo and Sharma (2004), and the USAID (2011) concluded that there are different approaches to conduct seismic slope stability analyses: the pseudo-static method, the Newmark sliding block method; the simplified displacements charts, and energy based methods. Baker et al., (2006) and Day (2002) concluded that the pseudo-static approach is the most common procedure employed for standard seismic slope stability evaluation. Day (2002) used the pseudo-static approach to analyze seismic slope stability using conventional limit equilibrium methods.

Basically, the effect of an earthquake is included in the analysis in the form of static horizontal and/or vertical force acting on the centroid of the sliding mass as shown in Figure 3-5.

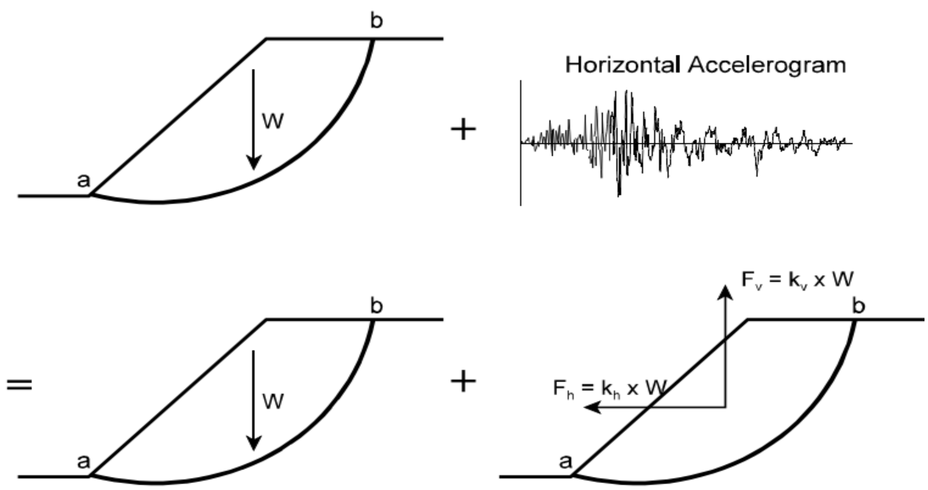

Figure 3-5 Pseudo-static analysis approach for stability analysis (Melo and Sharma, 2004)

The effect of the force on the shear strength can be observed in the reduction of the static factor of safety of the sliding mass (Baker et al., 2006; Melo and Sharma, 2004; USAID, 2011). The horizontal and vertical forces described by Terzaghi (1996) are:

$$F_h = \frac{a_h W}{g} = k_h W \qquad \textbf{(3- 22)}$$

$$F_v = \frac{a_v W}{g} = k_v W \qquad \textbf{(3- 23)}$$

where F_h and F_v are horizontal and vertical pseudo-static forces acting through the centroid of the sliding mass, in an out-of-slope direction in (kN). W is the total weight of sliding mass in (kN); a_h and a_v are the maximum horizontal and vertical acceleration at ground surface that is induced by the earthquake, also referred to as to the Peak Ground Acceleration (PGA) in (m/s^2); k_h and $_kv$ are the horizontal and vertical seismic coefficients, also known as pseudo-static coefficients (dimensionless); g is the earth's gravitational acceleration (9.81 m/s^2). The vertical force (F_v) is usually ignored in the standard pseudo-static analysis because it has much less effect on the stability of a slope (Day, 2002).

Pseudo-static slope stability analyses can be performed using the effective shear strength of the soil (Day, 2002; Duncan and Wright, 2005). Equation 3-24 shows the LEM - pseudo-static factor of safety equation proposed by the USAID (2011):

$$FOS = \frac{\text{Resisting Force}}{\text{Driving Force}} = FOS = \frac{\left[(1-k_v)\cos i - k_h \sin i\right]\tan\phi' + \dfrac{c'}{\gamma' D}}{(1-k_v)\sin i + k_h \cos i} \tag{3- 24}$$

where c′and ϕ′ are Mohr-Coulomb effective shear strength parameters on the failure plane, γ′ is the unit weight of the failure mass, *i* is the angle of the failure plane, K_h is the horizontal seismic coefficient, and D is the failure mass thickness.

3.7.1 The horizontal seismic coefficient (K_h)

The horizontal seismic coefficient increases the driving forces and decreases de resisting force, hence, it is usually the only force used in pseudo-static stability analyses. A general conclusion among researchers is that the selection of the seismic coefficient is the most critical criterion in pseudo-static analyses. An appropriate seismic coefficient will allow for the estimation of meaningful pseudo-static factors of safety (Day, 2002). Table 3-5 presents the summary of approaches for the selection of the horizontal seismic coefficient proposed by Melo and Sharma (2004).

Table 3-5 Recommended Horizontal Seismic Coefficients. (Melo and Sharma, 2004).

Horizontal Seismic Coefficient, K_h	Description and reference
0.05 - 0.15	In the United States (Melo and Sharma, 2004)
0.12 - 0.25	In Japan (Melo and Sharma, 2004)
0.1 “severe” earthquake	Terzaghi in 1950
0.2 “destructive” earthquake	
0.5 “catastrophic” earthquakes	
0.1 - 0.2	(Melo and Sharma, 2004)
0.10 Major Earthquake, FOS > 1.0	(Melo and Sharma, 2004)
0.15 Great Earthquake, FOS > 1.0	
0.5 to 0.33 of PGA/g	FOS > 1.0 (Melo and Sharma, 2004)
0.5 PGA/g	(Hynes-Griffin and Franklin, 1984), FOS > 1.0

Note: PGA = Peak Ground Acceleration in (m/s^2), gravitational acceleration (g) in (m/s^2).

In TSF pseudo-static stability analyses, the regional return period and probability of exceedance of major earthquake events should also be accounted for the horizontal seismic coefficient selection. Aguello et al.,(2003) indicated that the return period and annual exceedance probabilities of a seismic event are site specific.

3.7.2 Annual exceedance probability and return periods

The general and annual exceedance probabilities and the return period are hazard assessment definitions frequently used for pseudo-static analyses of TSFs (Aguello et al.,2003). The general exceedance probability (P_0) is the likelihood that an event will be met or exceeded during a given interval of years.

The annual exceedance probability (P) is the probability that an event level will be met or exceeded during a one-year interval. The return period (or mean recurrence) (T) is defined as the inverse of the annual exceedance probability T=1/P (Earthquakes Canada, 2010). Typical return periods and annual exceedance probabilities considered in this thesis are summarized in Table 3-6.

Table 3-6 Return Periods and annual probability of exceedance in Canada. (Earthquakes Canada, 2010)

General Probability of Exceedance (P_o)	Annual Exceedance Probability (P)	Return Period (T)	Event classification
40%/50 years	0.01	100 years	Frequent
10%/50 years	0.00211	475 years	Intermediate
5%/50 years	0.001	1000 years	Long
2%/50 years	0.000404	2475 years	Long

The MDDEP (2012), recommends a minimum return period of not less than 1:2475 years and a probability of exceedance of 2%/50 years for the mining industry hazard assessment. In the study by Julien et al., (2004) a 1:1000 (5%/50 years) return period for the sesimic analysis of a tailings storage facility in Val d'Or, Quebec for an earthquake of magnitude 6.8 was used. The CDA (2007) recommends 1:1000 years return period for hazard analysis and seismic assessment of dams.

3.7.3 Pseudo-static stability analysis with SRT

In pseudo-static SRT stability analyses the seismic coefficient is considered an additional body force applied to each finite element in the mesh. The seismic body force is vectorially added to the body force which exists due to gravity to obtain the total force acting on the element reduction factor. Pseudo-static analyses with Phase^2 yield contours of the horizontal displacement and maximum shear due to the seismic force applied (Rocscience, 2007). These contours can be associated with the zones of higher seismic liquefaction potential within the TSFs.

3.8 Transient Stability Analysis

Transient slope stability analyses consist on assessing the performance of the system taking into consideration changes in variables and other phenomena as a function of time (Saad, 2008). Transient stability analyses are necessary for TSFs staged-construction stability analyses (Vick, 1983). In this type of analysis, the strength gain and consolidation of the system depends on the time that the constitutive materials and boundary conditions require to drain water out of the system.

Generally, the Undrained Shear Analysis (USA) approach is used to conduct transient stability analyses of TSFs constructed under high rates of raise to analyze the pore pressure distribution and stress states in the system when water drainage occurs very slowly or does not happen at all (Moellmann et al.,2008; Ng and Shi 1998; Priscu, 1999; Saad 2008; Saad and Mitri 2011).

Transient stability analyses of TSF are fundamental in mining engineering because the stability of the facility at each stage of construction governs the ultimate height of the embankment, rate of raise, and expansion plans. Therefore, it should also be performed in combination with static and pseudo static stability analyses. The transient stability analysis is out of the scope of this thesis. In this thesis the interest is to estimate the long-term performance of TSFs due to embankment height increase and changes in phreatic surface location assuming steady state conditions.

3.9 Other common failure mechanisms of TSFs

The most common failure mechanisms observed in TSFs are slope instability, seismic/static liquefaction, foundation failure, flood overtopping, and internal erosion (Azam, 2010; Chambers and Higman, 2011; ICOLD, 1995; Kong et al., 2008; Rico et al., 2008; WISE, 2012). Generally, deficiencies in design and operation, poor site invesitgation, and unusual climatic events are importan triggers for failure.

The main focus of this thesis is static and pseudo-static slope instability due to embankment/ tailings height increase and phreatic surface location in a UTSF and a WRTD. Although, liquefaction and piping failure mechanisms are beyond the scope of this thesis, the concepts were taken into consideration because these two phenomena are the most probable causes or consequences associated with TSFs slope failure.

3.9.1 Liquefaction

Liquefaction is a state in which saturated non-cohesive tailings show very small or no shearing resistance due to pore pressure increase in the embankment. As a result of such strength reduction, tailings start to behave as a frictional fluid (Saad, 2008; Saad and Mitri, 2010; Saad et al., 2011).

Depending on the type of shear loading, tailings can undergo static liquefaction or seismic liquefaction. Liquefaction failure can have catastrophic impacts on the surrounding environment. Large volumes of hazardous materials can be released from the TSF and deposited at far distances from the discharge point causing massive pollution, loss of lives, and monumental economical liabilities for the mining (Lottermoser, 2003).

One of the many causes attributed to tailings liquefaction in UTSFs is high rate of embankment raise. Basically, when the time for pore pressure dissipation is insufficient before and a new raise takes place, the hydrostatic pressure and the phreatic surface increase to the point that shear strength vanishes and liquefaction occur. Poor drainage systems, unusual precipitation, and seismic events are also amongst the main triggers of this dangerous failure mechanism.

3.9.2 Piping

Piping is a phenomenon in which a pipe-shaped discharge channel forms when finer particles from one region of the TSFs move freely into and through the interstitial voids of adjacent coarser soil due to disproportion between particle sizes and under the influence of seepage forces (Terzaghi, et al., 1996). If the seepage velocity is large enough that erosion occurs due to the frictional heave exerted on the soil particles, an upwards seepage gradient is generated and jeopardizes the downstream toe of the tailings dam. In TSFs, piping occurs as a result of installing incompatible filters that allow for migration of particles between zones.

3.10 Deterministic and probabilistic approach for slope stability analyses

TSFs stability analyses are commonly conducted following the deterministic approach. According to Schweiger, et al., (2001) there a two main reasons for this practice: first, insufficient and reliable data from site investigation and/or laboratory testing. The second cause is unfamiliarity with the concepts and calculations behind stochastic analyses. Additionally, stochastic analyses are considered complex and time consuming (Christian, Ladd et al., 1994).

As stated before, in deterministic stability analysis the uncertainties associated with the physical and mechanical properties of the model's constitutive materials are not taken into account. The increasing failure cases of TSFs around the world have arisen concerns about the effectiveness of this approach and the extent to which it can accurately predict the performance of complex facilities that deal with uncertainties of various sources such as TSFs (Duncan 2000, Griffiths, Gordon et al., 2009). Probabilistic stability analyses counterpart the deterministic analyses not only because the variability of the input parameters is used to analyze the performance of the system, but also because additional information about the overall performance of the system is obtained based on stochastic methods. This advantage has made risk-based design of TSF gain significant popularity in the mining industry for conducting slope stability analyses (Christian, Ladd et al., 1994, Duncan 2000, Hamade, Saad et al., 2010).

3.10.1 Probabilistic and deterministic Factor of safety

The deterministic FOS is the ratio of the shear resistance to the shear stress of the system, and it is consider safe if the ratio is equals to or higher than unity. The result is a single value which is then subjected to the practitioner's judgment to determine whether or not it meets design and operational requirements. The probabilistic FOS, on the other hand, is the average value of multiple FOS obtained after treating the critical shear strength parameters as random variables and assigning a probabilistic distribution to each of them. The mean FOS allows for the estimation of the probability of failure (*pf*), and reliability Index (β) of the system. These complementary pieces of information provide better foundation for stability assessment and the decision making phase.

3.10.2 Uncertainty of soil parameters

The intrinsic variability of tailings mechanical and geotechnical properties affects the reliability of the FOS in TSF's stability analyses. Tailings like natural soils are highly variable in their properties and rarely homogenous. According to Griffiths et al., (2009), Hamade et al., (2011), Peterson (1999), and Xu and Low (2006), the uncertainty of tailings properties derives from the variability of milling and mineral processing techniques, sampling and testing methods.

Hamade et al., (2011) indicated that in the past, one approach to deal with the uncertainty in soil parameters was by increasing the value of the design FOS. However, the poor performance exhibited by some TSFs over the years indicates that this approach is inefficient. Thus, there is a need to use both deterministic and probabilistic methods to conduct stability assessment of mining infrastructure.

3.10.3 Probabilistic methods for slope stability analysis

The probabilistic methods most commonly used for slope stability analyses in geotechnical engineering are First Order Second Moment (FOSM), Monte Carlo Simulation, and PEM (Griffiths et al., 2009; Hamade et al., 2011; Peterson, 1999; Xu and Low, 2006).

Studies by Hamade et al., (2011), Wang et al.,(2011), Griffiths et al.,(2009), and Peterson (1999) present case studies of stability analysis in which First Order Second Moment Method (FOSM), Monte Carlo Simulation (MCS), Random Monte Carlo Simulation (RMCS), or the Point Estimate Method (PEM) are used for stability and risk assessment.

According to U.S. Army Corps of Engineers (1997), the first step in most probabilistic stability analyses is to characterize the model's random variables. The model's random variables are the parameters with the highest uncertainty and that may have the highest effect on the overall stability of the impoundment (Hamade et al., 2011).

Generally, the shear strength parameters are assumed as random variables in TSFs stability analyses (Griffiths et al., 2009; Peterson, 1999). Instead of having precise single values, random variables generally fluctuate along a range of values in conformity with a probability density function (Peterson, 1999) and the minimum and maximum values that the variable can possibly have. The best way to identify random variables is to conduct sensitivity analyses (Hamade et al., 2011).

The selection of the random variables and probabilistic distribution is followed by the assumption of their probabilistic moments. The probabilistic moments generally required for slope stability analyses are the mean value, the variance, standard deviation, and coefficient of variation (Griffiths et al., 2009; Hamade et al., 2011; Peterson, 1999; Kim and Sitar 2013). When the random variables are dependent, other probabilistic moments are required for the analysis (Griffiths et al., 2009; Hamade et al., 2011). A brief definition of these probabilistic moments is provided.

- **The Mean value (μ) or expected value** of a set of N measured values for the random variable X is obtained by summing the values and dividing by N. Similarly, the expected value of a random variable is the summation of mean value of all possible values of the random variable multiplied by its probability of occurrence (Haldar, 2000) as shown in Equation 3-25:

$$\mu_x = \frac{\sum_{i=1}^{N} X_i}{N} \quad \textbf{or} \quad E[X] = \mu_X \int Xf(X)dx = \sum p_X(X_i) \qquad \textbf{(3- 25)}$$

where $f(X)$is the probability density function of X for continuous random variables and p(X) is the probability of the value Xi for discrete random variables. The mean and expected value of a random variable are numerically considered the same (U.S. Army Corps of Engineers,1997; Haldar 2000).

- **The variance** of a random variable X, Var [X] is the expected value of the squared difference between the random variable and its mean value (Haldar, 2000). The variance of the data can be calculated by subtracting each value from the mean, squaring the result, and determining the average of these values (U.S. Army Corps of Engineers, 1997; Haldar, 2000):

$$Var\left[X\right]=\frac{\sum\left[\left(X_i-\mu_x\right)^2\right]}{N-1} \tag{3- 26}$$

- **The Standard deviation (σ_x)** determines the dispersion of a random variable about its mean value (U.S. Army Corps of Engineers,1997; Haldar, 2000). It is expressed in the same units as the random variable. The standard deviation is calculated taking the square root of the variance:

$$\sigma=\sqrt{Var\left[X\right]} \tag{3- 27}$$

- **The Coefficient of variation (COV)** is an expression of the uncertainty inherent in a random variable. It is usually expressed in percentage and is calculated by dividing the standard deviation by the expected value of the random variable (U.S. Army Corps of Engineers,1997; Haldar,2000; Hamade et al., 2011; Kim and Sitar, 2013).

$$COV_X=\frac{\sigma_X}{\mu_X}x100\% \tag{3- 28}$$

- **Covariance (CovX,Y) and Correlation coefficient (ρ):** when the random variables are correlated, the likelihood of a certain value of the random variable Y depends on the value of the random variable X (U.S. Army Corps of Engineers, 1997). The correlation coefficient may assume values from -1.0 to +1.0. A value of 1.0 or -1.0 indicates there is perfect linear correlation (Rocscience, 2006); given a value of X, the value of Y is known and hence is not random.

A value of zero indicates no linear correlation between variables (U.S. Army Corps of Engineers, 1997) . A positive value indicates the variables increase and decrease together; a negative value indicates that one variable decreases as the other increases.

$$Cov\left[X,Y\right]=\iint\left(X-\mu_X\right)\left(Y-\mu_Y\right)f(X,Y)dYdX \quad \textbf{or} \tag{3- 29}$$

$$Cov\left[X,Y\right]=\frac{1}{N}\sum(X_i-\mu_X)(Y_i-\mu_Y) \tag{3- 30}$$

$$\rho_{XY}=\frac{Cov[X,Y]}{\sigma_X\sigma_Y} \tag{3- 31}$$

3.10.4 Probability Distributions

The probability distribution refers to the function that defines a continuous random variable. The normal and the lognormal distribution are generally used to describe slope stability random variables (Smith 1986; Hamade et al., 2011; Peterson, 1999; U.S. Army Corps of Engineers, 1997). The Probability Density Function (PDF) of a random variable with normal or lognormal distribution can be calculated using equations 3-32 or 3-33, respectively:

$$f(X)_{normal}=\frac{1}{\sqrt{2\pi}*\sigma_X}e^{\left[-\frac{(X_i-\mu_X)^2}{2\sigma^2{}_X}\right]} \tag{3- 32}$$

$$f(X)_{\log normal}=\frac{1}{X\sigma_X\sqrt{2\pi}}e^{\left[-\frac{1}{2}\left(\frac{(\ln X-\mu_X)^2}{\sigma_X}\right)\right]} \tag{3- 33}$$

The U.S. Army Corps of Engineers (1997) indicated that the normal distribution is commonly assumed to characterize many random variables where the coefficient of variation is less than about 30%. Hamade et al., (2011) and Cao et al., (2011) conducted TSFs probabilistic stability analyses using normal and lognormal distributions for the random variables. The cumulative distribution function CDF or FX(X) measures the integral of the probability density function from minus infinity to X. For any value X, *f(X)* is the probability that the X random variable X is less than the given x as shown in Equation 3-34:

$$F_X(X)=\int_{-\infty}^{X}f_X(X)dX \tag{3- 34}$$

3.10.5 Monte Carlo Simulation (MCS)

The Monte Carlo simulation (MCS) involves the computation of deterministic solutions for a number of systematically generated realizations. The resulting set of solutions is analyzed statistically to estimate the mean, variance, standard deviation, and PDF of the random variables. After a probability distribution has been assigned, a random trial process is initiated for a fixed number of runs.

During each run, a random value is selected and entered into the calculation. Numerous solutions are obtained until a solution that matches the mean value and standard deviation of the variable of interest is found. The higher the number of runs applied to the model, the higher the reliability of the approximation to the performance of the system. The final result of a Monte Carlo simulation is a probability distribution of the parameter of interest.

The reliability index (β) and the probability of failure (p_f) are then calculated using the probability distribution. For slope stability analysis, the MCS can be conducted through any limit equilibrium method. In this case, spreadsheets can be used to conduct the random variables runs and manually feed the outputs into the LEM software, or by using LEM software with integrated probabilistic features.

3.10.6 Point Estimate Method (PEM)

In the PEM the deterministic value of the most critical random variable is replaced by a set of discrete points located plus or minus one standard deviation from the mean value (Rosenblueth, 1975) assuming that the random variables fit into a normal distribution (Rocscience, 2007). All possible solutions are calculated according to the 2^n condition, where n is the number of random variables as shown in Figure 3-6.

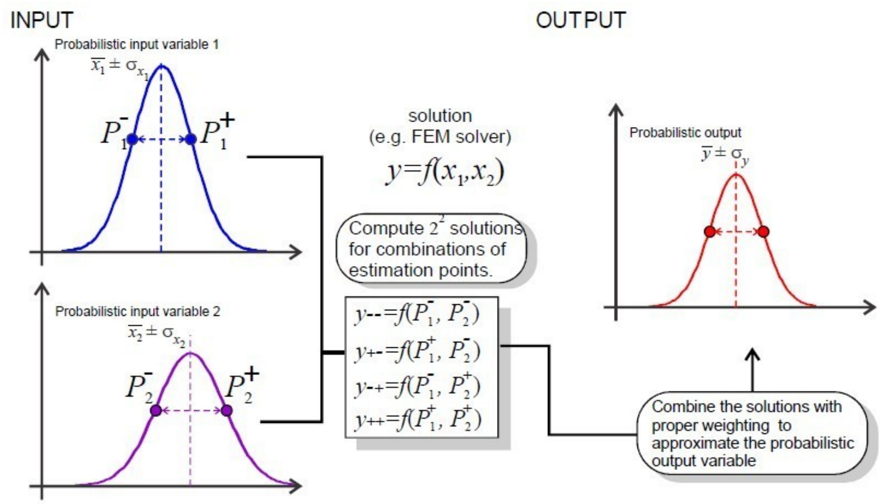

Figure 3-6 Principle of point estimate method assuming two random variables (Rocscience, 2007).

Figure 3-6 showns the procedure for two points or random variables. Rosenblueth (1975) used the following notation (Hamade et al., 2011):

$$E\left[Y^m\right] \approx P_+ y_+^m + P_- y_-^m \tag{3- 35}$$

Where:

Y is a deterministic function of X, Y = g(X), $E[Y^m]$ is the expected value of Y raised to the power m, y+ is the value of Y evaluated at a point x, which is greater than the mean, μ_X, y- is the value of Y evaluated at a point x^-, which is less than μ_X, and P^+, P^- are eights; and the problem then reduces to finding the appropriate values of x^+, x^-, P^+, and P^-

3.10.7 Probability of failure (p_f)

The stability of a TSF can be described by a limit-state function, *g(x)*, such that failure is defined when the condition *g(x)* ≤ 0 is satisfied, and x is the vector of the model's random variables (Villavicencio et al., 2010). The probability of failure is then given by:

$$p_f = P(g(x) \le 0) = \int_{g(x)\le 0} f(x)dx \tag{3- 36}$$

where *f(x)* is the joint PDF of x. Once the limit-state function g(x) and the distribution *f(x)* are selected, the probability of failure p_f can be estimated by computing the joint distribution *f(x)* within the failure domain defined by g(x) ≤ 0 (Kim and Sitar 2013; Villavicencio et al., 2010; Hassan et al., 2000).

If a normal distribution is selected, the probability of failure and reliability index can be calculated using Equation 3-37.

$$pf = 1 - \Phi\beta \tag{3- 37}$$

where Φ is the standard normal cumulative distribution function and β is the reliability index (Rocscience, 2007; Hammah and Yacoub, 2009)

3.10.8 Reliability index (β)

The mean value and standard deviation of the FOS obtained through probabilistic methods can be used to calculate the reliability index of the TSFs (Hassan et al., 2000; Wang, 2009). Depending on the probabilistic distribution that had been assigned to the FOS, the reliability index can be calculated using one of the following expressions (Rocscience, 2006 and 2007):

$$\beta_{(Normal)} = \frac{\mu_X - 1}{\sigma_X} \tag{3- 38}$$

$$\beta_{(Lognormal)} = \frac{\ln\left[\frac{\mu_X}{\sqrt{1+COV_X{}^2}}\right]}{\sqrt{\ln(1+COV_X{}^2)}} \tag{3- 39}$$

The expected level of performance of a TSF can be analyzed through the value of probability of failure and reliability index obtained in a probabilistic stability analysis as shown in Table 3-7.

Table 3-7 Relationship between reliability index (β) and probability of failure (p_f) (U.S. Army Corps of Engineers, 1997 and Wang, 2009):

Reliability Index (β)	Probability of Failure (p_f)	Expected level of performance
1.0	0.16	Hazardous
1.5	0.07	Unsatisfactory
2.0	0.023	Poor
2.5	0.006	Below average
3.0	0.001	Average
4.0	0.00003	Good
5.0	0.0000003	High

CHAPTER 4: METHODOLOGY AND NUMERICAL MODELLING

The stability analyses of the Upstream Tailings Storage Facility (UTSF) are based on the geometry and material properties presented by Saad and Mitri (2011) and Saad (2008). The stability analyses of the WRTD are based on the geometry and material properties presented by Hamade et al., (2011). In this section, a full description of the assumption, methodology, and additional design criteria considered to conduct the analyses of this thesis are provided. First, the design parameters and analytical criteria applicable for both TSFs are presented. Then, the particular considerations of each TSF are provided.

4.1 Design parameters and assumptions for the stability analyses

4.1.1 Tailings properties and site location

The studies by Saad (2008) and Hamade et al., (2011) were conducted for impoundments storing gold tailings materials. Figure 4-1 shows the grain size distribution of the mill tailings common to both types of dams.

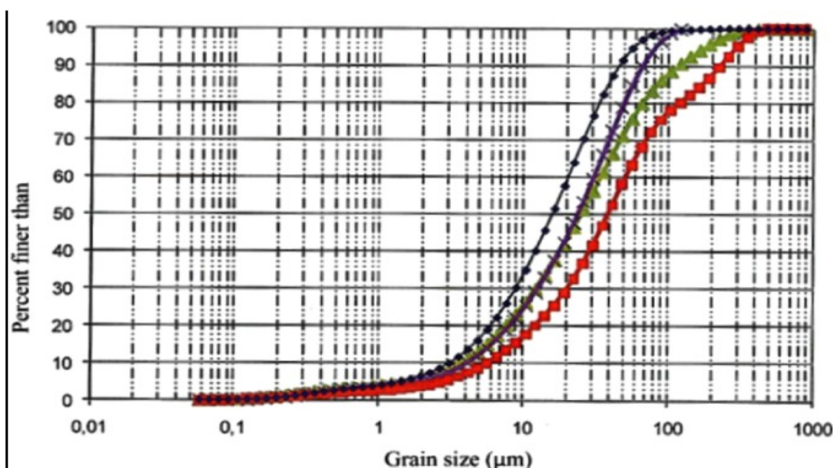

Figure 4-1 Grain size distribution of gold tailings adopted for the study (Hamade et al., 2011)

Saad (2008) and Hamade et al., (2011) indicated that gold tailings are classified as cohesionless non-plastic silts (USCS classification ML). Mill tailings are considered as normally consolidated and with high liquefaction potential.

The results of the grain size distribution presented by Hamade et al., (2011) and other mechanical properties of the mill gold tailings used for the UTSF and WRTD stability analyses are summarized in Table 4-1.

Table 4-1 Summary of mill tailings mechanical properties for the WRTD and UTSF. (Saad, 2008 and Hamade et al., 2011)

Property	Units	Value / Description
Clay size particles (<2μm)	%	5.3
Sand content (>0.06 mm)	%	33.3
Fines content (<74μm)	%	61.4
D10	μm	5
D30	μm	19
D50	μm	44.8
D60	μm	54
Specific Gravity (GS)	-	3.17
Average Void Ratio (e)	-	1.15
Max void ratio (emax)	-	0.72 to 1.23
Min void ratio (emin)	-	0.51 to 0.68
Saturation upon deposition (S)	%	100
Porosity (n)	-	0.5 to 0.53
Liquid Limit (LL)	%	-
Plasticity Index (PI)	%	-
Shrinkage Limit	%	21.6
Relative Density	%	30 to 50
γ_{sat}	kN/m^3	16 to 20
γ_{dry}	kN/m^3	13.5 14.7
Effective cohesion (c′)	kPa	0
Effective friction angle (φ′)	deg	20 to 30
Consolidation Pressure	kPa	20-25
Permeability	m/s	$1x10^{-6}$ to $1x10^{-7}$
Tailings permeability ratio k_h/k_v	Anisotropic	10

Based on the description and mechanical properties of the tailings materials obtained from Saad (2008) and Hamade et al., (2011), and with the need to determine a site location to assign realistic seismic coefficients into the stability analyses, the TSFs were assumed to be located in the city of Val d'Or, in the province of Quebec, Canada.

Figure 4-2 shows the location of the region assumed as mine site location in relation with the active gold mining operations in the province of Quebec as of September, 2012.

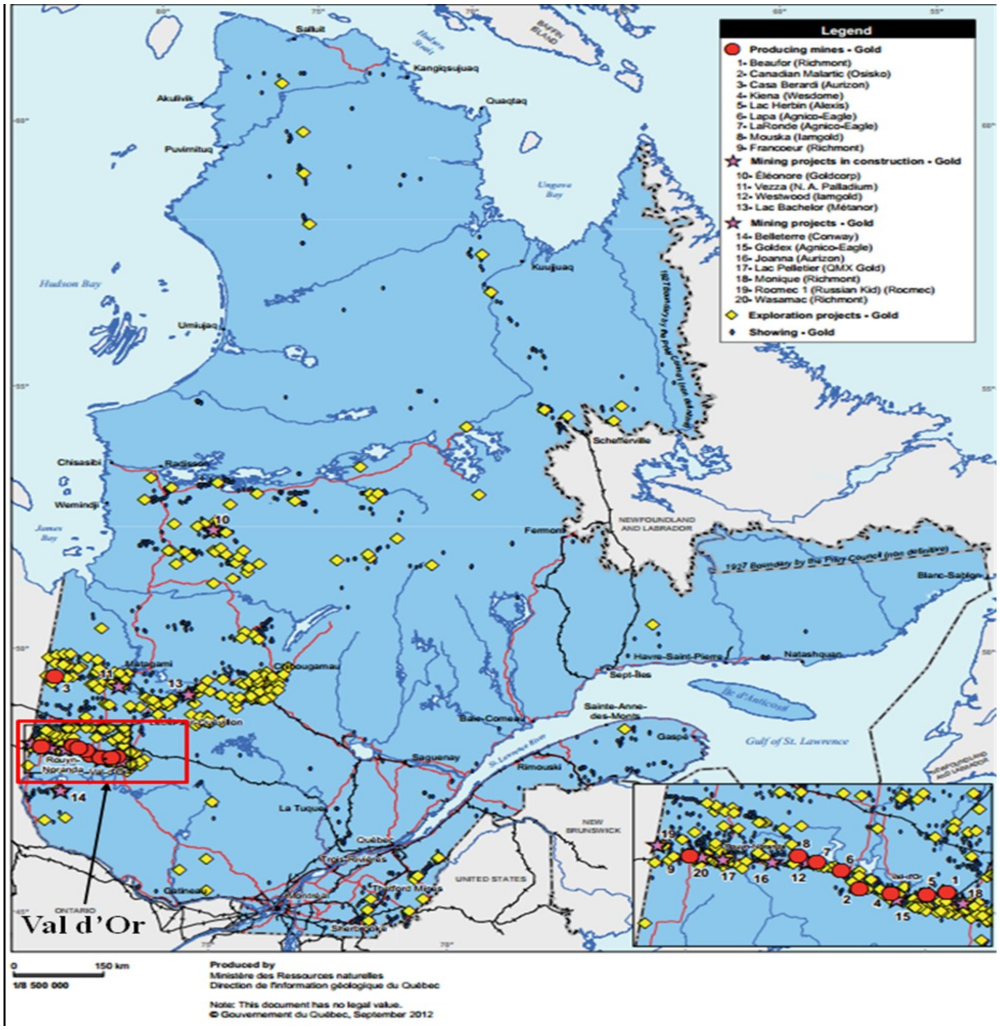

Figure 4-2 Major Gold Mining projects in the province of Quebec, Canada (Ressources Naturelles et Faune, 2012).

As shown in Figure 4-2, the largest gold mining operations in the province of Quebec (represented by the red circles on the map) are located in Val d'Or. By selecting this location for the UTSF and WRTD, the minimum TSFs stability design criteria and mining regulations applicable to this jurisdiction were adopted. For instance, the stability analyses presented in this thesis are based on the regulations and guidelines by the Ministère du Développement durable (2012), CDA (2007); CGS (2007); Environment Canada (2009); Environment Canada (2011), MAC, (1998); NRC (2010), and Earthquakes Canada (2010).

4.1.2 Climate and Seismic coefficients considerations

In a study by Camus and Duplessis (2012), the climate in Val d'Or, Québec is described as relatively dry, with cold winters and hot summers. The average annual precipitation in Val-d'Or is 954 mm. Rainfall is highest in September; averaging 103 mm. Snowfall is registered from late September to early May, with a peak period between November and March when the monthly average reaches 54 cm (Camus and Duplessis, 2012). The climate information was taken into consideration to decide whether a steady state analysis was reasonable for this region, the loading condition, and the assumptions made for the stability analyses. The seismic coefficients of this region were retrieved from the National Building Code Seismic Hazard Calculation system (Earthquakes Canada, 2010) by providing the position coordinates of the city of Val d'Or (48°05′51″N 77°46′26″W). The data obtained from this information system is presented in Table 4-2.

Table 4-2 Summary of Seismic Hazard parameters for Val d'Or Quebec (Earthquakes Canada, 2010 and Gouvernement du Quebec, 2002)

Probability of Exceedance	Return Period	Peak Ground Acceleration (g)	Horizontal Seismic Coefficient Kh
40%/50 years (0.01 per annum)	100 years	0.013 g	0.0065
10%/50 years (0.0021 per annum)	475 years	0.033 g	0.0165
5%/50 years (0.001 per annum)	1000 years	0.049 g	0.0245
2%/50 years (0.000404 per annum)	2475 years	0.076 g	0.038
Regional Seismic Coefficient after Centre d'expertise Hydrique, Quebec, 2002			0.05
Assumed worst case scenario, due to proximity to a high seismicity zones (e.g. Seismic Zones 3 and 4)			0.1

The seismic coefficients assumed are in good agreement with the seismic coefficients found in the literature review and correspond to the minimum return periods and exceedance probabilities indicated in regulations and guidelines for pseudo-static slope stability assessment.

The information obtained from Seismic Hazard Calculation system (Earthquakes Canada, 2010) was compared to the seismic zones map of the province of Quebec shown in Figure 4-3.

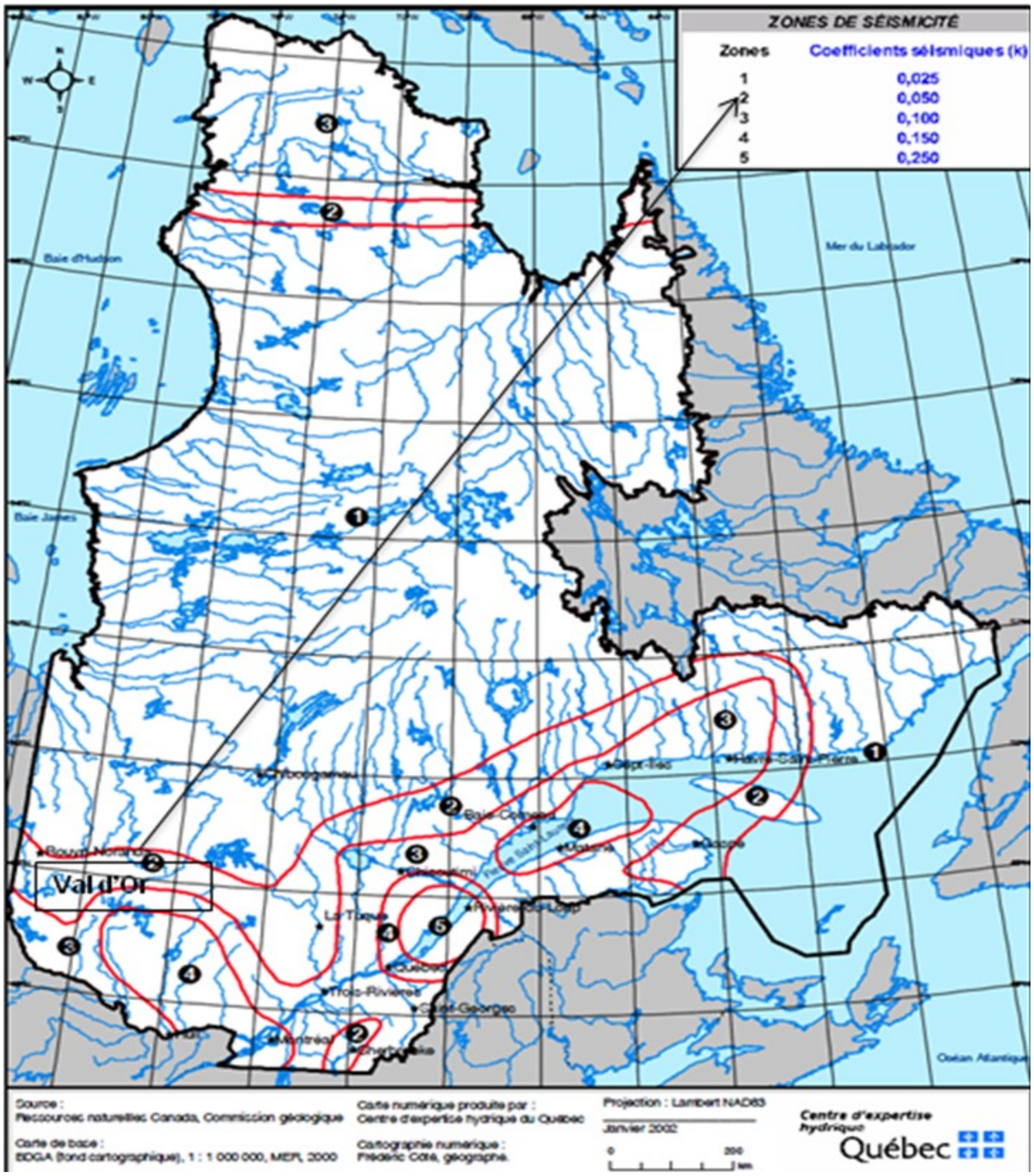

Figure 4-3 Seismic zones in the province of Quebec (Gouvernement du Quebec, 2002)

Figure 4-3 shows that Val d'Or is located in the seismic zone number 2, with a seismic coefficient equals to 0.05. It can also be seen in the figure that Val d'Or is close to seismic zones 3 and 4. Therefore, a worst case scenario of Kh=0.1 was used in some of the pseudo-static stability analyses of this thesis.

In summary, a seismic coefficient Kh=0.05 was used in those analysis in which the effect of the embankment/tailings height on the FOS was assessed. For the stability analyses in which the effect of the phreatic surface location, or the embankment to core permeability ratio was analyzed, 3 incrementally increasing seismic coefficients were used: Kh=0.038, Kh=0.05 and Kh=0.1, respectively.

4.1.3 Stability analyses and loading conditions

The static and pseudo-static stability analyses were conducted following the deterministic and the probabilistic approach for geotechnical slope stability assessment. The objective was to investigate the long-term behaviour of the impoundment under different loading conditions once steady-state equilibrium had been reached. The FOS was used as the stability criterion for all analyses.

The deterministic analyses were conducted using the simplified Ordinary-Fellenius (O-F) method, and the rigorous Morgenstern-Price (M-P) method. These analyses yielded graphs of the critical slip surface with its corresponding analysis of slices and contours of the FOS. The stability analyses with SRT-FEM provided the FOS or shear reduction factor along with the displacement and deformations occurring in the impoundment. The results were compared to determine the level of agreement between methods and performance of each type of storage facility.

The probabilistic approach was adopted with the purpose of including the uncertainty of material properties into the FOS computation. The Monte Carlo Simulation and the Point Estimate Method were used to conduct analyses. Additionally to the FOS, the probability of failure (p_f) and reliability index (β) were also calculated. The failure criterion was a FOS less than unity. The criterion for unsatisfactory performance were static and pseudo-static FOS below the minimum requirements for long-term steady-state seepage and normal reservoir level determined by mining regulations and guidelines in the province of Quebec and Canada as presented in table 4-3.

4.1.4 Minimum deterministic and probabilistic factors of safety

The minimum static and pseudo-static FOS and loading conditions assumed in this thesis are presented in table 4-3. The expected level of performance of each TSF was determined according to the probability of failure and reliability indices criteria proposed by the U.S. Army Corps of Engineers (1997) which were presented in Table 3-7 of this thesis.

Table 4-3 Factors of Safety for static and seismic slope stability assessment. (CDA, 2007 and MDDP, 2012)

Loading Conditions	Minimum FOS	Slope
End of construction before reservoir filling	1.3	Upstream and Downstream
Long-term (steady-stage seepage, normal reservoir level	**1.5**	**Downstream**
Rapid drawdown	1.2 to 1.3	Upstream
Pseudo-static	**1.1**	**Upstream and Downstream**
Post-earthquake	1.2-1.3	Upstream and Downstream

4.1.5 Loading conditions for the UTSF and WRTD

All static and pseudo-static analyses were performed assuming long-term-steady state; hence, the effective shear strength parameters (c' and ϕ') were used in the Effective Stress Analyses (ESA) approach. It was assumed that the load increase was slow enough during construction that every stage of embankment raise or tailings filling was allowed to reach equilibrium and pore pressures were dissipated by hydraulic boundary conditions before a new layer was applied.

All materials were assumed as elastic-perfectly plastic and following Mohr-Coulomb failure criteria. The ESA and long-term drained conditions assumptions were based on the studies by Saad (2008), Saad and Mitri (2011), Morsy et al., (1995), and Hamade, et al. (2011) in which no change in volume in the clayey glacial till foundation was observed.

Seepage through the impoundment was assumed to be controlled by a blanket drainage above the foundation. It was also determined that the free drainage zone outside the TSF in the downstream face of the embankment helped dissipate the pore pressure created by the deposited tailings. It was assumed that in both TSFs the tailings stream was discharged upstream of the starter dyke or embankment using multiple peripheral spigots. In the case of the UTSF, this deposition method allowed for the coarse fraction of tailings to settle out near the embankment creating a beach with a 2% slope.

4.1.6 Seepage conditions

The seepage analyses were conducted using the 2D-finite element method of the software Phase^2 8.0 by Rocscience (2007) to obtain the pore pressure distribution necessary to conduct the ESA using the LEM and the SRT. It was assumed steady-state flow in which Darcy’s law and Laplace’s equation were valid in confined flow. The porous media was assumed fully saturated and that the flow path changed directions within the impoundment with predominant vertical direction and a small component in the horizontal direction due to the effect of the gravitational force.

The interstitial fluid is water; it was considered laminar and incompressible, that is, there is no change in the void ratio of the porous media during seepage. However, the permeability of a given point within a tailings stratum was anisotropic. Therefore, in these cases, the modified Laplace’s equation and corrections for permeability was applied. The boundary conditions, permeability of the porous media, and hydraulic heads imposed by the model’s geometry were known and well defined.

4.2 The Upstream Tailings Storage facility (UTSF) design

According to Saad (2008) the UTSF was constructed in six stages at a raising rate of 5.25 m/year as shown in Figure 4-4. The embankment’s ultimate height is 41.75 m. as depicted in Figure 4-5. The embankment has an upstream slope of 3H: 1V and a downstream slope of 3.5H: 1V. The beach width at the end of construction is 162 m and has a slope of 2%. The freeboard maintained during the embankment raising and at the end of construction is 2 m. Tailings are considered fully saturated upon deposition.

The minimum design distance between the embankment crest and beach phreatic surface is 50 m. The material properties of the UTSF are presented in Table 4-4.

Figure 4-4 Stages 0 to 5 showing increasing embankment height - UTSF

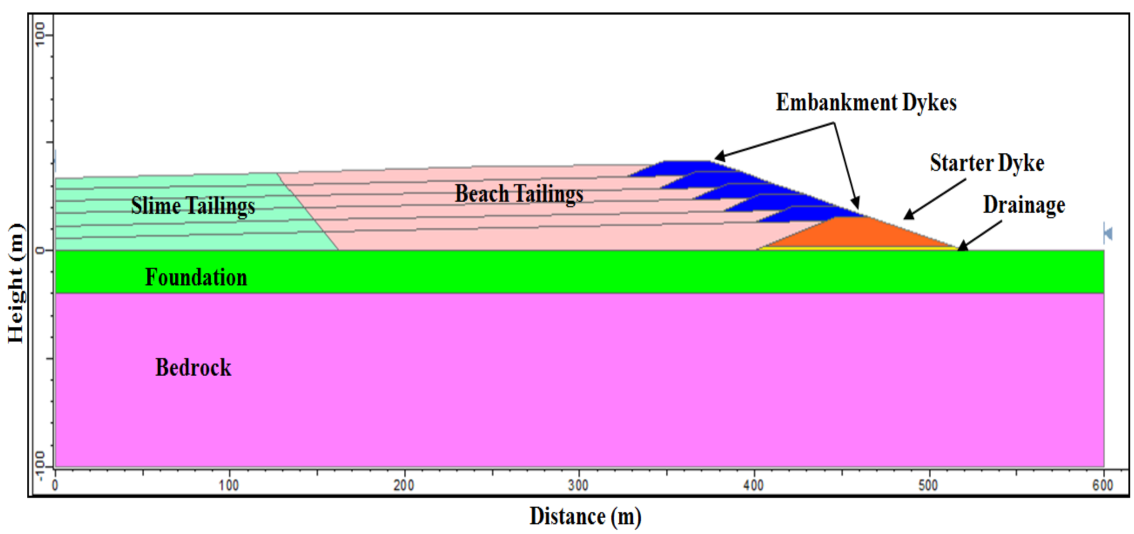

Figure 4-5 Stage 6: ultimate height (41.75m) - UTSF

Table 4-4 Material properties for the UTSF. Based on Saad and Mitri (2011), Morsy et al., 2005, Bardet (1997), Rajapakse (2008), Vermeulen (2001), and Vick (1983).

Material	γ_{sat} (kN/m^3)	γ_{dry} (kN/m^3)	ϕ' (deg)	c' (kPa)	E (kPa)	ν	k (m/s)	n
Bedrock	26	25.8	42	6000	1x10^{7}	0.23	1x10^{-8}	0.02
Top Foundation	17.9	15.9	21	0	25000	0.2	1x10^{-7}	0.2
Drainage	19.4	15.5	34	0	1x10^{7}	0.28	0.06	0.4
Starter Dyke	18.5	13.6	35	0	1x10^{6}	0.3	0.001	0.5
Beach Tailings	20	14.7	30	0	5575	0.33	7.3 x10^{-7}	0.53
Slime Tailings	19.7	14.5	5	5	5575	0.33	7.3x10^{-8}	0.53
Embankment Dykes	22.3	17.9	30	0	5575	0.33	0.000115	0.4

4.3 The Water Retention Tailings Dam (WRTD) design

According to Hamade et al., (2011), the WRTD is built to its complete height (16m) prior to the beginning of operations. The upstream slope is 2.5H: 1V and the downstream slope is 2.5H: 1V. The tailings height reduces from 4 m, in stages 0 to 3, to 2 m in stages 4 to 6 as depicted in Figure 4-6. Tailings reach an ultimate height of 18 m due to the construction of a small dyke near the end of operations as presented in Figure 4-7.The freeboard at the end of construction was 2 m. Tailings are considered fully saturated upon deposition. The material properties of the WRTD are presented in Table 4-5.

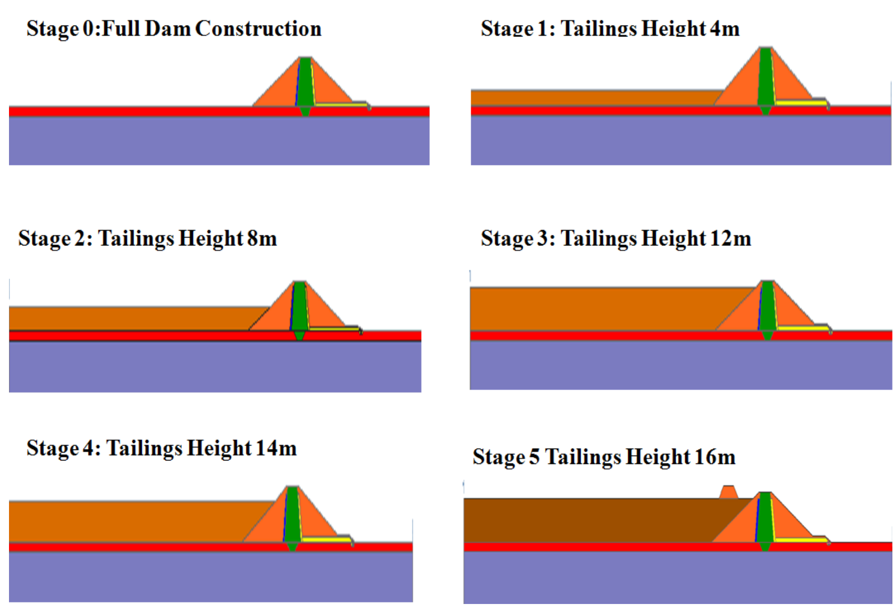

Figure 4-6 Stages 0 to 5 showing increasing tailings height - WRTD

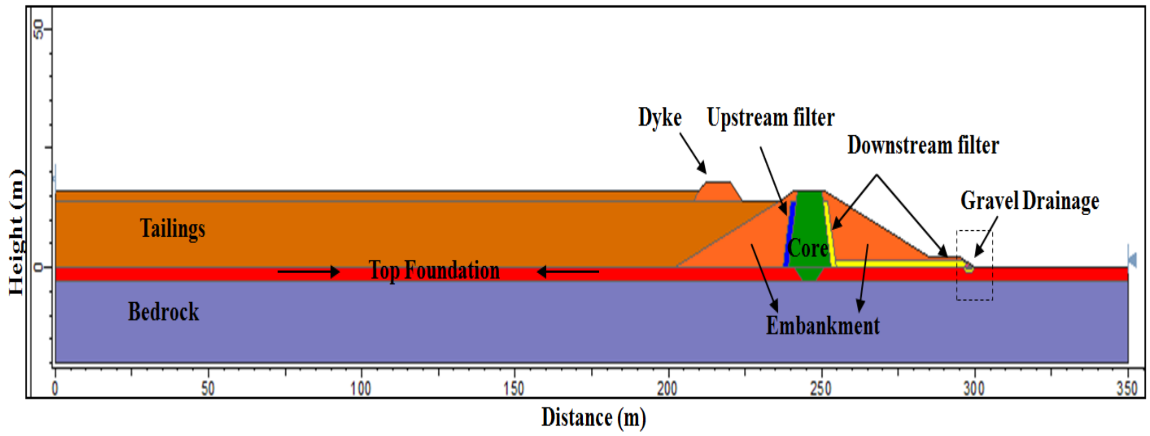

Figure 4-7 Stage 6: ultimate tailings height (18 m) - WRTD

Table 4-5 Material properties WRTD. Based on Hamade, et al., (2011), Saad and Mitri (2011), Morsy et al., 2005, Bardet (1997) Rajapakse (2008), Vermeulen (2001), and Vick (1983).

Material	γ_{sat} (kN/m^3)	ϕ' (deg)	c´ (kPa)	E (kPa)	ν	k (m/s)	n
Bedrock	27	42	6000	2.84×10^7	0.23	1×10^{-8}	0.02
Top Foundation	16.5	3	50	20000	0.25	1×10^{-7}	0.2
Core	21.5	28	12	150000	0.2	1×10^{-7}	0.35
Embankment	18.5	35	0	1×10^7	0.3	0.001	0.5
Downstream filter	18	34	0	70000	0.35	0.00025	0.5
Upstream filter	20	36	0	60000	0.28	0.06	0.45
Gravel Drainage	19	37	0	80000	0.3	0.1	0.4
Tailings (mill)	16	28	0	5575	0.33	1×10^{-7}	0.4

4.4 Phreatic surface location analysis

The influence of the phreatic surface location in the overall stability of the TSFs was analysed separately due to the different layouts and storage purposes of each type of impoundment. For the UTSF, a limit beach width ratio L/H= 6 and a critical beach ratio L/H=4 ratio were analyzed. The two scenarios are shown in Figures 4-8 and 4-9, respectively. This approach was adopted according to the method proposed by Vick (1983).

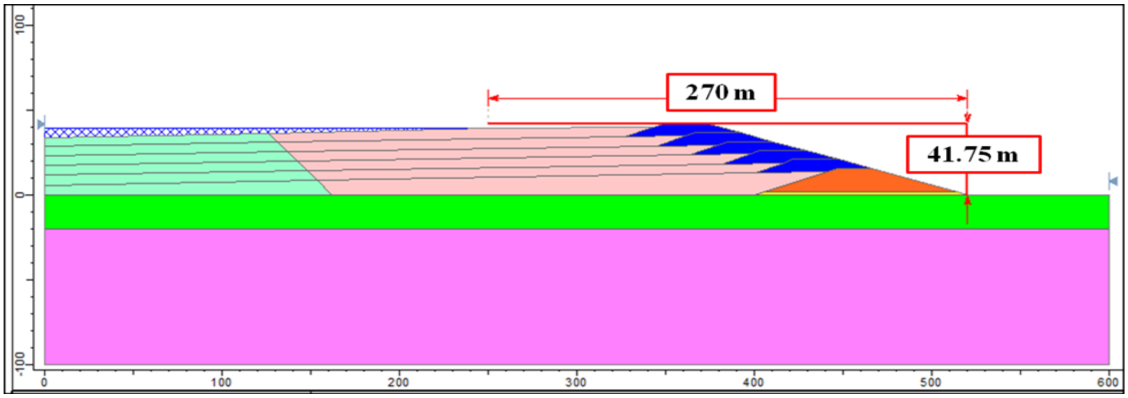

Figure 4-8 Cross section of the limit beach width for the UTSF - L/H = 6.

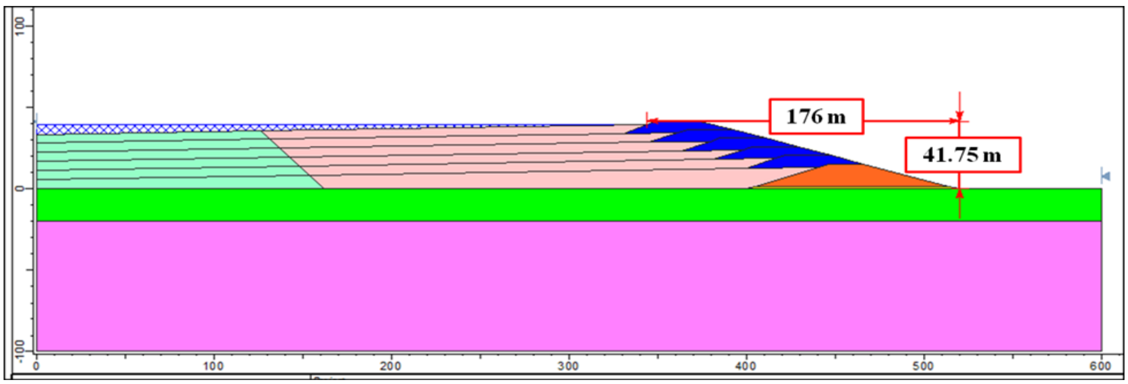

Figure 4-9 Cross section of the critical beach width for the UTSF - L/H = 4.

The effect of the phreatic surface in the WRTD was analyzed according to the method suggested by Vick (1983) in which the embankment to core permeability ratio (k_s/k_c) is reduced. The static and pseudo static analyses were conducted for the two scenarios shown in Figure 4-10. One scenario was for a k_s/k_c= 10000 (or the actual permeability ratio between the embankment and the core), and second scenario was for a k_s/k_c=100 in which the core's permeability increased two orders of magnitude due to filter incompatibility.

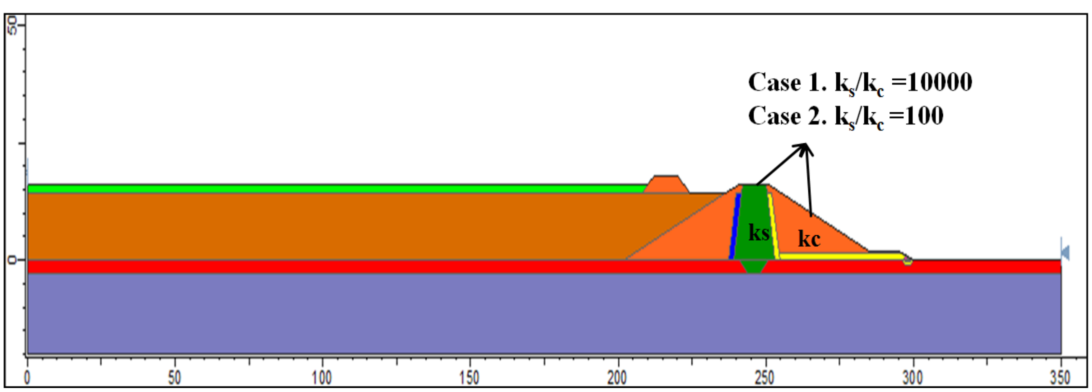

.

Figure 4-10 Cross section of the WRTD (ks) to core (ks) permeability ratio.

4.5 Discretization and mesh description - UTSF and WRTD

The deterministic and probabilistic stability analyses for the SRT and PEM of each TSF, respectively, were conducted with the 2-dimensional finite element plane strain software Phase2 8.0 by Rocscience (2007). All the materials in both TSFs were considered elastic-perfectly plastic with a Mohr-Coulomb failure criterion. The mesh and discretization criteria were based on studies by Chang et al.,(1995), Fourie et al., (2002); Griffiths and Lane (1999); Hamade et al., (2011); Matsui and San (1992), and Saad, (2008). A uniform 8-node quadrilaterals mesh with 4 Gauss-points per element was used for each model. The UTSF mesh consisted of 2904 elements (Figure 4-11), and the WRTD mesh contained 2300 elements (Figure 4-12), respectively.

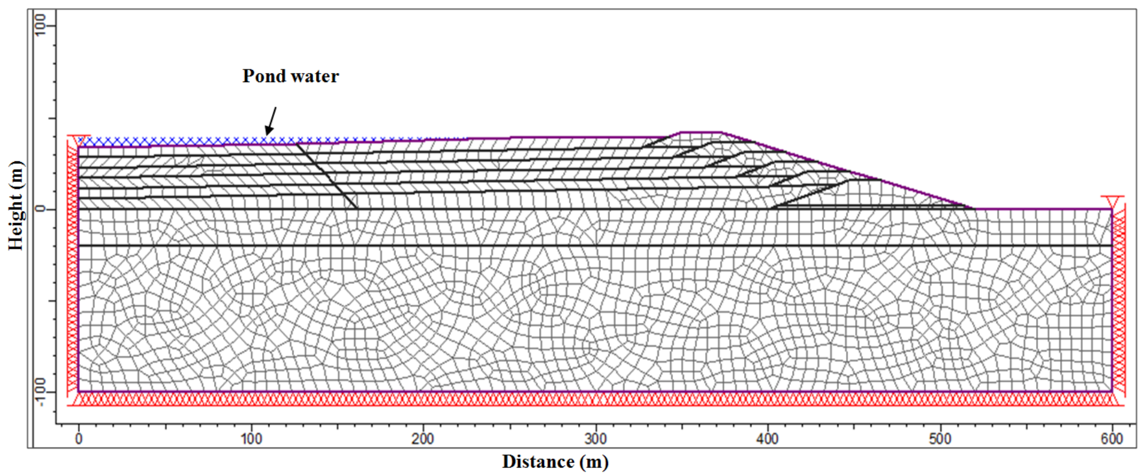

Figure 4-11 Cross section of the UTSF showing the FE mesh and restraints.

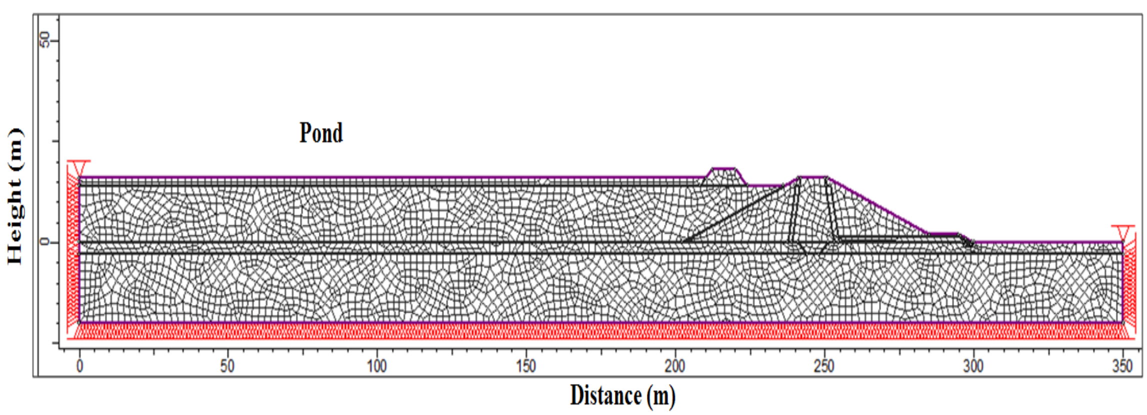

Figure 4-12 Cross section of the WRTD showing the FE mesh and restraints.

The initial element loading criteria of the embankment tailings, mill tailings and slime tailings, as well as the deposited tailings in the UTSFs were assigned body force element loading to simulate the self-weight consolidation at steady-state equilibrium. These same mesh and discretization criteria were used to conduct FEM groundwater seepage analyses for pore pressure. The LEM and SRT slope stability analyses in SLIDE 6.0 and Phase2 8.0 were performed with fully integrated 2D-FEM groundwater seepage analysis (Rocscience, 2007).

- **Boundary conditions and restrains**

The external and hydraulic boundary conditions for the embankment/tailings height increase varied as the total head changed, whereas the external and hydraulic boundary conditions for phreatic surface location and the embankment to core permeability ratio analyses remained constant.

It was assumed that the total head boundary conditions used to define the hydraulic boundary conditions did not define the weight of the ponded water. Each TSF was assigned external boundary conditions restrains in the x and y direction in the bedrock, top foundation and the pond water region only. As can be seen in Figures 33 and 34 the areas comprising the most probable slip surface were assigned free restrain to allow for displacement and deformation computation.

- **Convergence parameters**

The convergence or stopping criterion for all SRT-FEM stability analyses and Point Estimate Method was absolute energy imbalance. The tolerance value for this stopping criterion was 0.01 after 500 iterations. The convergence parameters were selected according to the parameters provided by Rocscience (2007) and Hammah et al., (2004).

4.6 Procedures and methodology for the UTSF and WRTS stability analyses

The analytical approaches, the type of analysis, loading conditions, and the analytical methods and software used in the thesis are summarized in Table 4-6. The input and output parameters considered for each case are also provided in this summary.

Table 4-6 Summary of analysis procedure and stability analyses methodology

Approach	Type of Analysis	Method	Modelling Tool	Procedure
Deterministic	**Static analysis with steady state seepage**	LEMs: M-P & O-F	SLIDE 6.0	**Input** Increasing embankment/tailings height UTSF and WRTD, ΔL/H ratio - UTSF, and $\Delta k_s/k_c$ ratio for WRTD. ESA- (c', ϕ') parameters. **Output** LEM—FOS - Slip surface graph. SRT—FOS, deformation, and displacement contours.
		FEM -SRT	$PHASE^2$	
	Pseudo-static analysis with steady state seepage	LEMs: M-P & O-F	SLIDE 6.0	**Input** Increasing seismic coefficients $K_{h=}$ 0.038, 0.05 and 0.1. Same loading criteria than static analysis used. **Output** LEM—FOS - Slip surface graph. SRT—FOS, deformation, and displacement contours.
		FEM -SRT	$PHASE^2$	
Probabilistic	**Sensitivity Analysis**	LEM: M-P	SLIDE 6.0 and Excel spreadsheets	**Input** Mean (μ), std. dev (σ), and COV of materials properties. Relative minimum and maximum values with μ±3σ rule to cover 99.74% of sample space. **Output** Random Variables of each TSF. Scatter plots. Correlation coefficient between FOS vs. R.Vs. Convergence plots for 1000 MCS
	Static and pseudo-static analyses with seepage	1000 MCS using LEM: M-P	SLIDE 6.0 and Excel spread sheets	**Input** Same loading criteria than for deterministic analyses. **Output** Mean FOS PDF CDF *Pf and β*. Failure and performance
	Static and pseudo-static analysis with seepage	FEM-SRT-PEM	$PHASE^2$	**Input** Same loading criteria than deterministic pseudo-static analyses. **Output** Probabilistic FOS Solutions=2^n; n=# of R.V *Pf and β*. Failure and performance

CHAPTER 5: TSF STABILITY ANALYSES WITH DETERMINISTC APPROACH - RESULTS AND DISCUSSION

The results of the effect of embankment/tailings height increase, the change in the beach width ratio for the UTSF, and the change in embankment to core permeability ratio for the WRTD on stability are presented in this chapter. The results were obtained from the static and pseudo-static analyses performed with a rigorous and simplified LEMs and the SRT under the deterministic approach. Only the M-P method global minimum slip surface graphs and the SRT maximum shear strain and horizontal displacement contours are presented for all analyses.

5.1 Effect of the embankment height increase on the UTSF stability

5.1.1 Static and Pseudo-static results

Table 5-1 Static and pseudo static FOS for increasing embankment height - UTSF

Embankment Height	LEMs				FEM-SRT	
	O-F		M-P			
	Static	Pseudo Static	Static	Pseudo Static	Static	Pseudo Static
15.5 m	1.30	1.08	1.57	1.28	1.49	1.29
20.75 m	1.28	1.06	1.55	1.27	1.63	1.32
26 m	1.27	1.05	1.50	1.24	1.61	1.28
31.25 m	1.25	1.04	1.46	1.21	1.61	1.24
36 m	1.24	1.04	1.44	1.20	1.51	1.23
41.75 m	1.24	1.04	1.42	1.19	1.44	1.20

Note: Pseudo-static analysis with Kh=0.05.

- **Discussion FOS under increasing embankment height - UTSF**

- Comparison between LEMs: O-F vs. M-P

The results in table 5-1 show that the average difference of the value of FOS between the O-F and M-P methods was 18.5% for the same loading conditions and embankment heights. Higher values of FOS were obtained for the M-P. The static FOS at the embankment's ultimate height was 1.42 for the M-P method and 1.24 for the O-F method.

The M-P method FOS results were considered more reliable. Even though the FOS with the M-P method was much higher than those of the O-F method, the FOS results did not meet the minimum requirement for long-term steady state conditions analyses in Quebec. Similarly, the pseudo-static FOS showed an average 17.4% variation between methods. The FOS obtained with the O-F method at the embankment's ultimate height was FOS =1.04 and did not meet the minimum requirement of Quebec's regulations.

The same analysis with the M-P method produced a FOS = 1.19 that met the requirements. These results show that conducting the analysis with only one method (especially with a simplified method) is not reliable and, this, it is not a good practice. The M-P results were assumed as more reliable and therefore were used to compare against the FEM-SRT results. The overall static safety reduction from the starter dyke (15.5m) until the embankment's ultimate height was reached was approximately 6.3%. The FOS went from FOS =1.57 to FOS= 1.42 using the M-P LEM analysis, and 12, 2% using the SRT (FOS=1.64 to 1.44)

- Comparison between LEMs and SRT

Good correspondence between the M-P LEM and the SRT results was found. The average difference of the static FOS between methods was 6%. A much better correspondence was observed for pseudo-static FOS in which the average difference between methods was 2.3%. The static FOS at the embankment's ultimate height did not meet the minimum requirements for any of the two methods. The FOS obtained with the SRT is considered the most reliable value and the one recommended for stability compliance assessment given the advantages it has over the LEM in terms of deformation and displacement calculation.

-Comparison between loading condition: static vs. pseudo-static analyses

The results show that applying a seismic coefficient reduces the FOS significantly. The results show an estimated safety reduction of 16% (FOS reduced from 1.42 to 1.19) . The pseudo-static FOS obtained at the embankment's ultimate height met the minimum requirements, but since it is a deterministic value, this value does not offer information regarding level of performance of the embankment.

5.2 Effect of the phreatic surface location on the UTSFs stability

The effect of the phreatic location on the stability of the UTSF at the embankment's ultimate height was investigated. Two phreatic surface locations were assumed: L/H=6, which is considered a limit location, and L/H=4, which is considered a critical location. After, a comparison between the value of FOS using the M-P method and SRT methods was made for each phreatic surface location.

The main objective was to retrieve information about the embankment's static and pseudo-static displacement and deformation additional to the FOS. The corresponding global minimums slip surface, max shear strain, and horizontal displacement contours of the L/H=6 and L/H=4 ratio are presented in Figures 5-1 to 5-4. Table 5-2 contains a summary of the static FOS obtained from the O-F, the M-P, and SRT deterministic analyses. Table 5-3 presents a summary of pseudo-static FOS obtained by increasing the Kh and using O-F method, the M-P method, and the SRT.

5.2.1 Static results

Table 5-2 Static FOS for different phreatic surface locations within the UTSF

Criteria	Static FOS		
	O-F	M-P	SRT
L/H= 6	1.24	1.42	1.44
L/H= 4	1.18	1.30	1.31

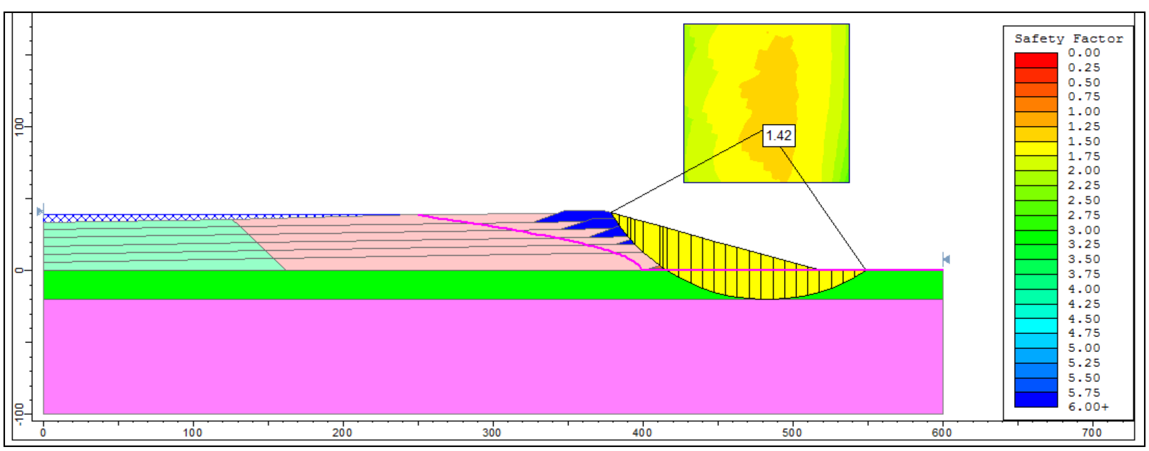

(a) Static FOS –M-P method

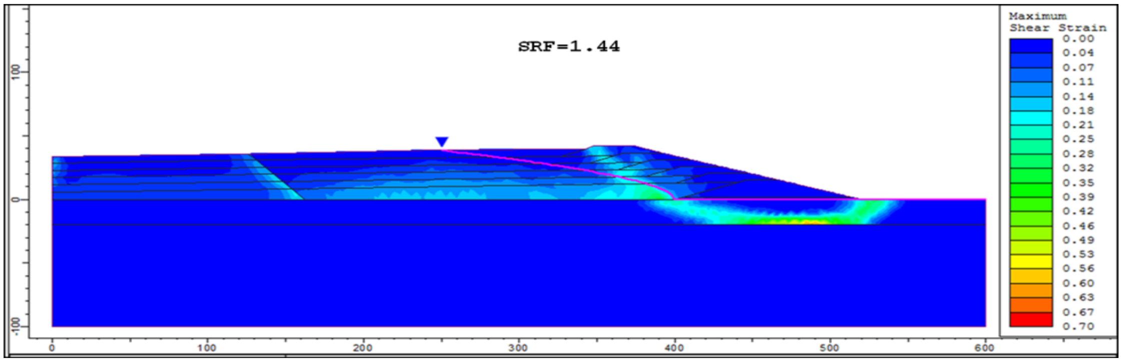

(b) Maximum shear strain - SRT

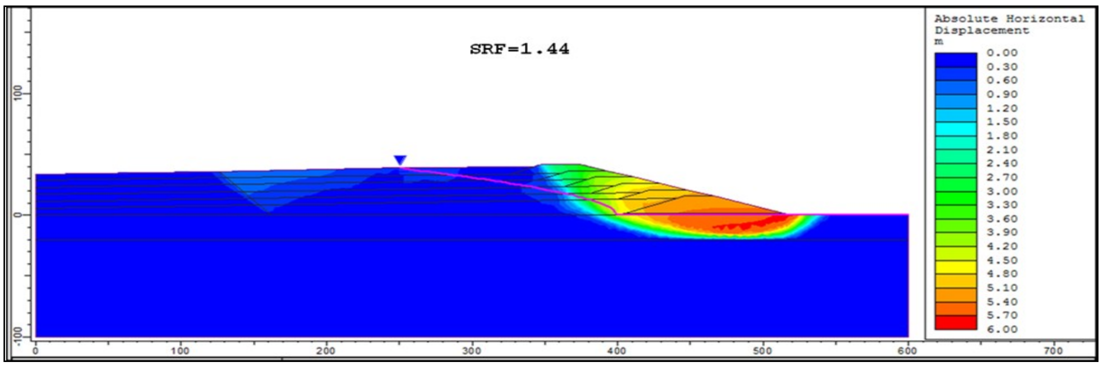

(c) Horizontal displacement (m) -SRT

Figure 5-1 Static analysis for a L/H=6 ratio - UTSF

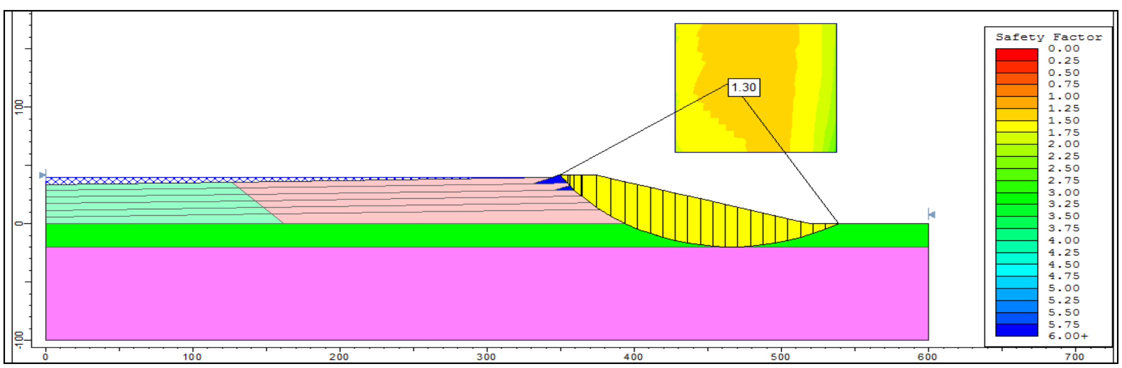

(a) Static FOS – M-P method

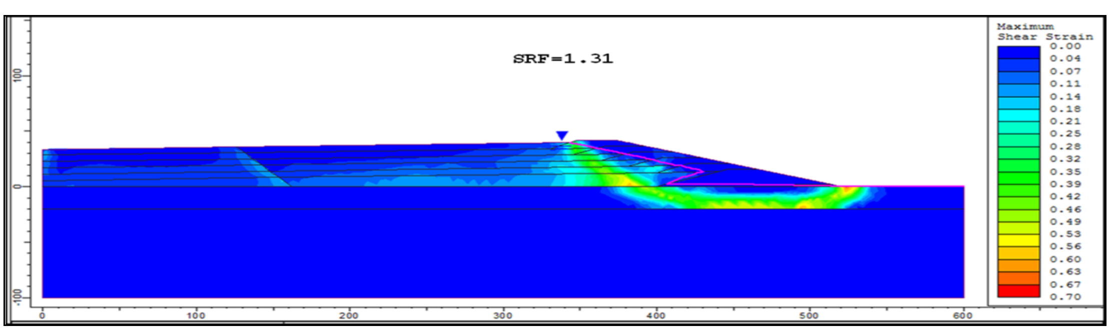

(b) Maximum shear strain - SRT

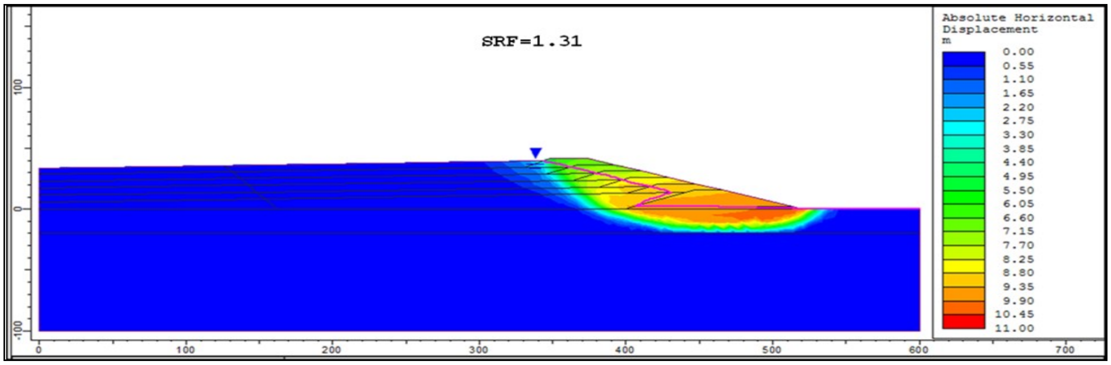

(c) Horizontal displacement (m) –SRT

Figure 5-2 Static analysis for a L/H=4 ratio - UTSF

5.2.2 Pseudo-static results

Table 5-3 Deterministic pseudo-static FOS for different phreatic surface locations within the UTSF

Criteria	Kh=0.038			Kh=0.05			Kh=0.1		
	O-F	M-P	SRT	O-F	M-P	SRT	O-F	M-P	SRT
L/H= 6	1.08	1.24	1.25	1.04	1.19	1.20	0.88	1.02	0.99
L/H= 4	1.04	1.13	1.14	1.00	1.08	1.08	0.85	0.92	0.93

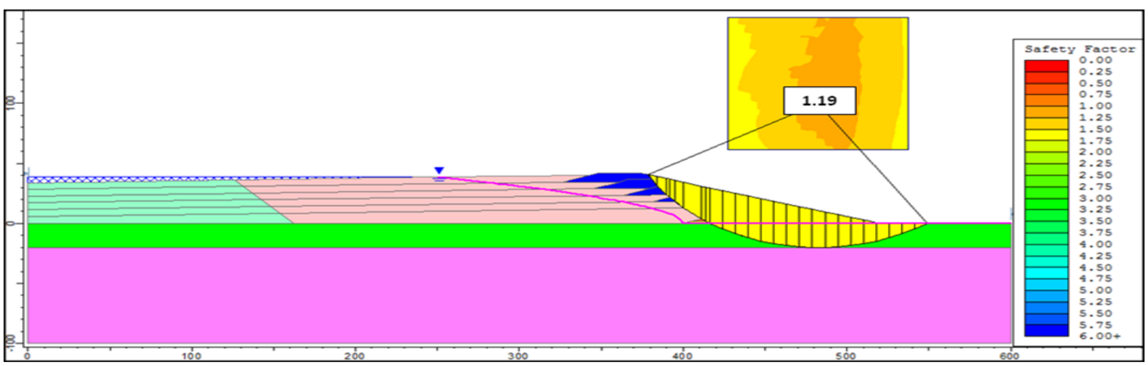

(a) Pseudo-static FOS – M-P method

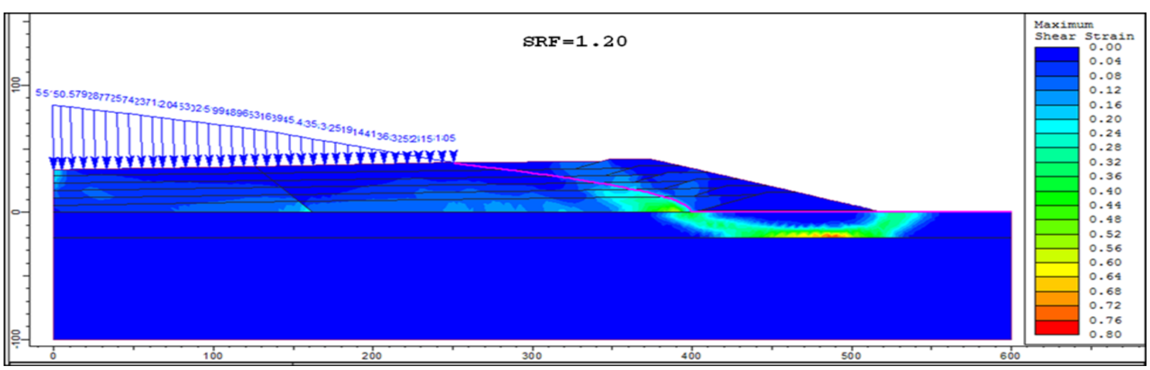

(b) Maximum Shear Strain - SRT

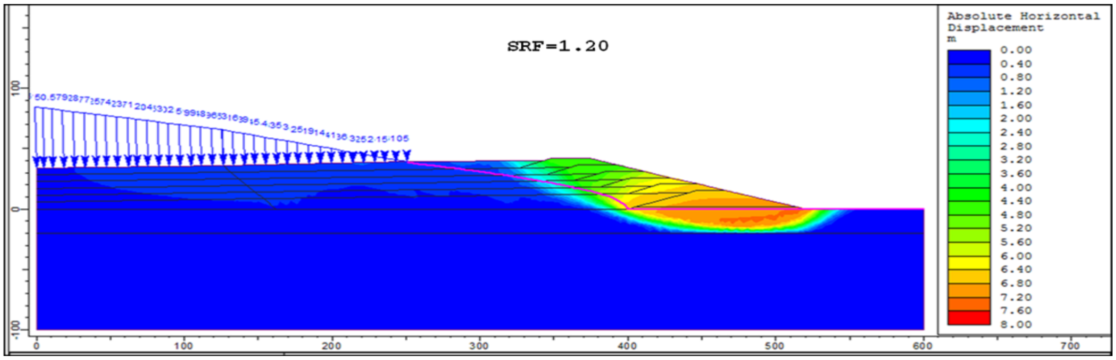

(c) Horizontal displacement (m) SRT

Figure 5-3 Pseudo-static FOS for a L/H=6 ratio given a Kh=0.05

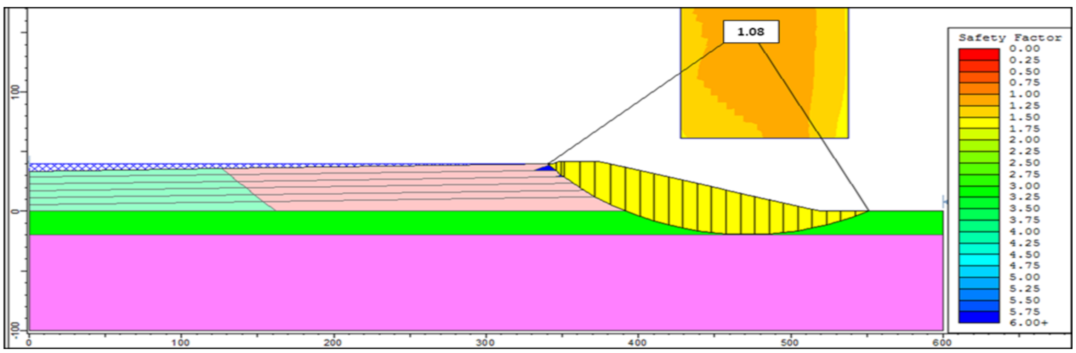

(a) Pseudo-static FOS – M-P method

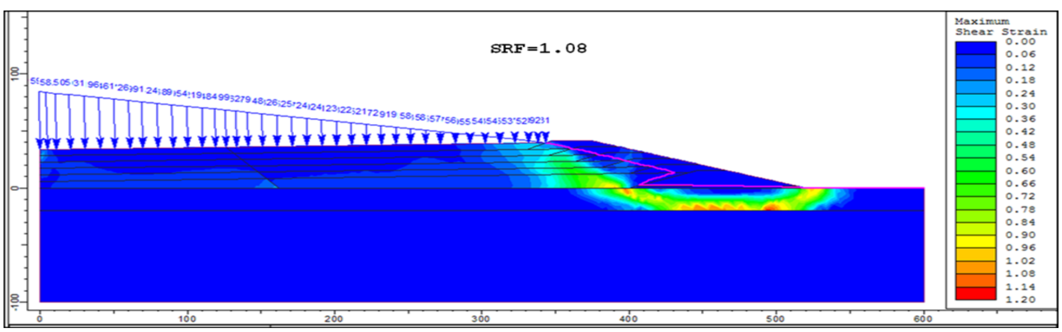

(b) Maximum Shear Strain - SRT

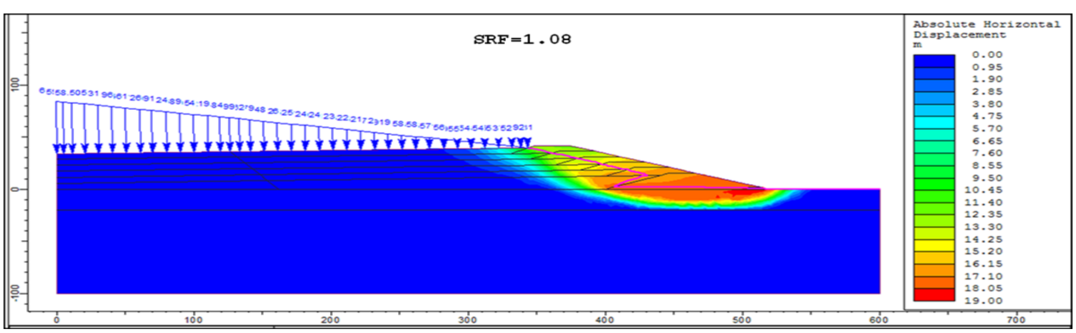

(c) Horizontal displacement (m) SRT

Figure 5-4 Pseudo-static FOS given for L/H=4 ratio given a Kh=0.05

- **Discussion stability and changing phreatic surface location–UTSF L/H=6 and L/H=4 – static and pseudo-static loading**

In general, a good correspondence between the FOS of the M-P method and SRT was obtained for the limit and critical phreatic surface location analyses. The static and pseudo-static FOS obtained were almost identical. The SRT analysis contours showed that the zones of maximum shear strain coincide with the location and shape of the global minimum slip surface obtained in the M-P method analysis. Figures 5-1b, 5-2b, 5-3b, and 5-4b show that the top foundation is the zone of maximum shear concentration in the UTSF.

All contours showed maximum deformation and horizontal displacement as the phreatic surface approached the embankment. For instance, for the L/H=6 ratio the maximum shear strain in the middle of the top foundation was approximately 0.56 and the horizontal displacement 6 m. For the critical beach width location ratio L/H=4, the maximum shear strain, at the same location, was 0.70 and a horizontal displacement 10.45m. A good agreement between the pseudo-static M-P method and SRT FOS was obtained. The pseudo-static force applied increased the shear strain in the middle of the top foundation. Figure 5-3b and 5-3c showed a maximum shear strain of 0.8 and a horizontal displacement of 7.4 m, respectively. Figures 5-4b and 5-4c The L/H=4 ratio contours showed a maximum shear strain of 1.20 and horizontal displacement of 19 m, respectively.

The large displacements obtained under static and pseudo static loading confirmed that the UTSF would not be suitable for water containment and has poor performance in zones of moderate to high seismicity. The results are in agreement with the effects of the phreatic surface location proposed by Vick (1983). Consequently, the beach width ratio should be as large as possible to keep the water at a safe distance from the embankment. Likewise, an appropriate drainage system should be installed to avoid pore pressure increase and subsequent reduction of the shear strength of the tailings materials that could result in static or seismic liquefaction.

5.3 Effect of tailings height increase on the WRTD stability

5.3.1 Static and pseudo-static results

Table 5-4 Static and pseudo-static FOS for increasing tailings height -WRTD

Tailings Height	LEMs				SRT	
	O-F		M-P			
	Static	Pseudo Static	Static	Pseudo Static	Static	Pseudo Static
4 m	1.63	1.41	1.70	1.49	1.62	1.60
8 m	1.62	1.40	1.70	1.47	1.60	1.58
12 m	1.58	1.34	1.64	1.38	1.59	1.50
14 m	1.54	1.30	1.58	1.33	1.59	1.48
16 m	1.54	1.30	1.58	1.32	1.56	1.48
18 m	1.54	1.30	1.58	1.30	1.54	1.47

Note: Pseudo-static analysis with Kh=0.05

- **Comparison between LEMs: O-F vs. M-P**

The value of FOS showed an average difference of 3.3% between the simplified O-F method and the rigorous M-P method for the same loading conditions and for the same tailings height. As shown in Table 5-4, higher values of FOS were obtained for the M-P method. The static FOS for the tailings ultimate height (18m) was 1.58 using the M-P method and 1.54 for the O-F method. The FOS obtained in both methods met the minimum requirements for long-term steady state analyses in Quebec. The pseudo-static FOS showed an average variation of 3.2% between methods. The pseudo-static FOS met the minimum requirements. The M-P method results were assumed more reliable and compared against the FEM-SRT. The overall static safety reduction from initial to ultimate tailings height was approximately 7% (FOS went from 1.70 to1.58) using the M-P LEM analysis, and 4.3% using the SRT (from FOS=1.60 to 1.53)

- Comparison between LEMs and SRT

The M-P method and the SRT results showed good correspondence. The average difference for the static FOS was 3.57%. In both methods the FOS for the tailings ultimate height met the minimum Quebec requirements (1.3 and 1.47 for the M-P method and SRT, respectively).The SRT results are considered more reliable to compare against the regulations of Quebec.

-Comparison between loading condition: static vs. pseudo-static analyses

A total safety reduction of 7% was observed under static loading (FOS went from FOS 1.70 to FOS 1.58 for the M-P method). However, the reduction did not reach values that indicated failure. The pseudo-static FOS at the embankment's ultimate height met the minimum pseudo-static FOS requirements as well. The safety reduction due to pseudo static loading was 13% for the M-P method and 11.2% for the SRT. The high values of pseudo-static FOS for the WRTD (1.3 for M-P method and 1.47 for the SRT) are in agreement with the literature review that indicates that WRTD have good seismic resistance compared to other types of tailings storage facilities.

5.4 Effect of embankment to core permeability ratio (ks/kc) on the WRTD stability

The effect of the embankment's to core permeability ratio variation when tailings reached their ultimate height in the WRTD was investigated. The initial embankment to core permeability ratio was reduced from ks/kc=10000 to ks/kc=100 assuming internal erosion processes and migration of particles due to filter incompatibility.

The FOS obtained with M-P method and SRT methods were compared. Table 5-5 shows a summary of the static FOS, followed by the LEM global minimum slip surface and maximum shear strain and horizontal displacement contours in Figures 5-5 and 5-6. Table 5-6 presents the results of the pseudo-static FOS, and Figures 5-7 and 5-8 show the corresponding pseudo-static slip surface, maximum shear, and horizontal displacement contours, respectively.

5.4.1 Static results

Table 5-5 Static FOS for initial and reduced embankment to core permeability ratio-WRTD

Criteria	Static FOS		
	O-F	M-P	SRT
k_s/k_c =10000	1.54	1.58	1.54
k_s/k_c 100	1.51	1.56	1.51

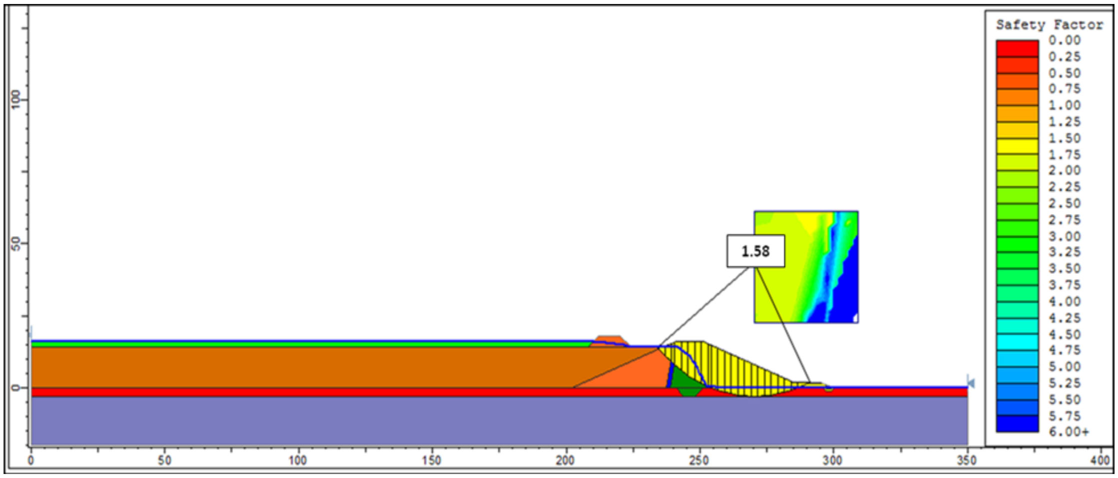

(a) Static FOS – M-P method

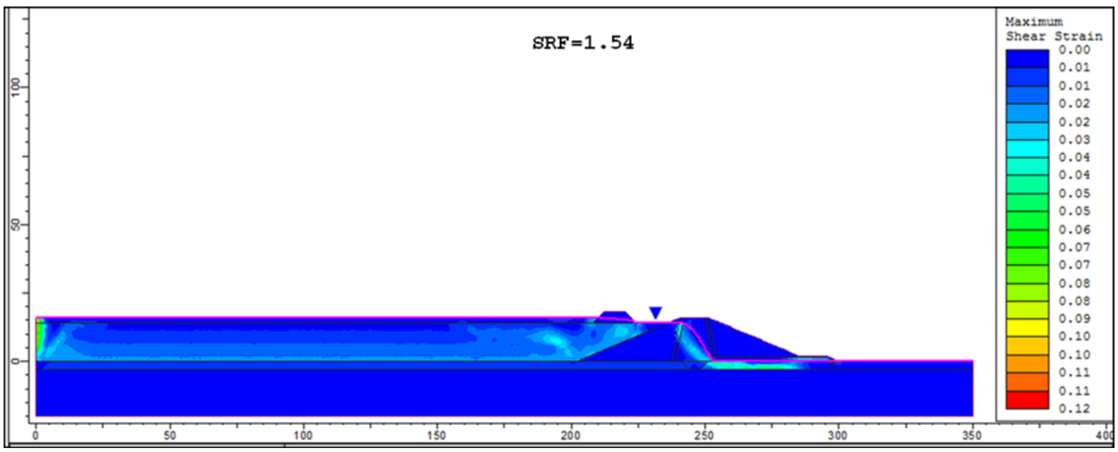

(b) Maximum shear strain -SRT

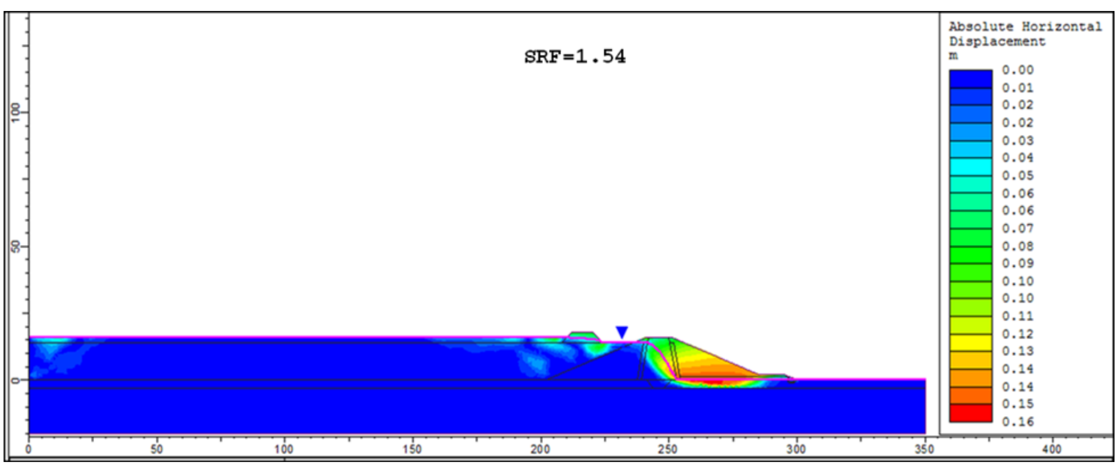

(c) Horizontal displacement (m) - SRT

Figure 5-5 Static analysis for the ks/kc =10000 - WRTD

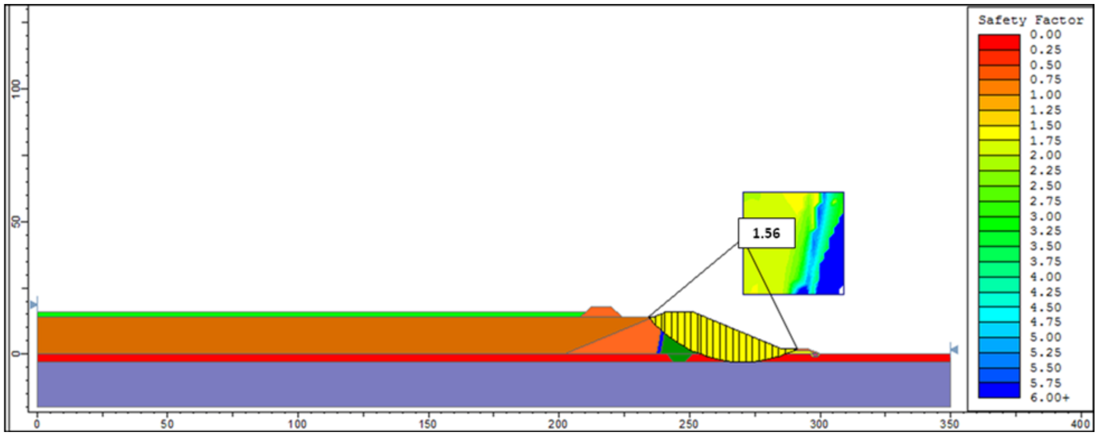

(a) Static FOS M-P method

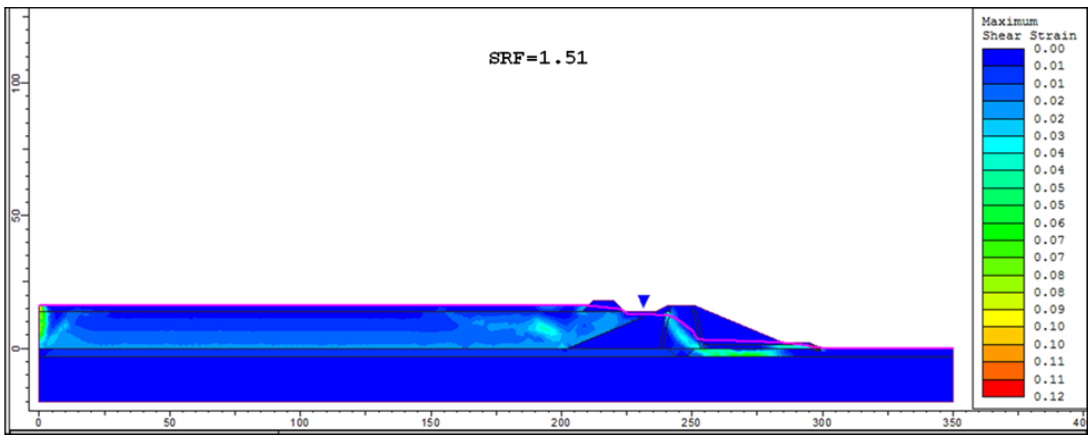

(b) Maximum shear strain-SRT

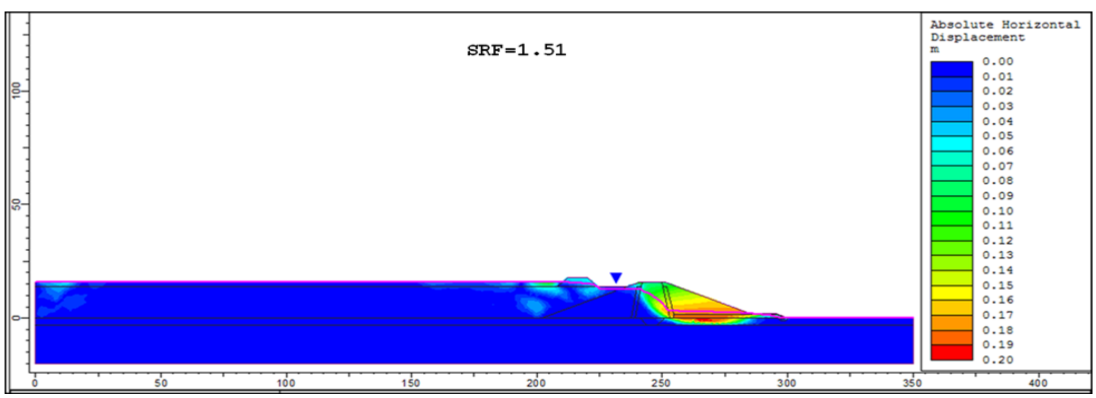

(c)Horizontal displacement (m) –SRT

Figure 5-6 Static analysis for the ks/kc =100 - WRTD

A good agreement between the static M-P method and SRT FOS results was obtained. The SRT contours showed that the zones of maximum shear strain, that is, the core and top foundation, coincide with the location and shape of the global minimum slip surface obtained in the M-P method analysis.

5.4.2 5.4.2 Pseudo-static results

Table 5-6 Pseudo-static FOS for initial and reduced core permeability ratio - WRTD

	Kh=0.038			Kh=0.05			Kh=0.1		
k_s/k_c	O-F	M-P	SRT	O-F	M-P	SRT	O-F	M-P	SRT
10000	1.35	1.380	1.48	1.30	1.32	1.47	1.12	1.140	1.35
100	1.32	1.350	1.47	1.27	1.30	1.47	1.10	1.110	1.35

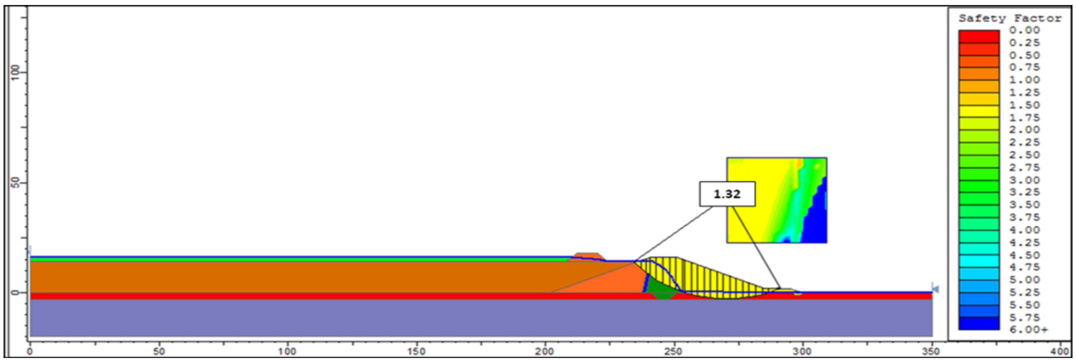

(a) Pseudo-static FOS M-P method

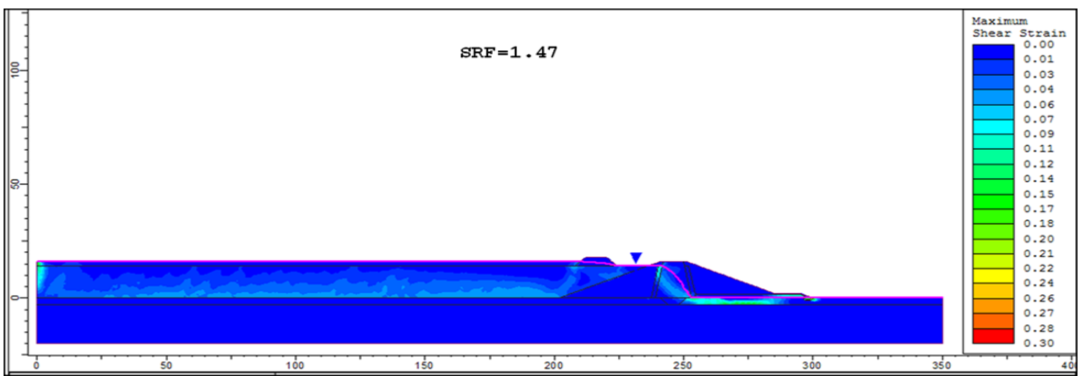

(b) Maximum shear strain - SRT

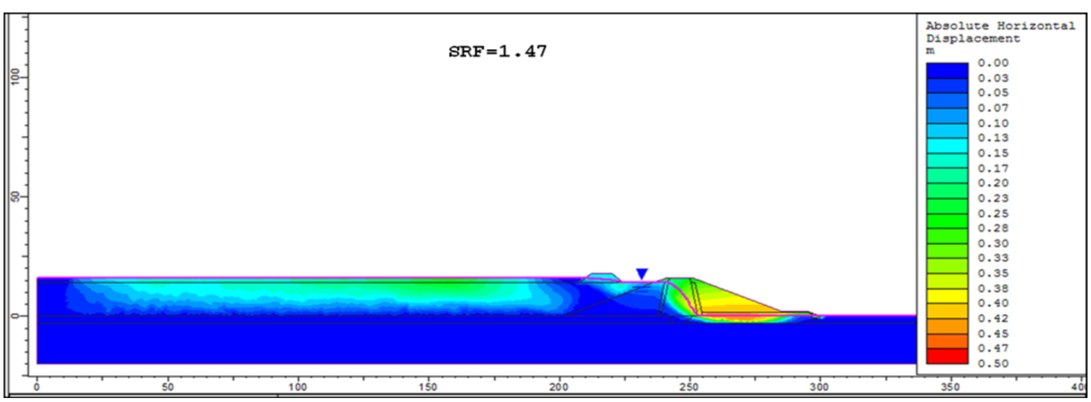

(c) Horizontal displacement (m) –SRT

Figure 5-7 Pseudo-static FOS for ks/kc =10000 WRTD; Kh=0.05

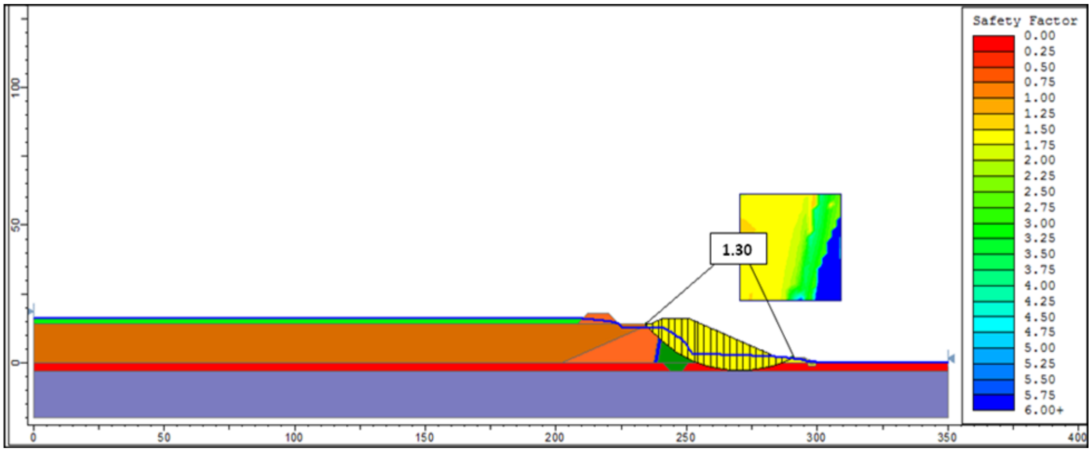

(a) Pseudo-static FOS M-P method

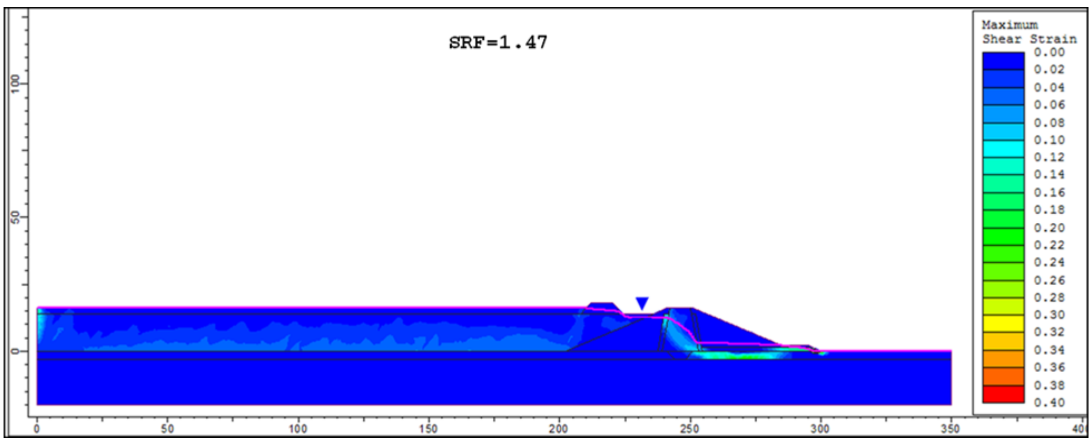

(b) Maximum shear strain - SRT

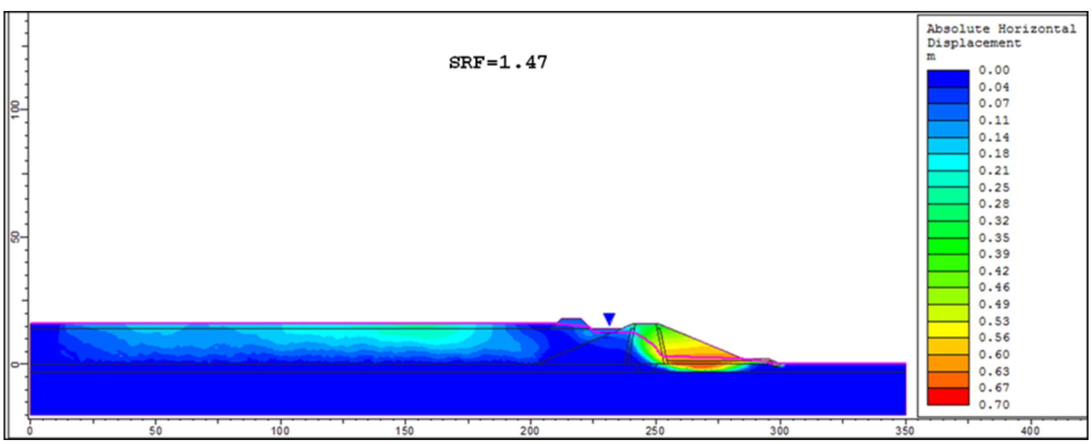

(c) Horizontal displacement (m) - SRT

Figure 5-8 Pseudo-static FOS for ks/kc=100 WRTD; Kh=0.05

- **Discussion ks/kc=10000 and ks/kc=100 static and pseudo-static loading**

The contours indicate that both the maximum shear strain and horizontal displacement increased as the permeability ratio reduced under static and pseudo-static loading. However, this increase was not substantial.

For instance, for the ks/kc=10000 ratio, the maximum shear strain at the core and top foundation was approximately 0.02, and the horizontal displacement 14 cm. For the ks/kc=100 the maximum shear strain reached a value of 0.03 and a horizontal displacement of 20 cm.

Good agreement between the pseudo-static FOS for the M-P method and SRT was obtained. As expected, the pseudo-static analysis with a Kh=0.05 showed an increase in the maximum shear strain of the facility compared to the static loading. The pseudo-static contours for the ks/kc=10000 ratio showed maximum shear strain of 0.07, and horizontal displacement of 50 cm. The ks/kc=100 ratio contours indicated a maximum shear strain of 0.12 and horizontal displacement of 70 cm.

The small displacements observed both under static and pseudo static analyses are indicators of the shear strain resistance of the constitutive materials of the WRTD. The results also confirmed that WRTD are good for water containment and have good seismic resistance.

The results are in agreement with the effects of embankment to core ratio on phreatic surface location and stability proposed by Vick (1983). It was observed that the higher the difference in permeability between the core and the embankment, the lower the phreatic surface through the core and less risk of internal erosion of the core. A high embankment to core permeability ratio is important to control seepage and to avoid pining due to migration of fine particles into other regions within the dam.

CHAPTER 6: TSF STABILITY ANALYSES WITH PROBABILISTIC APPROACH - RESULTS AND DISCUSSION

6.1 Sensitivity Analyses

The effect of material properties variability on the factor of safety was explored conducting a sensitivity analysis for each TSF. In each sensitivity analyses, the model parameters were varied across a range of values to identify those that governed the overall stability of the TSF. The critical parameters obtained from the sensitivity analyses were assumed as the random variables in the probabilistic analyses.

The sensitivity analyses were performed using the software Slide 6.0 by Rocscience (2006) and the M-P LEM. The effective shear strength parameters of the constitutive materials in each TSF were used for the analyses. The deterministic input values of each parameter were assumed as the mean values. A coefficient of variation (COV) was assigned to each material property based on the criteria presented in Table 6-1.

Table 6-1 Coefficients of variation for selected parameters

Property	COV	Source
Effective friction angle ϕ´ (deg)Overall tailings and non-tailings materials	5 to 20% 10 to 40 %	Summary of values reported by Cho (2007); Duncan (2000); Nadim, (2007); Sample et al.,(2009); Srivastava et al., (2010)
Effective friction angle ϕ´ (deg)Core	25 %	Hamade et al.,(2011)
Effective friction angle ϕ´ (deg)Tailings	25%	Assumed by the author based on the ranges proposed by Arnaouti (2012; Hamade et al., 2011; Villavicencio et al., 2011)
Effective cohesion c´ (kPa)	10-40%	Duncan (2000); Sample et al., (2009)
Bulk unit weight (kN/m^3)	2-13%	Cho (2007); Duncan (2000); Srivastava et al., (2010)

The standard deviation of each parameter was obtained from equation 3.28 in Chapter 3. The values of mean and standard deviation were used to specify the minimum and maximum value according to the ‘‘*Three-Sigma Rule*’’ proposed by Duncan (2000), Haldar (2000), and Rocscience (2006 and 2007).

Under this rule, 99.73% of all values of a normally distributed parameter fall within three standard deviations of the mean value. Therefore, the maximum and minimum values of the parameters are calculated as follows,

$$\begin{aligned} \text{Minimum value} &= \mu - 3\sigma \\ \text{Maximum value} &= \mu + 3\sigma \end{aligned} \qquad \textbf{(6- 1)}$$

The input parameters of sensitivity analyses for the UTSF and the WRTD are presented in tables 6-2 and 6-3 respectively.

Table 6-2 Input parameters for the sensitivity analysis of the UTSF

TSF regions	Material	Parameter	P.D	COV (%)	μ	σ	Min	Max
Bedrock	Limestone	c′	N	20	6000	1200	2400	9600
		ϕ′	N	7	42	2.94	33.2	50.82
		γ′	N	10	26	2.6	18.2	33.8
Foundation	Clayey Glacial Till	ϕ′	N	25	21	5.25	5.25	36.75
		γ′	N	10	17.9	1.79	12.53	23.27
Drainage	Mixed Sand and Gravel	ϕ′	N	10	34	3.4	23.8	44.2
		γ′	N	10	19.4	1.94	13.58	25.22
Starter Dyke	Native Borrow	ϕ′	N	25	35	8.75	8.75	61.25
		γ′	N	13	18.5	2.41	11.27	25.73
Mill Tailings	Silty-Sand	ϕ′	N	25	30	7.5	7.5	52.5
		γ′	N	25	20	5	5	35
Slime Tailings	Silty-Clay	c′	N	25	5	1.25	1.25	8.75
		ϕ′	N	25	5	1.25	1.25	8.75
		γ′	N	25	19.7	4.93	4.91	34.49
Embankment Dykes	Coarse Sand	ϕ′	N	25	30	7.5	7.5	52.5
		γ′	N	25	22.3	5.57	5.56	39.04

Each parameter was varied between in 50 equal increments, and the safety factor for the Global Minimum slip surface was calculated at each increment.

Table 6-3 Input parameter for the sensitivity analysis of the WRTD

TSF Regions	Material	Parameter	P.D	COV (%)	μ	σ	Min	Max
Bedrock	Limestone	c′	N	20	6000	1200	2400	9600
		ϕ′	N	7	42	2.94	33.18	50.82
		γ′	N	10	27	2.7	18.9	35.1
Core	Glacial Till	c′	N	20	12	2.4	4.8	19.2
		ϕ′	N	25	28	7	7	49
		γ′	N	10	21.5	2.15	15.05	27.95
Top Foundation	Silty Clay	c′	N	20	3	0.6	1.2	4.8
		ϕ′	N	20	50	10	20	80
		γ′	N	10	16.5	1.65	11.55	21.45
Embankment	Natural Borrow	ϕ′	N	7	35	2.45	27.65	42.35
		γ′	N	10	18.5	1.85	12.95	24.05
Tailings	Slimes	ϕ′	N	25	28	7	7	49
		γ′	N	10	16	1.6	11.2	20.8
Downstream Filter	Sand	ϕ′	N	7	34	2.38	26.86	41.14
		γ′	N	10	18	1.8	12.6	23.4
Upstream Filter	Mixed Sand and Gravel	ϕ′	N	10	36	3.6	25.2	46.8
		γ′	N	10	20	2	14	26
Drainage	Gravel	ϕ′	N	7	37	2.59	29.23	44.77
		γ′	N	10	19	1.9	13.3	24.7

The results of the parametric analyses were plotted in sensitivity graphs of safety factor versus the parameter value. All parameters were plotted on a normalized scale of 0 to 100 percent, where 0 represents the minimum value of each parameter, and 100 represents the maximum value of each parameter (Rocscience, 2006).

The sensitivity plots of the UTSF and the WRTD are presented in Figure 6-1 and Figure 6-2, respectively.

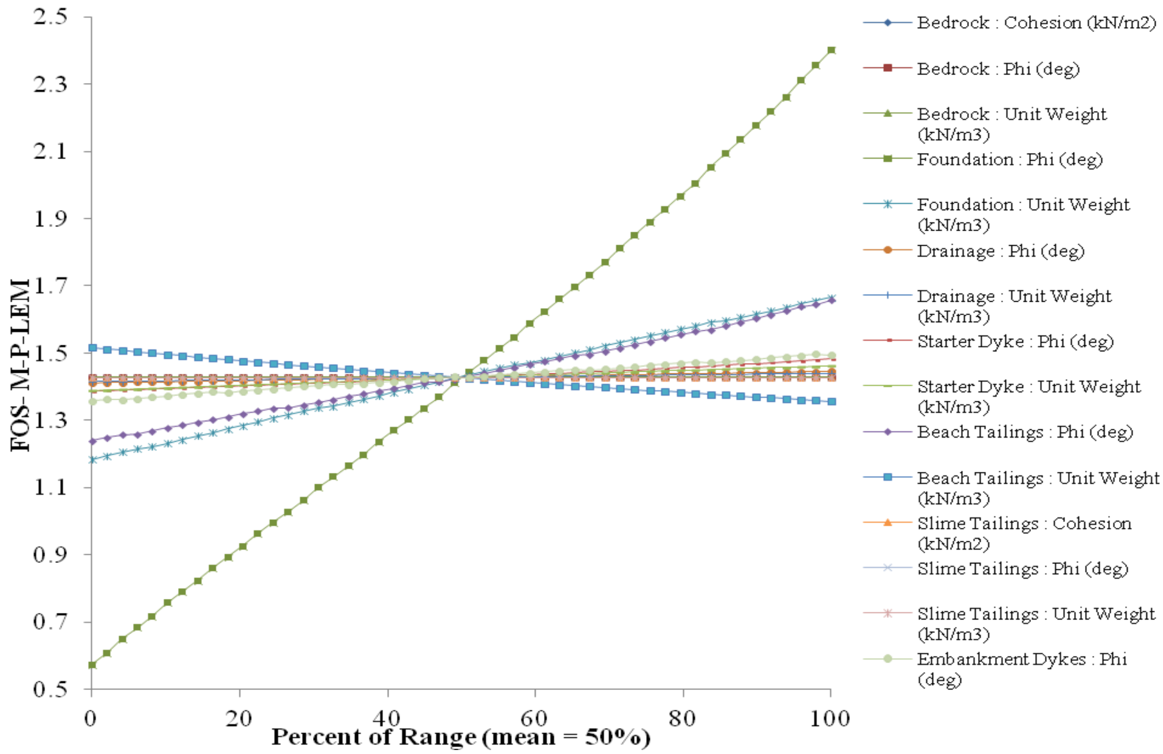

Figure 6-1 Sensitivity Analysis plot for the UTSF

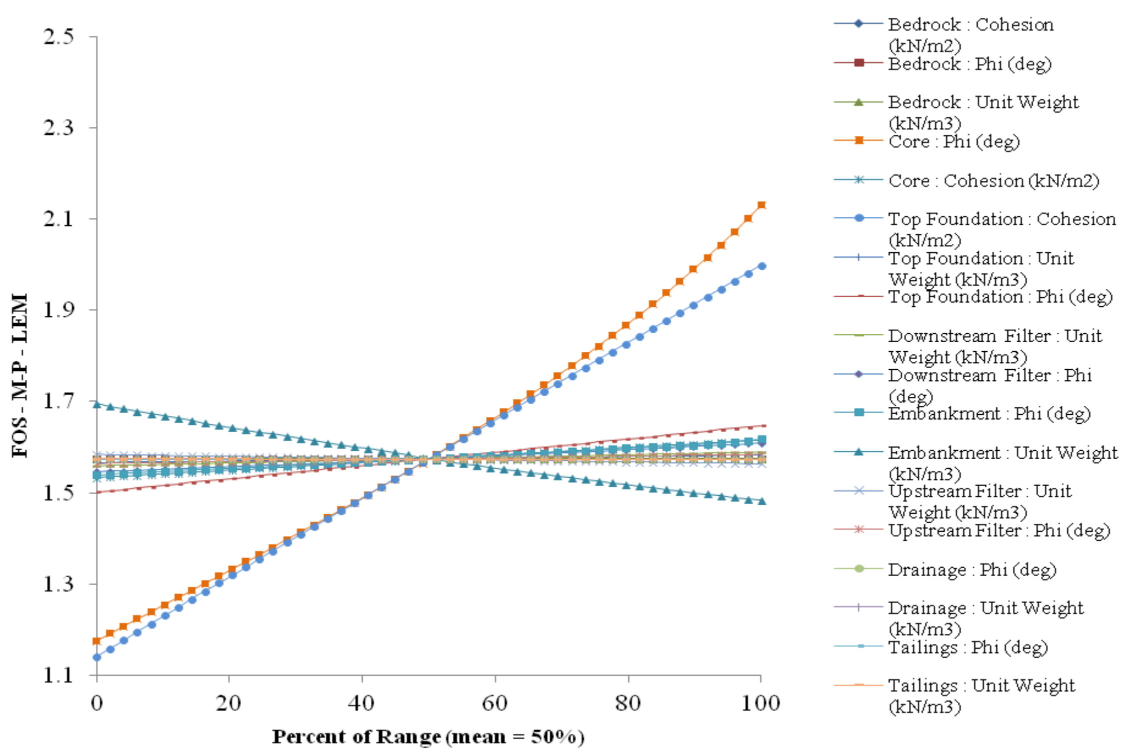

Figure 6-2 Sensitivity Analysis plot for the WRTD

6.2 Random variables

The results of the sensitivity analysis of the UTSF presented in Figure 6-3 shows that the foundation's friction angle is the parameter that governs the overall stability of the impoundment with mean value of 21.4˚ and standard deviation of 5˚. In the case of the WRTD, the sensitivity analysis indicated that the overall stability is governed by two parameters: the core's friction angle, with a mean value of 28.6˚ and standard deviation of 6.7˚ (Figure 6-4), and the top foundation's effective cohesion, with a mean value of 49.8 kPa and a standard deviation of 10 kPa (Figure 6-5). All random variables were considered independent and with a normal distribution.

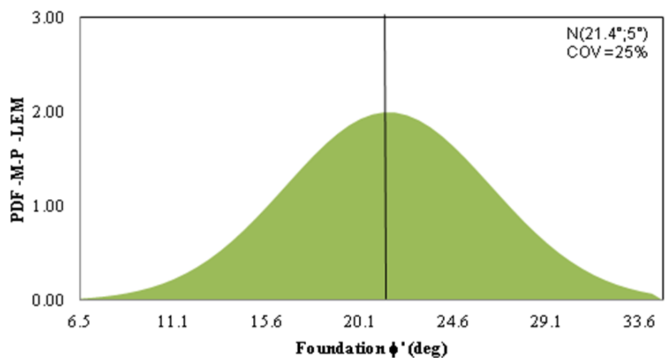

Figure 6-3 PDF of foundation's effective friction angle – UTSF

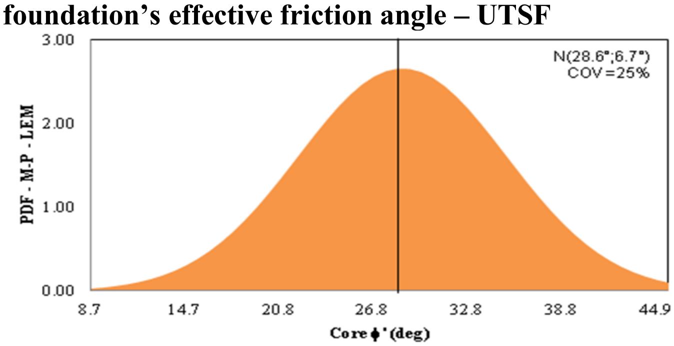

Figure 6-4 PDF of core's effective friction angle – WRTD

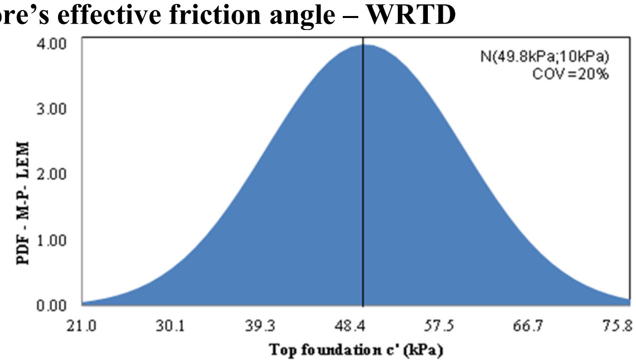

Figure 6-5 PDF of the top foundation's effective cohesion – WRTD

6.3 Probabilistic Analyses methods applied to the case studies

The objectives of the probabilistic analysis were: to complement the information provided by the deterministic analysis by obtaining a distribution of the FOS of each TSF; to identify the zones within the TSFs that bear the highest risk for instability: to incorporate the variability of material properties into the FOS calculation; to obtain an estimate of the probability of failure the TSFs under different loading conditions; and to obtain the reliability index to assess the estimated level of performance of each TSFs. Accordingly, the following sections present the results of the UTSF and WRTD stability analyses using the probabilistic approach using the same rationale loading conditions of the deterministic approach.

6.3.1 Monte Carlo Simulation MCS

The MCS consisted in 1000 runs of the R.V and recalculation of the FOS using the rigorous M-P LEM. The probability density functions of the static and pseudo-static FOS were calculated according to equations 3-23 in Chapter 3. The probability of failure and reliability index for each loading condition were calculated using the outcome of the MCS runs in conformity to equation 6-2 and equation 3-37, respectively:

$$p_f = \frac{number\ \text{failed}}{number\ \text{samples}} x100\% \quad \textbf{(6- 2)}$$

$$\beta_{RI(Normal)} = \frac{\mu_{FS} - 1}{\sigma_{FS}} \quad \textbf{(3-37)}$$

6.3.2 Point Estimate Method PEM

The probabilistic analyses with the PEM were conducted using the 2^n criteria. For the UTSF, 2 point estimates were ran twice 1 random variable as follows:

- UTSF PEM weight points (2^1=2) at $\mu \pm 1\sigma \rightarrow$ P++ = P-- = (1/2)

For the WRTD, 4 point estimates were ran for 2 random variables as follows:

- WRTD PEM weight points (2^2=4) at $\mu \pm 1\sigma \rightarrow$ P++ = P- - = (1/4)

  P+ - = P- + = (1/4)

6.4 Convergence graphs

In order to investigate whether the MCS converged to a final answer with the number of runs selected, convergence graphs of the mean FOS vs. number of samples were prepared. The convergence graphs of the UTSF and the WRTD are presented in Figures 6-6 and 6-7, respectively. The figures show that the FOS becomes relatively stable after approximately 600 runs and the analysis converges to a final answer after the 1000 runs. It can be inferred from these graphs, that a smaller number of runs, e.g., 800 runs, would also have been a good number to conduct the probabilistic stability analyses.

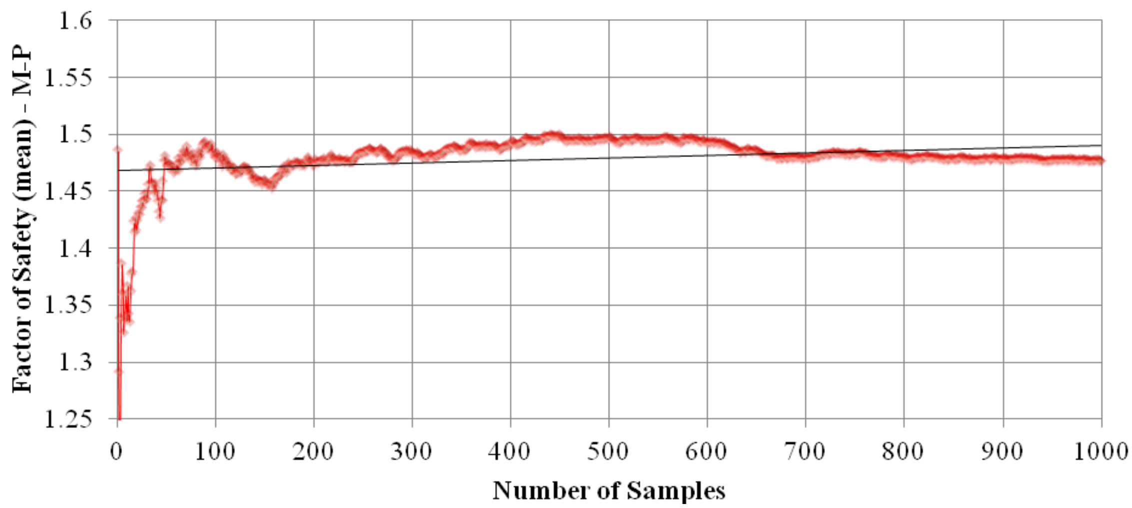

Figure 6-6 Convergence plot 1000 MCS Static FOS – M-P method – USTF

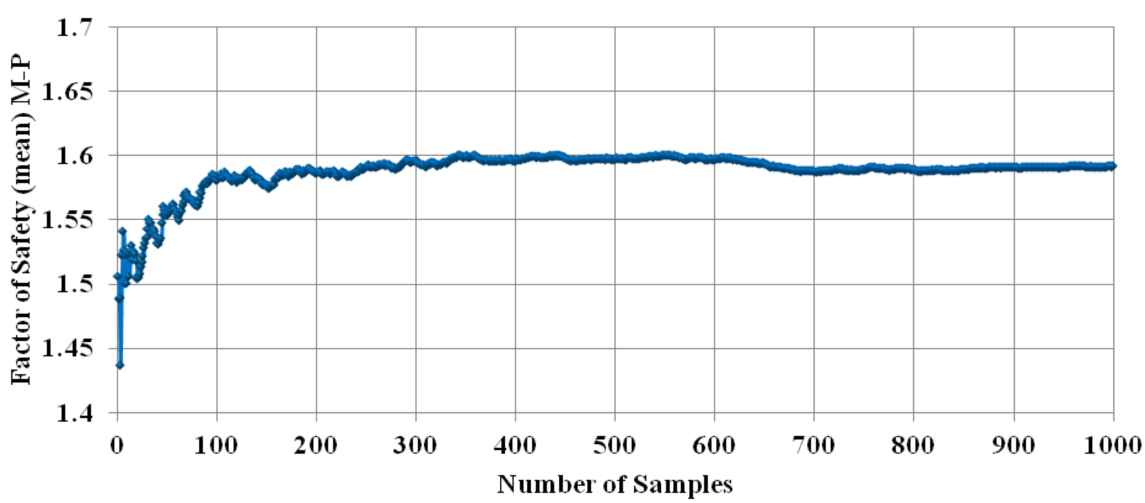

Figure 6-7 Convergence plots for 1000 MCS Static FOS M-P method – WRTD

The degree of correlation between each random variable and the factor of safety was examined through scatter correlation plots. The correlation coefficient can vary between -1 and 1; numbers close to zero is a sign of poor correlation, and numbers close to 1 or -1 signify a good correlation (Rocscience, 2006). The obtained scatter correlation plots of each random variable are presented in Figures 6-8, 6-9 and 6-10, respectively.

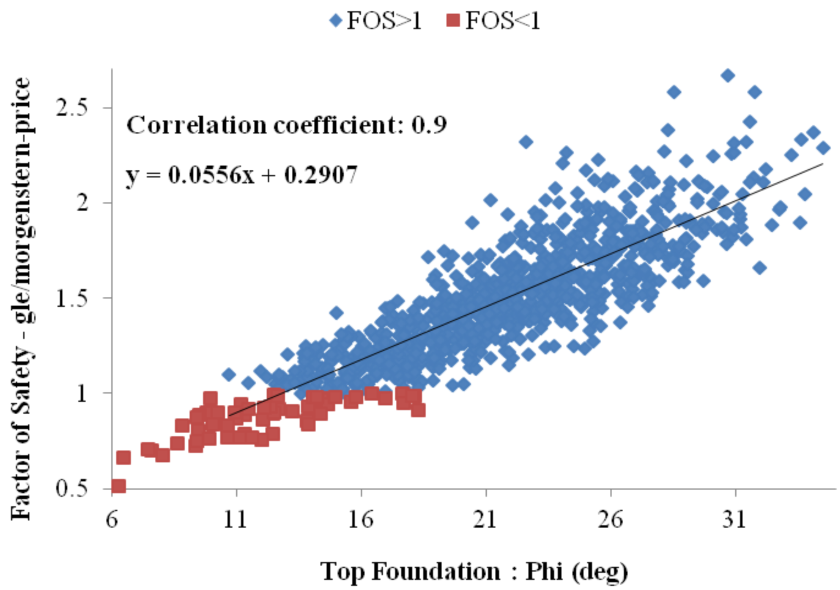

Figure 6-8 Scatter Plot FOS vs. Top Foundation's Friction Angle – UTSF

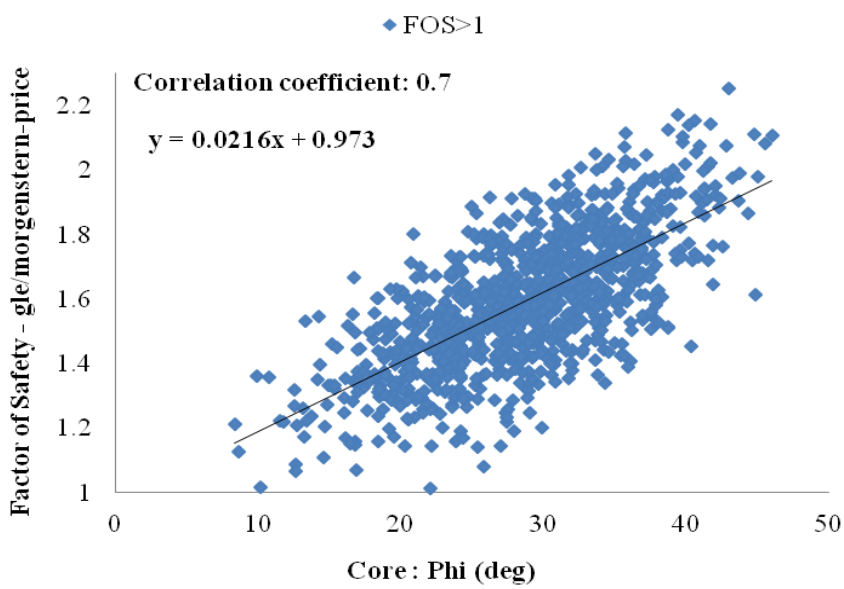

Figure 6-9 Scatter Plot FOS vs. Core's Friction Angle – WRTD

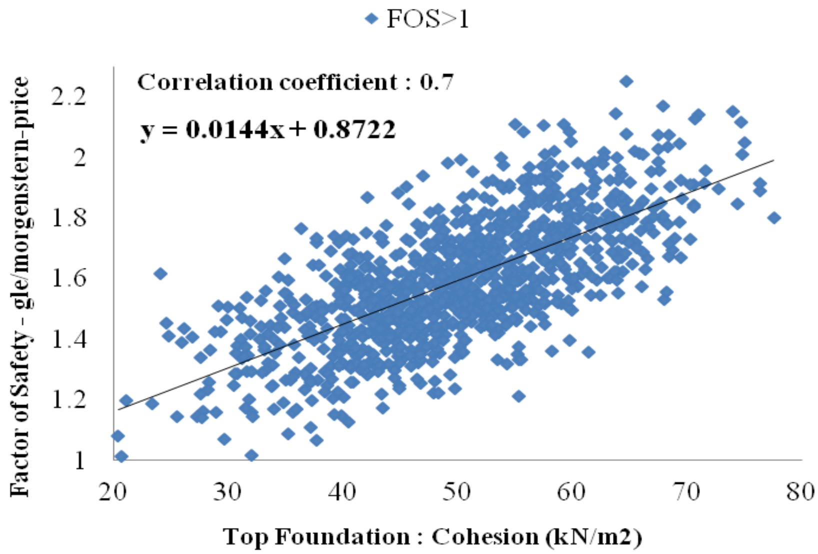

Figure 6-10 Scatter Plot FOS vs. Top Foundation's cohesion – WRTD

6.5 Effect of embankment height increase on the UTSF stability

The deterministic stability analysis of the UTSF gave evidence of the reduction in the FOS as the embankment increased in height. The most critical FOS reduction occurred at the embankment's ultimate height. The embankment's ultimate height is a very important stage of analysis because it frames the final configuration of the TSF for closure and long-term stability analyses.

The results show that the UTSF did not meet the minimum requirements for static steady state - long term analyses (FOS obtained 1.48, minimum 1.5) in Quebec. The difference is not significant, but the results provided information about the probability of failure or level of expected performance of the UTSF that could be used for decision making purposes. Consequently, the usefulness of probabilistic analysis under static and pseudo static loading was reinforced.

Table 6-4 summarizes the results of mean FOS, probability of failure (*pf*) obtained for the static and pseudo-static probabilistic analyses of the UTSF after fitting the FOS into a normal distribution. The standard deviation and reliability index obtained at each height increase are also provided in the summary.

Table 6-4 Probabilistic analysis for increasing embankment height –UTSF using MCS and-M-P method

Embankment Height (m)	Static				Pseudo-static			
	Mean FOS	σ	P_f	β	Mean FOS	σ	P_f	β
15.5	1.61	0.36	0.03	1.71	1.32	0.30	0.14	1.05
20.75	1.59	0.37	0.05	1.61	1.30	0.30	0.15	0.99
26	1.54	0.36	0.06	1.48	1.27	0.29	0.16	0.92
31.25	1.51	0.36	0.07	1.43	1.24	0.29	0.18	0.84
36	1.48	0.34	0.07	1.41	1.23	0.28	0.19	0.82
41.75	1.48	0.33	0.07	1.40	1.23	0.26	0.22	0.86

Note: Kh=0.05 for pseudo-static analysis

6.5.1 Static and pseudo-static results

Form the results in Table 6-4 a safety decrease of 8.07% decrease from the starter dyke construction until the ultimate height of the embankment was calculated. The probability of failure at the embankment's ultimate height is 0.07. The expected level of performance is unsatisfactory because the static FOS is below the minimum requirement in Quebec. Nonetheless, the reliability index and probability of failure indicate that no catastrophic behaviour should be expected from the embankment. Under pseudo-static loading, a safety reduction of nearly 7% was observed (FOS went from 1.32 to 1.23). The the probability of failure increased and reached 0.22. The reliability index was 0.86 and indicates a hazardous perfomance of the UTSF. Figure 6-11 shows the variation the of mean FOS with increasing embankment height for static and pseudo-static loading.

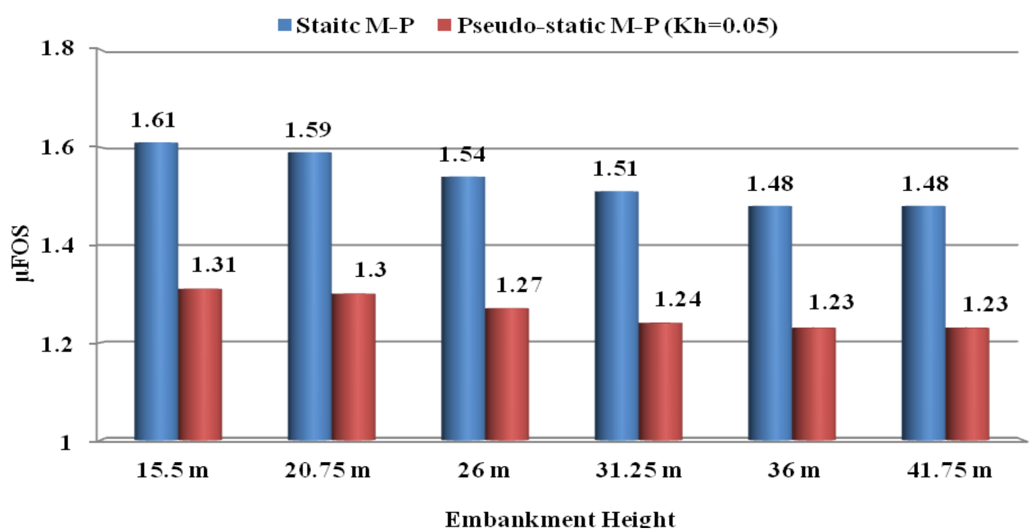

Figure 6-11 Static and Pseudo-static FOS for increasing embankment height using MCS – M-P method; USTF

The pseudo-static PDFs presented in Figure 6-12 shows a larger area under the curve for the pseudo-static FOS compared to the static PDF. However, possibility of failure is observed under both loading conditions. This means that under variable gradation, strength conditions, or unusual events, the UTSF has the potential to develop a hazardous performance. Therefore, optimum maintenance and operational practices must be sustained through the life time of the facility.

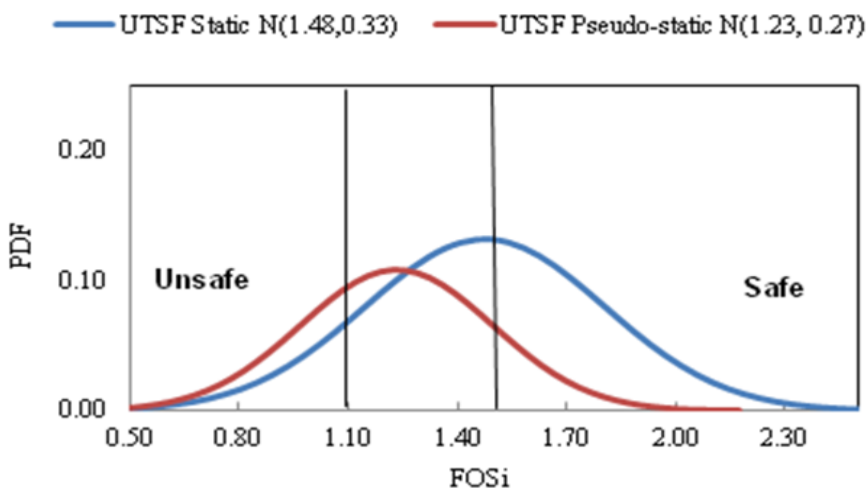

Figure 6-12 Static and Pseudo-static PDF of FOS at embankment's ultimate height – MCS and M-P method

The decrease in FOS with embankment height implies an increase in the probability of failure under static and pseudo static loading of the UTSF as shown in Figure 6-13.

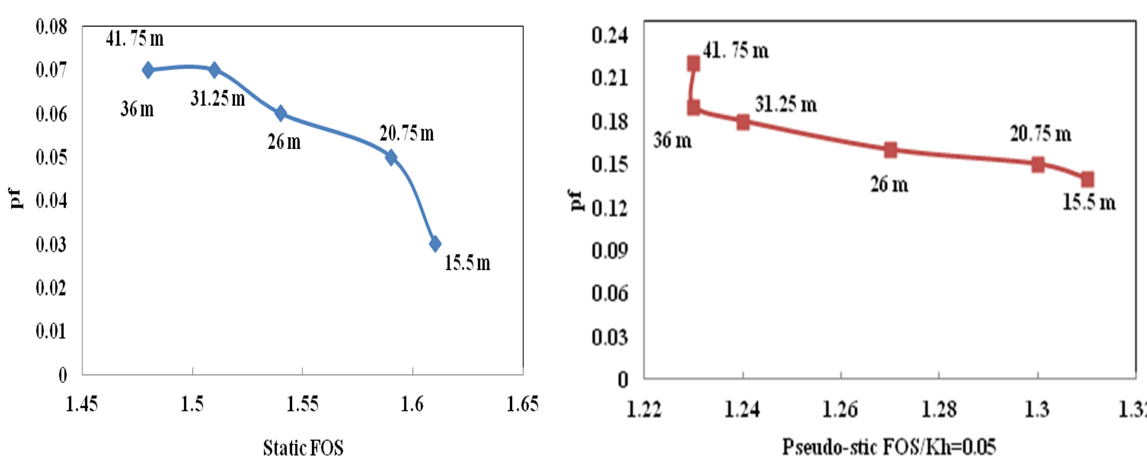

(a) Static (b) Pseudo-static

Figure 6-13 Probability of failure respect to the static FOS for increasing embankment height - UTSF

6.6 Effect of phreatic surface location and beach width ratio (L/H) on the UTSF stability

The results of beach width ratio reduction on the UTSF stability showed that as the distance between the phreatic surface and the embankment reduces, the FOS reduces and the probability of failure increases. The reduction in the FOS is an indicator of loss of shear strength of the constitutive materials of the embankment due to pore pressure increase. Overall good correspondence between the MCS and PEM results of mean FOS was obtained. The mean FOS under static and pseudo static loading was below the minimum requirement. Both probabilistic methods yielded similar probabilities of failure and reliability indices that helped classify the level of performance as unsatisfactory for a limit beach width ratio (L/H=6), and hazardous for a critical beach width ratio (L/H=4), however, higher probabilities of failure were obtained with the PEM. The results of the static probabilistic are summarized in Table 6-5.

6.6.1 Static results

Table 6-5 Probabilistic analysis for limit and critical phreatic surface locations for static state using LEM and SRT - UTSF

L/H=6	MCS M-P	PEM -SRT	L/H=4	MCS M-P	PEM- SRT
μFOS	1.48	1.42	μFOS	1.35	1.31
σFOS	0.33	0.38	σFOS	0.31	0.40
Pf	0.06	0.14	Pf	0.13	0.22
Β	1.45	1.10	β	1.13	0.78

As expected, the PDF and CDF presented in Figure 6-14 shows a larger area under the curve within the failure zone for the critical beach width ratio (L/H=4).

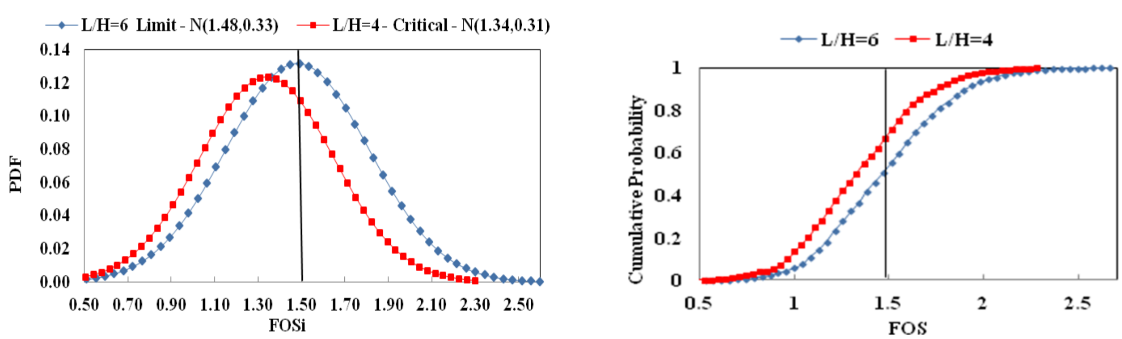

(a) PDF (b) CDF

Figure 6-14 PDF and CDF of the FOS for L/H=6 and L/H=4 ratio using MCS and M-P method

The results in figure 6-15 show that UTSF stability is highly dependent on the water management methods applied to keep the phreatic surface at a safe distance from the embankment and avoid strength loss. Strength loss is the fundamental trigger for liquefaction and slope instability related failure.

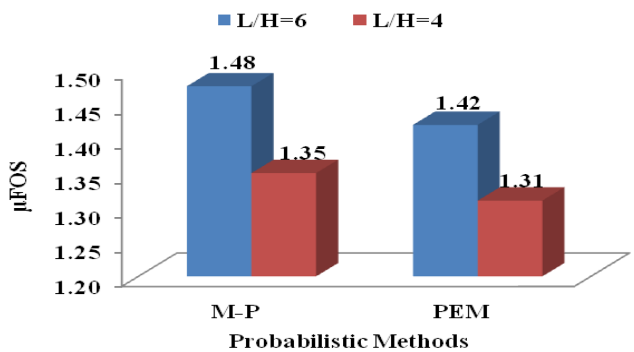

(a) Mean static FOS

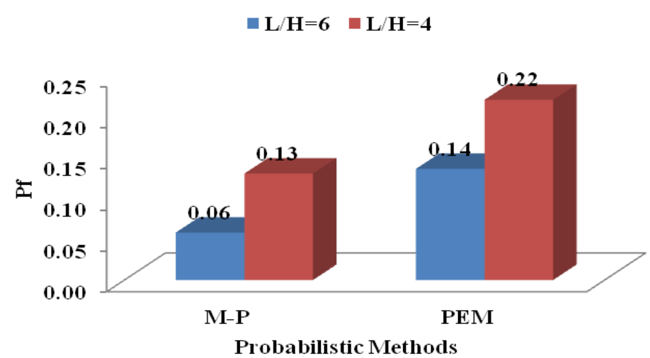

(b) Probability of failure

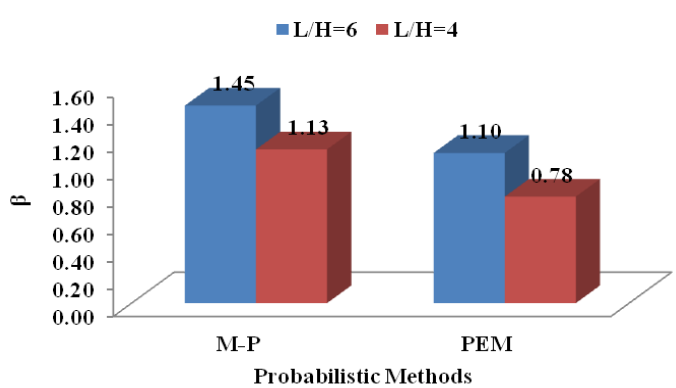

(c) Reliability index

Figure 6-15 Summary of static probabilistic analysis for L/H=6 and L/H= 4 using MCS and PEM.

6.6.2 Pseudo -static results

Table 6-6 Pseudo-static probabilistic analysis of the UTSF with (L/H=6) and (L/H=4) using MCS and PEM

L/H=6	Kh=0.038		Kh=0.05		Kh=0.1	
	MCS-M-P	PEM	MCS-M-P	PEM	MCS-M-P	PEM
μFOS	1.28	1.23	1.23	1.18	1.05	0.83
σFOS	0.28	0.37	0.27	0.38	0.22	0.10
Pf	0.15	0.27	0.22	0.32	0.43	0.69
B	1.00	0.61	0.86	0.47	0.22	-1.72
L/H=4	**MCS-M-P**	**PEM**	**MCS-M-P**	**PEM**	**MCS-M-P**	**PEM**
μFOS	1.16	1.12	1.11	1.09	0.95	0.89
σFOS	0.26	0.38	0.25	0.36	0.30	0.32
Pf	0.28	0.38	0.34	0.41	0.60	0.73
B	0.63	0.31	0.46	0.25	-0.16	-0.35

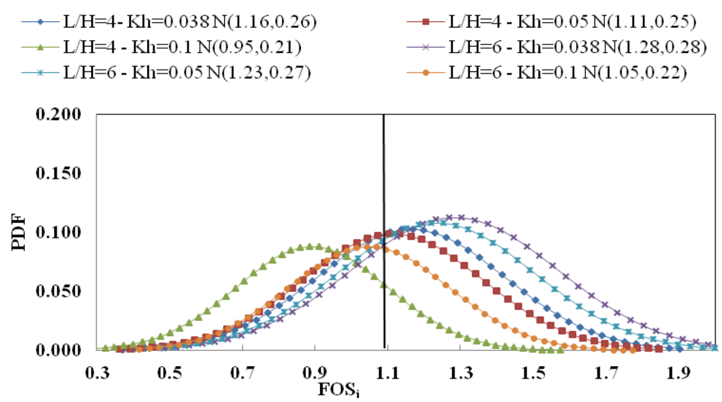

Figure 6-16 PDF of the pseudo-static FOS of the UTSF with L/H=6 and L/H=4 for increasing seismic coefficients; MCS using M-P method

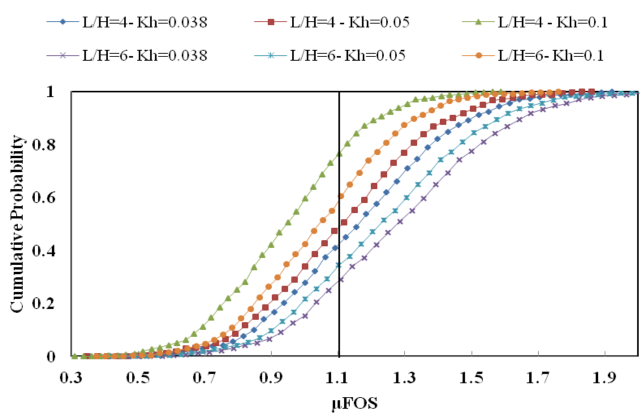

Figure 6-17 CDF of the pseudo-static FOS of the UTSF with L/H=6 and L/H=4 for increasing seismic coefficients

Figures 6-16 and 6-17 showed a direct relation between Kh and probability of failure. The larger the Kh the larger the area under the curve in the failure zone for all beach width ratio.

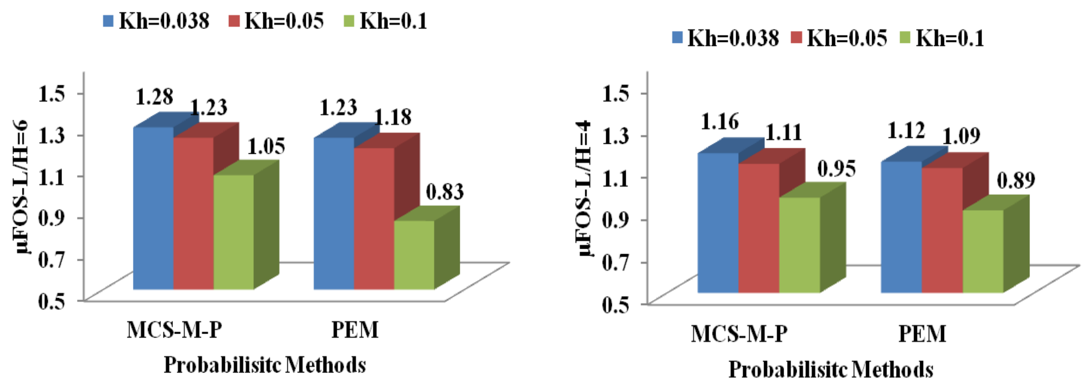

(a) Mean pseudo- static FOS

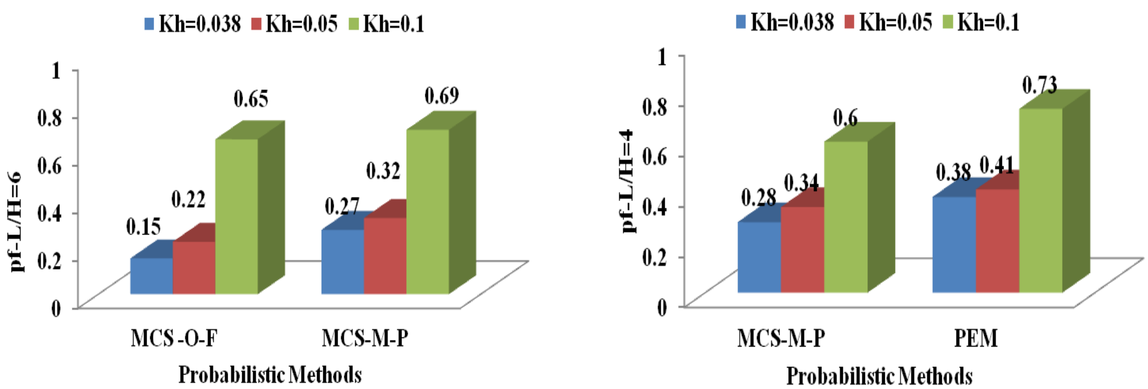

(b) Probability of failure

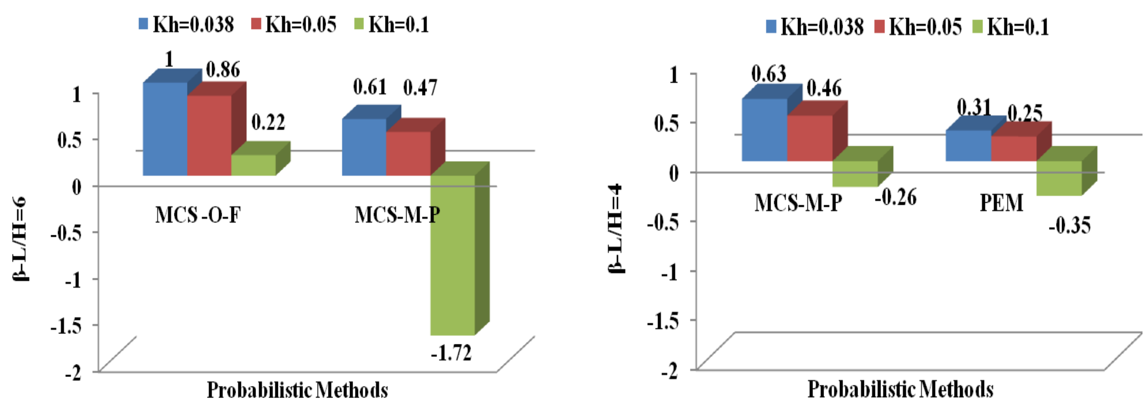

(c) Reliability index

Figure 6-18 Summary of pseudo-static probabilistic analysis for L/H=6 and L/H= 4 using MCS and PEM.

The probability of failure and reliability indices of the pseudo-static analysis showed in Figure 6-18 depicts a hazardous level of performance for UTSF under all seismic conditions. This confirms that UTSF are not recommended for zones of moderate to high seismicity or water storage. Good association between MCS and PEM was observed.

Effect of Tailings Height increase on the WRTD stability

6.6.3 Static and pseudo-static results

The probabilistic analysis on the effect tailings height increase on the WRTD stability showed that as the dam is filled with tailings the FOS decreases and the probability of unsatisfactory performance increases. The reliability indices and probabilities of failure of the WRTD showed high levels of performance under static and pseudo-static loading. However, when tailings reach the ultimate operational height, the reliability index reduces significantly, and a poor level of performance can be expected. The results of the analysis are summarized in Table 6-7 and Figure 6-19.

Table 6-7 Probabilistic analysis–WRTD for increasing tailings height using MCS and M-P method

Tailing Height	Static				Pseudo-static Kh=0.05			
	Mean FOS	Σ	Pf	β	Mean FOS	σ	Pf	β
4 m	1.78	0.21	0.00	3.62	1.55	0.18	0.000	3.05
8 m	1.74	0.21	0.00	3.54	1.47	0.17	0.001	2.76
12 m	1.66	0.20	0.00	3.37	1.40	0.16	0.008	2.50
14 m	1.60	0.19	0.00	3.18	1.34	0.15	0.011	2.26
16 m	1.59	0.19	0.00	3.11	1.34	0.14	0.011	2.11
18 m	1.59	0.21	0.00	2.96	1.33	0.17	0.024	1.95

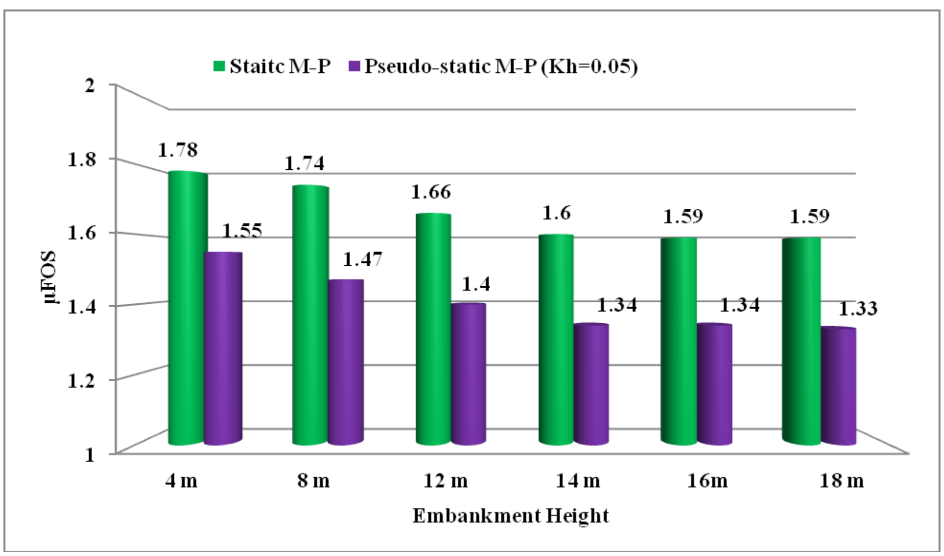

Figure 6-19 Static and Pseudo-static FOS of the WRTD for increasing tailings height using MCS – M-P method

The probability density function of the static and pseudo-static FOS shown in Figure 6-20 show that even under seismic loading, the WRTD meets the minimum requirements in Quebec. For instance, the average pseudo-static FOS with a Kh-0.05 was 1.34.

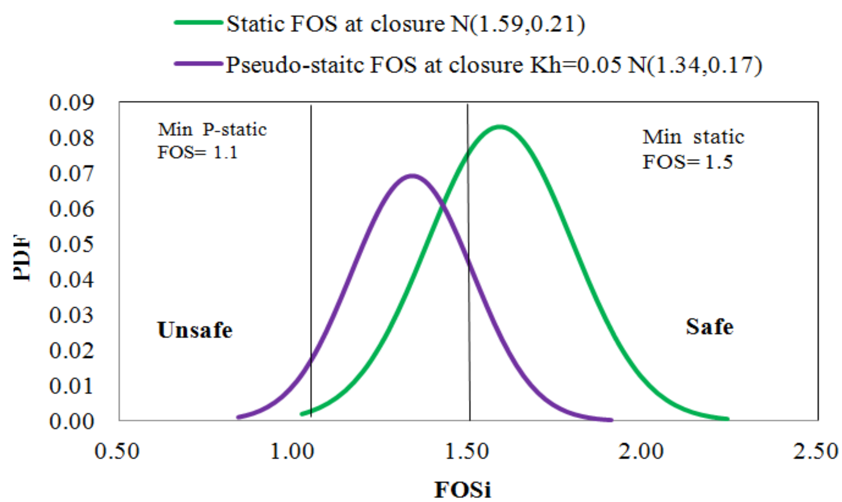

Figure 6-20 PDF of the static and pseudo-static FOS at the tailings' ultimate height using MCS- M-P method; Kh =0.05 -WRTD

Nonetheless, it is important to highlight that seismicity should always be taken into consideration in stability analyses because it acts as a major cause of instability. For the case of the WRTD shown in Figure 6-21a and b, tailings at 18 m of height in steady state had zero probability of failure, whereas with the effect of seismicity, safety decreased in a 16.4 %. As mentioned before, even if the risk increase is not remarkable, it might increase under more severe seismic events or in combination with other unusual events such as floods or unexpected precipitation or snow.

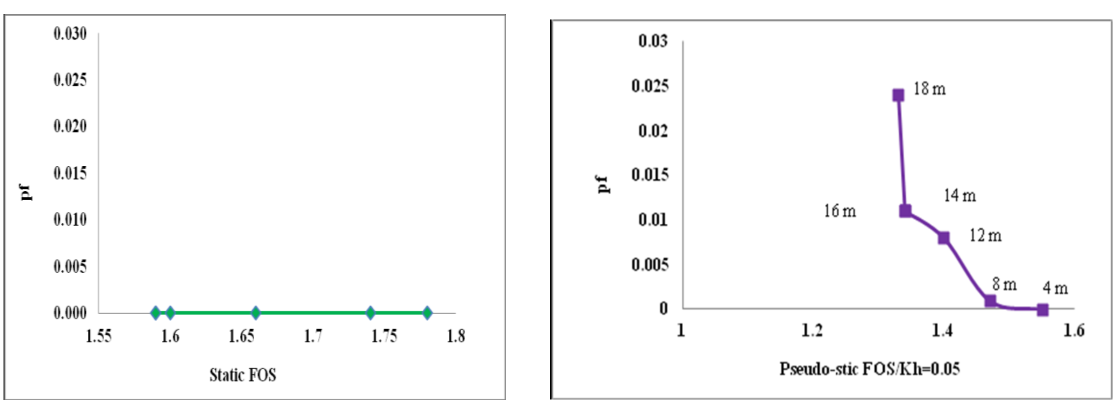

(a) Static (b) Pseudo-static

Figure 6-21 Probability of failure vs. static and pseudo-static FOS for increasing tailings height - WRTD

6.7 Effect of the embankment to core permeability ratio (ks/kc) reduction on the WRTD stability

6.7.1 Static results

Table 6-8 Static probabilistic analysis of the WRTD for changing ks/kc using MCS and PEM

k_s/k_c =1000	MCS-M-P	PEM	k_s/k_c =100	MCS- M-P	SRT
μFOS	1.59	1.58	**μFOS**	1.56	1.51
σFOS	0.21	0.14	**σFOS**	0.21	0.18
Pf	0.000	0.000	**Pf**	0.002	0.003
Β	2.84	4.30	**β**	2.74	2.81

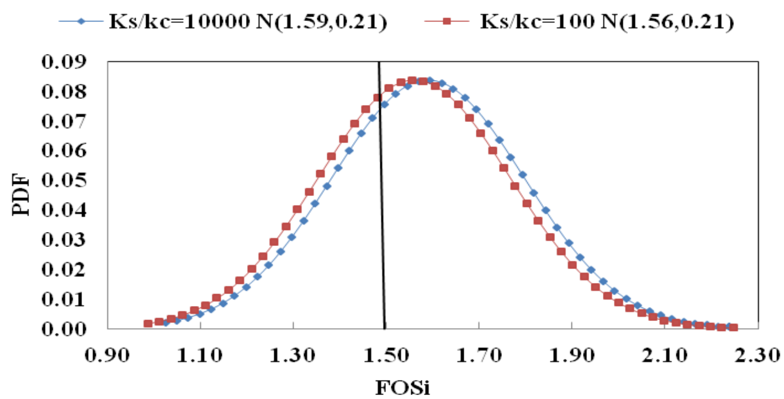

Figure 6-22 PDF of the static FOS for ks/kc=10000 and ks/kc=100 using MCS and M-P method -WRTD

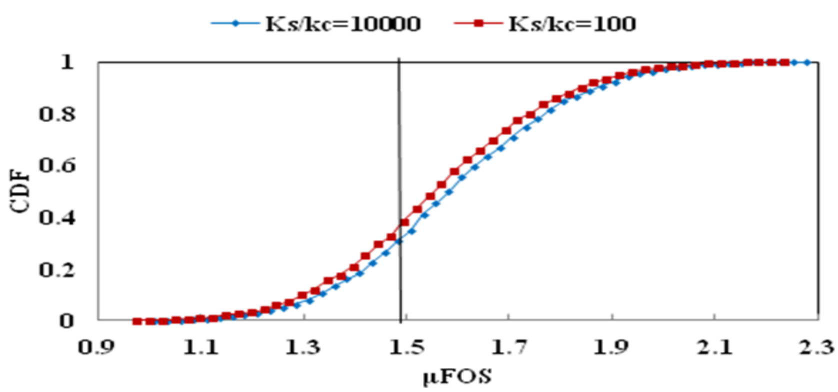

Figure 6-23 CDF of the static FOS for ks/kc=10000 and ks/kc=100 - WRTD

The conclusion of this particular static probabilistic analysis is that a variation in the embankment to core permeability of the WRTD does not have a significant effect on the stability of the impoundment. As shown in Table 6-8, and Figures 6-22 and 6-23, the PDF and CDF for ks/kc=10000 and ks/kc=100 were almost the same. Figure 6-24 contains a summary of the static analysis results.

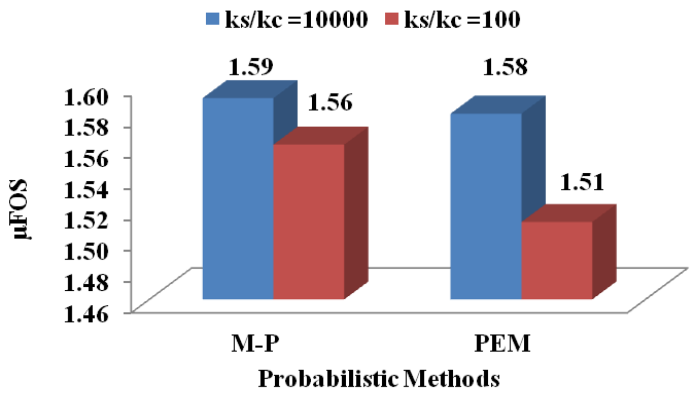

(a) Mean static FOS

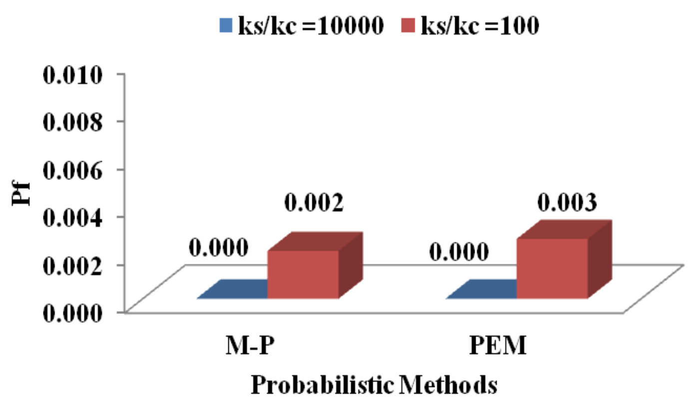

(b) Probability of failure

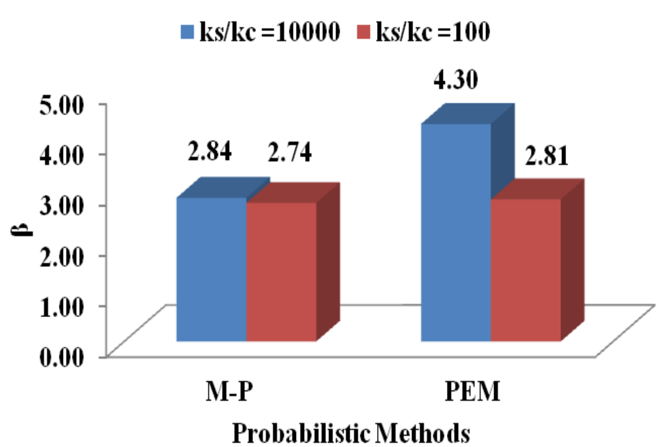

(c) Reliability Index

Figure 6-24 Summary of static probabilistic analysis of the WRTD with ks/kc=10000 and ks/kc=100 using MCS and PEM.

6.7.2 Pseudo-static results

Table 6-9 Pseudo-static probabilistic analysis of the WRTD with ks/kc=10000 using MCS and PEM

k_s/k_c =10000	Kh=0.038		Kh=0.05		Kh=0.1	
	MCS-M-P	PEM	MCS-M-P	PEM	MCS-M-P	PEM
μFOS	1.39	1.44	1.34	1.42	1.15	1.32
σFOS	0.18	0.18	0.17	0.19	0.15	0.20
Pf	0.010	0.006	0.024	0.013	0.187	0.058
β	2.17	2.50	1.95	2.21	0.90	1.55
k_s/k_c = 100	MCS-M-P	PEM	MCS-M-P	PEM	MCS-M-P	PEM
μFOS	1.36	1.41	1.31	1.40	1.12	1.31
σFOS	0.18	0.19	0.17	0.20	0.15	0.23
Pf	0.019	0.014	0.028	0.025	0.202	0.077
β	2.03	2.18	1.81	1.97	0.85	1.37

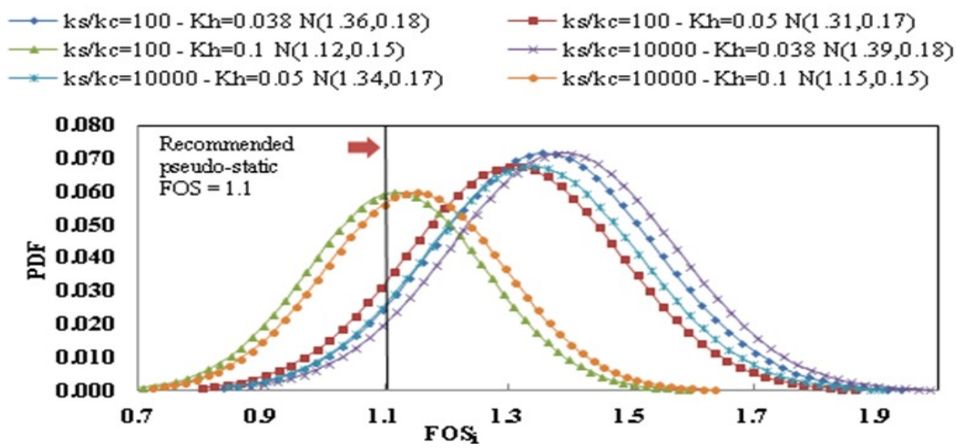

Figure 6-25 PDF of pseudo-static FOS for ks/kc=10000 and ks/kc=100 and increasing seismic coefficients using MCS using M-P method - WRTD

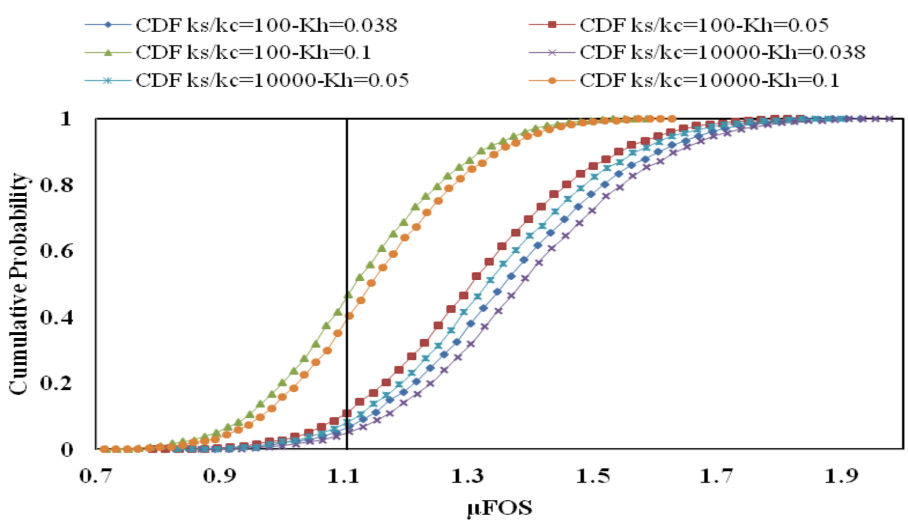

Figure 6-26 CDF of the pseudo-static FOS for ks/kc=10000 and ks/kc=100 for MCS using M-P method -WRTD

Table 6-9, along with Figures 6-25 and 6-26 show a decreasing level of performance of the WRTD as the seismic coefficient increases. This implies that WRTD despite their good seismic resistance, WRTD could also attain hazardous performance under a severe seismic event (e.g. Kh=0.1 or higher).

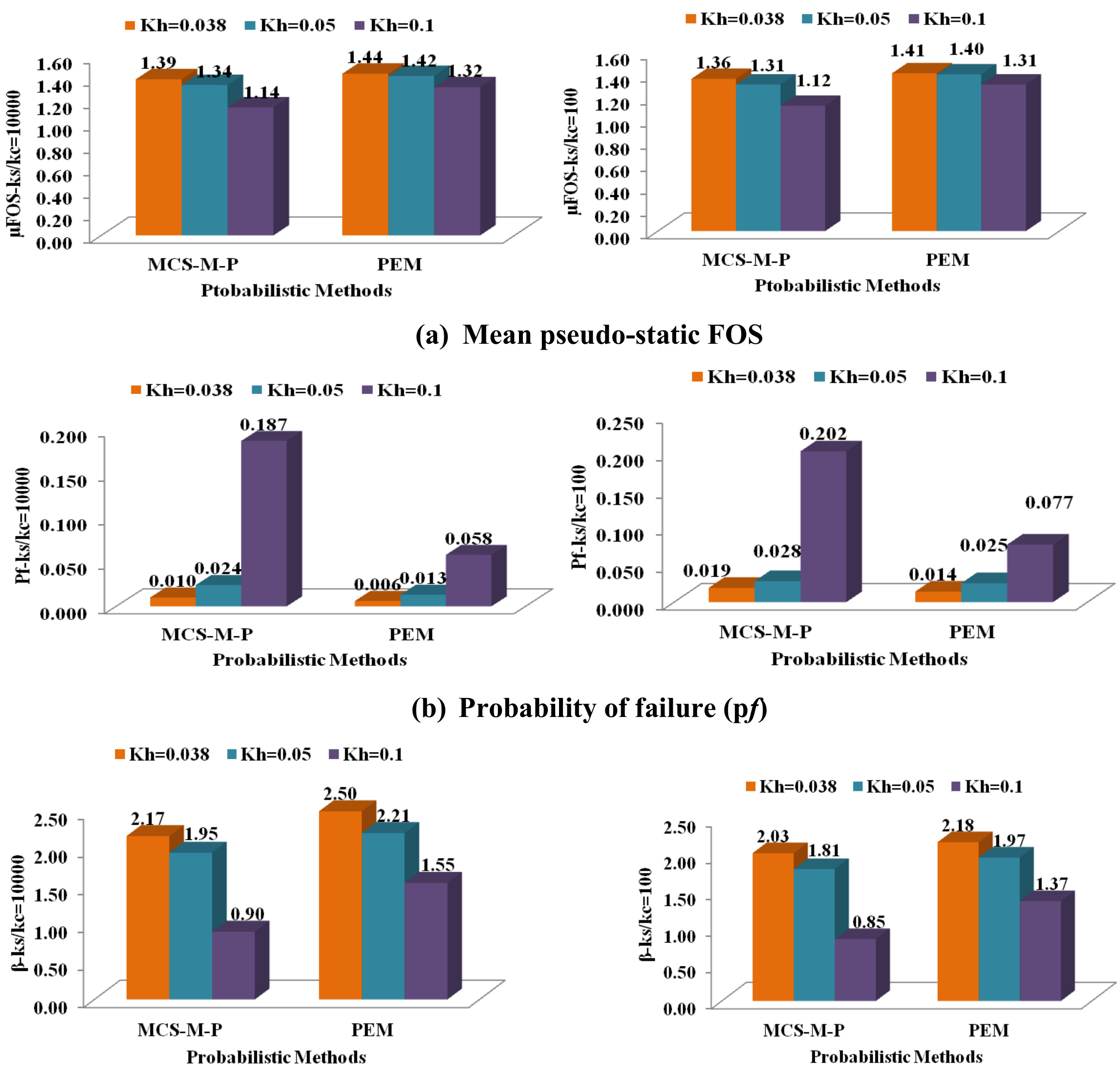

(a) Mean pseudo-static FOS

(b) Probability of failure (p*f*)

(c) Reliability Index (β)

Figure 6-27 Summary of pseudo-static probabilistic analysis for ks/kc=10000 and ks/kc=100 using MCS and PEM.

The results of the pseudo-static probabilistic analysis of the effect of embankment to core permeability reduction were similar than those of the static case. Figure 6-27 shows that the overall behaviour of the WRTD of the dam was not affected by the permeability ratio variation. Good agreement between probabilistic MCS and PEM was observed.

CHAPTER 7: CONCLUSIONS

- A comparative stability analysis of two typical tailings storage facilities under static and pseudo-static states was conducted. The analyses were performed for different loading conditions and following the deterministic and probabilistic approach. Likewise, the advantages and limitations of using Limit Equilibrium Methods compared to the Finite Element Method and Shear Reduction Technique for TSF stability analysis were analysed.

- The comparative analyses showed that the water retention tailings dam exhibits smaller horizontal displacements, lower shear strain levels, and hence, a larger factor of safety. For all loading conditions smaller probability of failure and higher reliability indices were obtained compared to those of the upstream tailings storage facility. The pseudo- static analyses confirmed larger displacements and significant reduction in the FOS at all stages of construction and methods for both tailings facilities. Overall, the WRTD exhibited a better and higher level of performance under static and pseudo-static compared to the UTSF.

- It was found that the factor of safety varied within the rigorous Morgenstern-Price LEM and simplified Ordinary-Fellenius LEM under identical analysis conditions. These variations affect the stability assessment if just one LEM is considered. It is important to use at least one rigorous method that satisfies moment and force equilibrium and takes into consideration the interslice forces and to compare it to a non-rigorous method for a better understanding of the static behaviour of the TSF.

- Generally, a better correspondence of the factor of safety calculation between the Morgenstern-Price Limit Equilibrium Method and Strength Reduction Technique results was observed. However, a higher degree of confidence is given to the Shear Reduction Technique results because information about displacement, deformation, stress, and pore pressure distribution were obtained along with the FOS without making assumptions about the failure mechanisms.

- Analyses on the effect of embankment or tailings height on stability showed that the vertical load increase applied by the weight of the embankment or the tailings decreases the FOS. However, more remarkable changes were observed in the UTSF.

- The analysis of the effect of beach width ratio variation on the USTF stability showed that as the phreatic surface approaches the embankment there is a significant reduction in the FOS and the level of performance became unsatisfactory or hazardous. These observations confirmed the fact that UTSF is not recommended for sites of high seismicity or water storage due to the high liquefaction susceptibility of non-cohesive tailings of low plasticity.

- The reduction in the embankment to core permeability ratio on the WRTD stability did not have a significant effect on the overall behaviour of this type of TSF. Nonetheless, a slight reduction in the FOS, reliability index, and higher probability of failure was obtained for ks/kc=100, more specifically, under pseudo-static conditions. It was confirmed, however, that WRTD are good options for sites with high water storage requirements and moderate to high seismicity because all FOS met Quebec requirements under static and pseudo-static states.

- It was concluded that adopting the probabilistic approach is the best geotechnical practice for TSFs stability analyses because the intrinsic uncertainty of material properties is accounted for and the probability of failure and reliability index provide valuable information about the most likely behaviour of the impoundment that can support engineering judgment and decision making processes.

- The Monte Carlo and Point Estimate probabilistic analyses showed lower factors of safety, higher probability of failure Pf, and lower reliability index β for the upstream tailings dam. This could be attributed to the intrinsic low consolidation rate of deposited tailings. In general, good agreement between these two probabilistic methods was found.

7.1 Recommendations for future research

It is considered that future research on the topics that were either a limitation or out of the scope of the present thesis are of great importance in tailings storage facilities stability assessment and mining applications. Some of these subjects would be:

- Conduct a full coupled hydrodynamic stability analysis of the models using advanced numerical modelling tools.
- Use the First Order Second Moment or Random Monte Carlo Simulation to conduct the probabilistic analysis and compare it to the Point Estimate Method.
- Explore the effect of using other simplified and/or rigorous limit equilibrium methods on the factor of safety (e.g. Corrected Janbu and Spencer)
- Conduct a study about liquefaction potential of the UTSF under pseudo-static loading at each stage of construction using the Undrained Shear Analysis approach at each stage of construction.
- Evaluate the effect of a Probable Maximum Precipitation on the phreatic surface location in the UTSF.
- Apply these methodologies to other types of raised embankment TSFs (e.g. centerline or downstream) and compare it to a water retention tailings dam.
- Conduct post-failure back analyses for each type of TSFs to identify the optimum shear strength conditions for long-term stability.

REFERENCES

Abadjiev, C.B., 1976. Seepage Through Mill Tailings Dams, Douzième Congrès international des grands barrages: Mexico, Mexique, 29 mars-2 avril 1976 : comptes rendus. Twelfth International Congress on Large Dams,. ICOLD, International Commission on Large Dams, Mexico City, Mexico, pp. 381-393.

Abadjiev, C.B., Germanov, T.S. and Markov G.T, 1987. Determination of Tailings Consolidation For a High Spigotted Upstream Tailings Dam, Groundwater effects in geotechnical engineering :proceedings of the ninth European Conference on soil mechanics and foundation. A.A . Balkema, SMFE, Dublin, Ireland, pp. 355-357.

Abitew, A., 2010. Hydro-Geotechnical Study of Tailings at Aitik Mine. Emphasis on Hydraulic Conductivity Deposit, Luleå University of Technology, Luleå

Aguello, A.J., Joshi, D. and Kidd, A.D., 2003. Seismic slope stability and deformation analyses for a heap leach facility, Proceedings of the Tenth International Conference on Tailings and Mine Waste, . Tailings and Mine Waste Vail, Colorado, USA.

Alencar, J., Morgenstern, N.R. and Chan, D.H., 1994. Analysis of Foundation Deformations beneath the Syncrude Tailings Dyke. Can Geotech J, 31(6): 868-884.

ANCOLD, 1999. Guidelines on tailings dams design, construction and operation. Australian National Committee on Large Dams, pp. 1-52.

Auvinet, G. and González, J.L., 2000. Three-dimensional reliability analysis of earth slopes. Computers and Geotechnics, 26(3-4): 247-261.

Avila, J., 2011. The Drained Stacking of Granular Tailings: A Disposal Mehtod for a Low Degree of Saturation of the Tailings Mass, Proceedings Tailings and Mine Waste, 2011, Vancouver, B.C., pp. 1-11.

Azam, S.L., Q., 2010. Tailings Dams Failures: A Review of the Last One Hundred Years, Geotechnical News. Waste GeOTechnics, pp. 50-53.

Babu, G.L.S., Srivastava, A. and Murthy, D.S.N., 2006. Reliability Analysis of the Bearing Capacity of a Shallow Foundation Resting on Cohesive Soil. Canadian Geotechnical Journal, 43: 217-223.

Babu, G.L.S., Srivastava, A. and Sahana, V., 2007. Analysis of Stability of Earthen Dams in Kachchh Region, Gujarat, India. Engineering Geology, 94: 123-136.

Baecher, G.B. and Christian, J.T., 2003. Reliability and Statistics in Geotechnical Engineering. John Wiley & Sons Ltd, The Atrium, Southern Gate, Chichester, West Sussex, England.

Baker, R., Shukha, R., Operstein, V. and Frydman, S., 2006. Stability charts for pseudo-static slope stability analysis. Soil Dynamics and Earthquake Engineering, 26(9): 813-823.

Bardet, J-P., 1997. Experimental Soil Mechanics. Prentice Hall.

Barrera, S., Velenzuela, L. and Campaña, J., 2011. Sand Tailings Dams: Design, Construction and Operation, Tailings and Mine Waste 2011. John Wiley & Sonds, Vancouver, pp. 1-13.

Blight, G.E., 1979. Properties of Pumped Tailings Fill. J S Afr I Min Metall, 79(15): 446-453.

Blight, G.E. and Bentel, G.M., 1983. The Behavior of Mine Tailings during Hydraulic Deposition. J S Afr I Min Metall, 83(4): 73-86.

Blight, G.E., Robinson, M.J. and Diering, J.A.C., 1981. The Flow of Slurry from a Breached Tailings Dam. J S Afr I Min Metall, 81(1): 1-8.

Blight, G.E., Thomson, R.R. and Vorster, K., 1985. Profiles of Hydraulic-Fill Tailings Beaches, and Seepage through Hydraulically Sorted Tailings. J S Afr I Min Metall, 85(5): 157-161.

Blight, G.E., Troncoso, J.H., Fourie, A.B. and Wolski, W., 2005. Issues in the geotechnics of mining wastes and tailings GeoEng. 2000 Int. Conf. on Geotechnical and Geological Engineering, Melbourne, Australia, pp. 1253-1285.

Bowles, D.S., Anderson, L.R. and Glover, T.F., 1996. Risk Assessment Approach to Dam Safety Criteria: Uncertainty in Geologic Environment, from Theory to Practice, Proceedings of ASCE, STP, pp. 451-473.

Calderon, A., Catalan, A. and A., K., 2003. Modelo de Riesgo Geotecnico y Bases Geotecnicas, Plan Minero CBV-2003, Mina Chiquicamata, CODELCO, Chile.

Camus, Y. and Duplessis, C., 2012. NI 43-101 Technical Report Mineral Resource Val-d'Or East Property Abitibi, Qc, Canada Adventure Gold Inc. . SGS Canada Inc, Blainville, Québec Canada, pp. 150.

CDA, C.D.A., 2007. Guidelines for Dam safety, 1. Canadian Dam Association, Edmonton.

CGS, C.G.S., 2007. Canadian foundation engineering manual. Canadian Geotechnical Society,, Richmond, B.C.

Chambers, D.M. and Higman, B., 2011. Long Term Risks of Tailings Dam Failure. Center for Science in Public Participation, Bozeman, MT, pp. 1-21.

Chang, C.H., Tung, Y.-K. and Yang, J.-C., 1995. Evaluation of probability point estimate methods. Applied Mathematical Modelling, 19: 95-105.

Chang, C.S. and Duncan, J.M., 1983. Consolidation Analysis for Partly Saturated Clay by Using an Elastic-Plastic Effective Stress-Strain Model. International Journal for Numerical and Analytical Methods in Geomechanics, 7(1): 39-55.

Chang, Y. and Huang, T., 2005. Slope stability analysis using strenght reduction technique. Journal of the Chinese Institute of Engineers, 28(2): 231-240.

Cheng, Y.M. and Lau, C., K, 2008. Slope stability analysis and stabilization : new methods and insight Routledge Taylor and Francis Group, London and New York.

Cho, S.E., 2007. Effects of spatial variability of soil properties on slope stability. Engineering Geology, 92(3–4): 97-109.

Chouinard, L.E., 2012. Risk Engineering - Course Notes and lectures, CIVE 609. Civil Engineering and Applied Mechanics McGill University, Montreal, Quebec, Canada.

Christian, J.T., 2004. Geotechnical Engineering Reliability: How Well Do We Know What We Are Doing? Journal of Geotechnical and Geoenvironmental Engineering, 130(10): 985-1003.

Christian, J.T. and Baecher, G.B., 1999. Point-Estimate Method as Numerical Quadrature. Journal of Geotechnical and Geoenvironmental Engineering, 125(9): 779-786.

Christian, J.T., Ladd, C. and Beacher, G.B., 1994a. Reliability Applied to Slope Stability Analysis. Journal of Geotechnical Engineering, 120(12): 2180-2207.

Christian, J.T., Ladd, C.C. and Baecher, G.B., 1994b. Reliability Applied to Slope Stability Analysis. Journal of Geotechnical Engineering, 120(12): 2180-2207.

Clayton, C.R.I., Theron, M. and Vermeulen, N.J., 2004. The effect of particle shape on the behaviour of gold tailings. In: R.J. Jardine, D.M. Potts and K.G. Higgins (Editors). Advances in Geotechnical Engineering: The Skempton Conference, London, pp. 393-404.

Committee on Large Dams - USCOLD, 1994. Tailings Dams Incidents, U.S Commeettee on Large Dams, Denver, Colorado, Denver, Colorado, pp. 82.

Craig, R.F., 2004. Craig's soil mechanics. Spon Press, London ; New York.

Das, B.M., 2007. Principles of foundation engineering. Thomson, Toronto, Ontario, Canada.

Davies, M.P. and Martin, T.E., 2000. Mine Tailings Dams: When Things Go Wrong, ASDSO Conference, Las Vegas, Nevada.

Day, R.W., 2002. Slope stability analyses for earthquakes, Geotechnical Earthquake Engineering Handbook. McGraw Hill, New York.

Dimitrova, R.S. and Yanful, E.K., 2012. Factors affecting the shear strength of mine tailings/clay mixtures with varying clay content and clay mineralogy. Engineering Geology, 125(0): 11-25.

Ding, Y., Wang, B.W. and McLeod, H., 2010. Characterizing Tailings to Better Predict Consolidation During Deposition, CDA 2010 Annual Conference. Canadian Dam Association, Niagara Fall, Ontario, Canada, pp. 1-13.

DOME, 1999. Guidelines on Safe Design and Operating Standards For Tailings Storage. In: D.o.M.a.E.W. Australia (Editor). Government of Australia, pp. 57.

Duncan, J.M., 1996. State of the art: Limit equilibrium and Finite Element Analysis of Slopes. Journal of Geotechnical and Geoenvironmental Engineering, 122(7): 577-596.

Duncan, J.M., 2000. Factors of Safety and Reliability in Geotechnical Engineering. Journal of Geotechnical and Geoenvironmental Engineering, 126: 307-316.

Duncan, J.M. and Wright, G.W., 2005. Soil Strength and Slope Stability. John Wiley&Sons, Inc, Hoboken, New Jersey, 295 pp.

Earthquakes Canada, G., Earthquake Search (On-line Bulletin), Nat. Res. Can.,, 2010. National Building Code Seismic Hazard Calculation. In: N.R. Canada (Editor). Goverment of Canada.

El-Ramly, H., Morgenstern, N.R. and Cruden, D.M., 2002. Probabilistic Slope Stability Analysis for Practice. Canadian Geotechnical Journal, 39: 665-683.

Elkateb, T., Chalatumyk, R. and Robertson, P.K., 2003. An Overview of Soil Heterogeniety: Quantification and Implications on Geotechnical Field Problems. Canadian Geotechnical Journal, 40: 1-15.

Environment Canada, 2009. Environmental Code of Practice for Metal Mines. In: M.a.P.D. Mining Section (Editor). Environment Canada, pp. 72.

Environment Canada, 2011. Guidelines for the Assessment of Alternatives for Mine Waste Disposal. In: E. Canada (Editor). Goverment of Canada, Ottawa, Ontario, Canada, pp. 1-40.

Fell, R., MacGregor, P. and Stapledon, D., 2005. Mine and Industrial Dams. In: C. Press (Editor), Geotechnical Engineering of Dams. Technology & Engineering pp. 767-818.

Fenton, G.A. and Griffiths, D.V., 2005. A Slope Stability Reliability Model, Proceedings of the K.Y. Lo Symposium (on CD), London, Ontario, Canada.

Fetter, C.W., 2001. Applied hydrogeology. Prentice Hall, Upper Saddle River, N.J.

Fishman, G.S., 1995. Monte Carlo: Concepts, Algorithms, and Applications. Springer, New York.

Fourie, A.B., Blight, G.E. and Papageorgiou, G., 2002. Static liquefaction as a possible explanation for the Merriespruit tailings dam failure: Reply. Can Geotech J, 39(6): 1441-1442.

Fredlund, D.G., 1984. Analytical methods for slope stability analysis, Proceedings of the Fourth International Symposium on Landslides, State-of the-Art, Toronto, Canada, pp. 229-248.

Fredlund, D.G. and Krahn, J., 1977. Comparison of slope stability methods of analysis, 29th Canadian Geotechnical Conference, Vancouver B.C, pp. 429-439.

Gouvernement du Quebec, 2002. Zones de Seismicite Province du Quebec. In: S.C.i.t.p.o. Quebec (Editor), Pdf. Centre d'expertise hydrique, Ressources Naturelles Canada, Comission Geologique, Quebec, Quebec.

Griffiths, D.V. and Fenton, G.A., 1998. Probabilistic Analysis of Exit Gradients Due to Steady Seepage. Journal of Geotechnical and Geoenvironmental Engineering, 124(9): 789-797.

Griffiths, D.V. and Fenton, G.A., 2004. Probabilistic Slope Stability Analysis by Finite Elements. Journal of Geotechnical and Geoenvironmental Engineering, 130(5): 507-518.

Griffiths, D.V. and Fenton, G.A., 2007. Probabilistic Methods In geotechnical Engineering, International Centre for Mechanical Sciences -CISM courses and lectures. CISM, Udine, Italy, pp. 149.

Griffiths, D.V., Fenton, G.A. and Lemons, C.B., 2002a. Probabilistic Analysis of Underground Pillar Stability. International Journal for Numerical and Analytical Methods in Geomechanics, 26: 775-791.

Griffiths, D.V., Fenton, G.A. and Manoharan, N., 2002b. Bearing Capacity of Rough Rigid Strip Footing on Cohesive Soil: Probabilistic Study. Journal of Geotechnical and Geoenvironmental Engineering, 128(9): 743-755.

Griffiths, D.V. and Lane, P.A., 1999. Slope stability analysis by finite elements. Geotechnique, 49(3): 387-403.

Haldar, A. and Mahadevan, S., 2000. Probability, Reliability, and Statistical Methods in Engineering Design. John Wiley & Sons, Inc., New York, NY.

Hamade, T., Saad, B. and Mitri, H., 2010. Probabilistic Assessment of Tailings Dam Stability, CDA 2010 Annual Conference, Niagara Falls, ON, Canada.

Hamade, T., Saad, B. and Pouliot, S., 2011. Stochastic Analysis of Tailings Dams Stability Using Numerical Modelling, Pan-Am CGS Geotechnical Conference. Canadian Geotechnical Society, Toronto, Ontario, Canada, pp. 8.

Hammah, R.E., Curran, J.H., Yacoub, T.E., and Corkum, B. 2004. Stability analysis of rock slopes using the finite element method. In Proceedings of the ISRM Regional Symposium EUROCK 2004 and the 53rd Geomechanics Colloquy, Salzburg, Austria.

Hammah, R.E., Yacoub, T.E., Corkum, B. an Curran, J.H. 2005. A comparison of finite element slope stability analysis with conventional limitequilibrium investigation. In Proceedings of the 58th Canadian Geotechnical and 6th Joint IAH-CNC and CGS Groundwater Specialty Conferences – GeoSask 2005. Saskatoon, Canada.

Hoek, E., 1998. Rock engineering: The application of modern techniques to underground design, Brazilian Rock Mechanics Committee (CBMR), Brazilian Tunneling Committee (CBT), Brazilian Society for Soil Mechanics and Geotechnical Engineering (ABMS), Sao Paulo, Brazil.

Holtz, R.D., & Kovacs, W.D. (1981). An Introduction to Geotechnical Engineering. Englewood Cliffs, New Jersey: Prentice Hall.

Hsu, Y.-C., Lin, J.-S. and Kuo, J.-T., 2007. Projection Method for Validating Reliability Analysis of Soil Slopes. Journal of Geotechnical and Geoenvironmental Engineering, 133(6): 753-756.

Hynes-Griffin, M.E. and Franklin, A.G., 1984. Rationalizing the Seismic Coefficient Method. In: D.o.t. Army (Editor), U.S Army Corps of Engineers. U.S Army Corps of Engineers, Vicksburg, Mississippi, pp. 1-40.

ICOLD, 1986. Static Analysis for Embankments Dams, 53, Paris.

ICOLD, 1993. Embankment Dams Upstream Slope Protection. Review and Recommendations, 91. ICOLD, Paris, 118 pp.

ICOLD, 1995. Dam Failures Statistical Analysis, 99. ICOLD, Paris, 62 pp.

ICOLD, 1996. A Guide to Tailings Dams and Impoundments. Design, construction, use and rehabilitation. ICOLD series, 106. UNEP-PNUE, Paris, 239 pp.

ICOLD, 2001. Tailings Dams Risk of Dangerous Occurrences. Lessons learnt from practical experiences, ICOLD Series, pp. 1-98.

James, M., Aubertin, M., Wijewickreme, D. and Wilson, G.W., 2011. A laboratory investigation of the dynamic properties of tailings. Can Geotech J, 48(11): 1587-1600.

Jeeravipoolvarn, S., Scott, J.D. and Chalaturnyk, R.J., 2009. 10 m standpipe tests on oil sands tailings: long-term experiment results and prediction. Can Geotech J, 48: 875-888.

Julien, M. and Kissiova, M., 2011. Benefits and Challenges in Using Tailings as Foundation and Construction Material to Increase Capacity of Tailings Storage Facilities. In: G.A. Ltee (Editor), Symposium 2011-Rouyn-Noranda Nubes and the Development, Rouyn-Noranda, Quebec, Canada, pp. 1-14.

Julien, M., Lemieux, M., Cayouette, J. and Talbolt, D., 2004. Performance and monitoring of the Louvicourt mine tailings disposal area, Proceedings of the 36th Annual Meeting of the Canadian Mineral Processors, Ottawa, Ont.

Kong, X.J., Pan, J.P. and Zou, D.G., 2008. Analysis of liquefaction-induced flow deformation of tailings dam. Dalian Ligong Daxue Xuebao/Journal of Dalian University of Technology, 48(4): 541-545.

Krahn, J., 2003. The 2001 R.M. Hardy Lecture: The limits of limit equilibrium analyses. Can Geotech J, 40(3): 643-660.

Lade, P.V. and Yamamuro, J.A., 2011. Evaluation of static liquefaction potential of silty sand slopes. Can Geotech J, 48(2): 247-264.

Liu, H., Yang, C., Zhang, C. and Mao, H., 2012. Study on static and dynamic strength characteristics of tailings silty sand and its engineering application. Safety Science, 50(4): 828-834.

Lopez-Caballero, F. and Modaressi-Farahmand-Razavi, A., 2010. Assessment of variability and uncertainties effects on the seismic response of a liquefiable soil profile. Soil Dynamics and Earthquake Engineering, 30(7): 600-613.

Lottermoser, B. G. (2003). Mine wastes : characterization, treatment, and environmental impacts. Berlin ; New York: Springer.

MAC, M.A.o.C., 1998. A guide to the management of tailings facilities. The Mining Association of Canada, Ottawa, Ontario.

Malkawi, A.I.H., Hassan, W.F. and Abdulla, F.A., 2000. Uncertainty and reliability analysis applied to slope stability. Struct Saf, 22(2): 161-187.

Martin, T. and Morrison, K., 2012. Tailings Management, Design and Operation, Webcast notes, Tailings 101. Edumine, Vancouver, B.C, pp. Conventional Dams vs. Tailings Embankments.

Martin, T.E., 1999. Characterization of pore pressure conditions in upstream tailings dams. In: T.a.M.W. '99 (Editor), Proceedings of the Sixth International Conference,. Taylor & Francis, Fort Collins, Colorado, USA, pp. 303-313.

Matsui, T. and San, K.-C., 1992. Finite Element Slope Stability Analysis by SSR Technique. Japanese Society of Soil Mechanics and Foundation Engineering, Soils and Foundation., 32(1): 59-70.

Meguid, M.A., 2012. CIVE 416, Geotechnical Engineering Lecture Notes. Department of Civil Engineering and Applied Mechanics, McGill University.

Melo, C. and Sharma, S., 2004. Seismic Coefficients for Pseudo-static slope analysis, 13th World Conference on Earthquake Engineering, Vancouver, B.C, Canada, pp. 1-15.

Ministère du Développement durable, d.l.E., et des Parcs - MDDEP., 2012. Directive 019 Sur l'industrie Miniere. Gouvernement du Quebec., Quebec, Quebec.

Mittal, H.K., 1974. Design and Performance of Tailings Dams, University of Alberta, Edmonton. Alberta, 345 pp.

Mittal, H.K. and Morgenstern, N.R., 1976. Parameters for the Design of Tailings Dams Geotechnical and Geological Engineering, 12: 235-261.

Moellmann, A., Vermeer, P.A. and Huber, M., 2008. A probabilistic Finite Element Analysis of Embankment Stability Under Transient Seepage Conditions, Proceedings of the 6th International Probabilistic Workshop, Darmstadt, pp. 551-562.

Morgenstern, N.R., 2000. Common Ground.

Morsy, M.M., Morgenstern, N.R. and Chan, D.H., 1995. Simulation of creep deformation in the foundation of Tar Island Dyke. Can Geotech J, 32: 1002-1023.

Ng, C.W. and Shi, Q., 1998. A Numerical Investigation of the Stability of Unsaturated soil slopes subjected to transient seepage. Computers and Geotechnics, 22(1): 1-27.

NRC, N.R.C., 2010. National building code of Canada, 1. ,National Research Council, Ottawa, Ont.

Peterson, J.L., 1999. Probability Analysis of Slope Stability, College of Engineering and Mineral Resources, University of West Virginia, Morgantown, West Virginia, 91 pp.

Phoon, K.-K. and Kulhawy, F.H., 1999. Characterization of Geotechnical Variability. Canadian Geotechnical Journal, 36: 612-624.

PHP Billiton, 2010. Tailings storagge facility design report- Appendix F1, pp. 1-105.

Priscu, C., 1999. Behavior of mine tailings dams under high tailings deposition rates, McGill University, Montreal, Quebec, Canada, 330 pp.

Qiu, Y. and Sego, D.C., 1998a. Engineering Properties of Mine Tailings, 51st Canadian Geotechical Conference. Canadian Geotechical Society, Alliston, Ont, pp. 149 -154.

Qiu, Y. and Sego, D.C., 1998b. Laboratory Test Methods on Mine Tailings, 51st Canadian Geotechical Conference. Canadian Geotechical Society, Alliston, Ont, pp. 155-162.

Qiu, Y. and Sego, D.C., 2006. Optimum deposition for sub-aerial tailigns disposal; concepts and theories. International Journal of Mining, Reclamation and Environment, 20(4): 272-285.

Qiu, Y.X. and Sego, D.C., 2001. Laboratory properties of mine tailings. Can Geotech J, 38(1): 183-190.

Rademeyer, B., 2007. The Influence of Environmental Impaxts on Tailings Impoundment Design, University of Pretoria, Pretoria.

Rajapakse, R., 2008. Geotechnical engineering calculations and rules of thumb. Elsevier/Butterworth-Heinemann, Amsterdam ; Boston.

Rassam, D.W. and Williams, D.J., 1999. Engineering properties of gold tailings. International Journal of Surface Mining, Reclamation and Environment, 13(3): 91-96.

Rico, M., Benito, G., Salgueiro, A.R., Diez-Herreiro, A. and Pereira, H.G., 2008. Reported tailings dam failures. A review of the European in the world context. Journal of Hazardous Materials, 152: 846-852.

Riela, J., Urzua, A., Christian, J.T., Karzulovic, A. and Flores, G., 1999. Sliding Rock Wedge Reliability Analysis of Chuquicamata Mine Slopes, Proceedings of the 11th Pan-American Conference on Soil Mechanics and Geotechnical Engineering, Foz do Iguacu, brazil.

Robertson, A.M., 1987. The Influence of Depositional Methods on the Engineering Properties of Tailings, International Conference on Mining and Industrial Waste Management, August. Robertson Geoconsultants Inc, Johannesburg, South Africa.

Rocscience, 2006. Slide 6.0 2D limit equilibrium slope stability analysis, Atlanta, pp. 29.

Rocscience, 2007. Phase2. 2D Finite Element Analysis for Excavations and Slopes.

Rocscience, 2012. Factor of safety and probability of failure. , pp. 1-14.
Rosenblueth, E., 1975. Point Estimates for Probability Moments. Proceedings of the National Academy of Sciences, 72(10): 3812-3814.

Rosenblueth, E., 1981. Two-point estimates in probabilities. Applied Mathematical Modelling, 5(5): 329-335.

Saad, B., 2008. Transient coupled analysis of upstream tailings disposal facilities construction, McGill University, Montreal, Quebec, Canada, 342 pp.

Saad, B. and Mitri, H., 2010. Staged construction analysis of surface tailings disposal facilities. International Journal of Mining, Reclamation and Environment, 24(1): 44-63.

Saad, B. and Mitri, H., 2011. Hydromechanical Analysis of Upstream Tailings Disposal Facilities. Journal of Geotechnical and Geoenvironmental Engineering, 137(1): 27-42.

Saad, B., Mitri, H. and Hamade, T., 2011. Evaluating Pore Pressure building up in upstream tailings dams, CDA 2011 Annual Conference, Frerericton, N.B Canafa.

Sarsby, R.W., 2000. Environmental Geotechnics. Thomas Telford, New York.

Selvadurai, A.P.S., 2006. Geotechnical Mechanics - Course Notes. McGill Universoty, Montreal, Quebec, Canada.

Schweiger, H. F., et al. (2001). "Reliability Analysis in Geotechnics wit deterministic finite elements." The International Journal of Geomechanics 1(4): 389-413.

Shamsai, A., Pak, A., Bateni, S.M. and Ayatollahi, S.A., 2007. Geotechnical Characteristics of Cooper Mine Tailings: A Case Study. Geotechnical and Geological Engineering, 25: 591-602.

Starchan, C. and Caldwell, J.A., 2010. New Directions in Tailings Management In: T.a.M.W. '10 (Editor), Committee of the 14th International Conference on Tailings and Mine Waste CRC Press. Taylor and Francis Group, Vail, Colorado, pp. 41-48.

Strachan, C., 2001. Tailings dam performance from USCOLD incident-survey data. Mining Engineering, 53(3): 49-53.

Terzaghi, K., Peck, R.B., & Mesri, G. (1996). Soil Mechanics in Engineering Practice (Third Ed.): John Wiley & Sons.

U.S. Army Corps of Engineers, 1986. Seepage analysis and control for dams. In: D.o.t. Army (Editor), Washington.

U.S. Army Corps of Engineers, 1997. Introduction to probability and reliability methods for use in geotechnical enigneering. Department of the Army, ETL 1110-2-547: 1-11.

U.S. EPA, 1994. Design and evaluation of tailing dams. Technical Report. In: O.o.S.W. U.S Environmental Protection Agency, Special Waste Branch (Editor). EPA, Washington D.C.

UNEP, 1996. Environmental and safety incidents concerning tailings dams at mines. Results of a survery for the years 1980-1996. Prepared by Mining Journal Research Service for the United Nations Environment Programme. UNEP, Paris, pp. 130.

USAID.-. 2011. Sesimic hazard analysis and seismic slope stability evaluation in northwestern pakistan. USAID, Whashington D.C, USA, pp. 158.
Uzielli, M., 1987. Statistical analysis of geotechnical data. In: U.S.A.E.W.E. Station (Editor), pp. 145.

Vermeulen, N.J., 2001. The Composition and State of Gold Tailings, University of Pretoria, Pretoria.

Vick, S.G., 1983. Planning, Design, and Analysis of Tailings Dams, 1. Jonh Wiley & Sons, New York; Chichester; Brisbane; Toronto; singapore, 369 pp.

Vick, S.G., 1990. Planning, Design and Analysis of Tailings Dams. BiTech Publishers Ltd.

Watts, B.D., 1981. Lateral Creep Deformations in the Foundation of a High Dam, University of Alberta, Civil Engineering, 251 pp.

Whitman, R.V., 2000. Organizing and Evaluating Uncertainty in Geotechnical Engineering. Journal of Geotechnical and Geoenvironmental Engineering, 126(7): 583-593.

WISE, 2012. Properties of Tailings dams and Chronology of major tailings dam failures.
Woodward, P.K. and Griffiths, D.V., 1996. Comparison of the pseudo-static and dynamic behaviour of gravity retaining walls. Geotechnical and Geological Engineering,, 14: 26-9-290.

Xu, B. and Low, B., 2006. Probabilistic Stability Analyses of Embankments Based on Finite Element Method. Journal of Geotechnical and Geoenvironmental Engineering, 132(11): 1444-1454.

APPENDIX

Probabilistic analyses data - PDF and CDF –UTSF different stability criteria

PDF-FOS- UTSF - Ultimate Height				L/H=6 Beach ratio		L/H=4 Beach ratio		L/H=6 Beach ratio		L/H=4 Beach ratio	
S		PS		PDF-MP LEM - Static		PDF-MP LEM- Static		CDF -Static		CDF-Static	
μFOS	1.48	μFOS	1.23	μFOS	1.48	μFOS	1.34	μFOS	1.48	μFOS	1.34
σFOS	0.33	σFOS	0.27	σFOS	0.33	σFOS	0.31	σFOS	0.33	σFOS	0.31
σ^2FOS	0.11	σ^2FOS	0.07	σ^2FOS	0.11	σ^2FOS	0.09	σ^2FOS	0.11	σ^2FOS	0.09
FOSi	*f*FOS	FOSi	*f*FOS	FOSi	*f*FOS	FOSi	*f*FOS	FOSi	*f*FOS	FOSi	*f*FOS
0.50	0.00	0.44	0.00	0.51	0.00	0.43	0.00	0.49	0.00	0.41	0.00
0.55	0.00	0.47	0.00	0.55	0.00	0.47	0.00	0.53	0.00	0.45	0.00
0.59	0.00	0.51	0.00	0.59	0.00	0.51	0.00	0.57	0.00	0.49	0.00
0.63	0.00	0.54	0.00	0.64	0.01	0.54	0.00	0.62	0.00	0.52	0.00
0.68	0.01	0.57	0.00	0.68	0.01	0.58	0.01	0.66	0.00	0.56	0.00
0.72	0.01	0.61	0.01	0.72	0.01	0.62	0.01	0.70	0.00	0.60	0.00
0.76	0.01	0.64	0.01	0.77	0.01	0.65	0.01	0.74	0.01	0.63	0.01
0.81	0.02	0.68	0.01	0.81	0.02	0.69	0.01	0.79	0.01	0.67	0.01
0.85	0.02	0.71	0.02	0.85	0.02	0.73	0.02	0.83	0.02	0.71	0.02
0.89	0.03	0.74	0.02	0.89	0.03	0.76	0.02	0.87	0.02	0.74	0.02
0.94	0.03	0.78	0.02	0.94	0.03	0.80	0.03	0.91	0.03	0.78	0.03
0.98	0.04	0.81	0.03	0.98	0.04	0.84	0.03	0.96	0.04	0.82	0.04
1.02	0.05	0.85	0.04	1.02	0.05	0.87	0.04	1.00	0.06	0.85	0.04
1.06	0.06	0.88	0.04	1.06	0.06	0.91	0.05	1.04	0.07	0.89	0.05
1.11	0.07	0.91	0.05	1.11	0.07	0.95	0.05	1.09	0.11	0.93	0.07
1.15	0.08	0.95	0.06	1.15	0.08	0.98	0.06	1.13	0.14	0.96	0.10
1.19	0.09	0.98	0.07	1.19	0.09	1.02	0.07	1.17	0.18	1.00	0.13
1.24	0.10	1.02	0.08	1.23	0.10	1.05	0.08	1.21	0.23	1.04	0.17
1.28	0.11	1.05	0.09	1.28	0.11	1.09	0.09	1.26	0.28	1.07	0.20
1.32	0.12	1.09	0.09	1.32	0.12	1.13	0.10	1.30	0.33	1.11	0.25
1.37	0.12	1.12	0.10	1.36	0.12	1.16	0.11	1.34	0.36	1.15	0.28
1.41	0.13	1.15	0.10	1.41	0.13	1.20	0.11	1.38	0.42	1.18	0.33
1.45	0.13	1.19	0.11	1.45	0.13	1.24	0.12	1.43	0.46	1.22	0.38
1.50	0.13	1.22	0.11	1.49	0.13	1.27	0.12	1.47	0.51	1.26	0.42
1.54	0.13	1.26	0.11	1.53	0.13	1.31	0.12	1.51	0.55	1.29	0.46
1.58	0.12	1.29	0.11	1.58	0.13	1.35	0.12	1.55	0.60	1.33	0.50
1.63	0.12	1.32	0.10	1.62	0.12	1.38	0.12	1.60	0.65	1.37	0.55
1.67	0.11	1.36	0.10	1.66	0.11	1.42	0.12	1.64	0.70	1.40	0.58
1.71	0.10	1.39	0.09	1.70	0.10	1.46	0.12	1.68	0.74	1.44	0.62
1.75	0.09	1.43	0.08	1.75	0.10	1.49	0.11	1.72	0.77	1.48	0.67
1.80	0.08	1.46	0.07	1.79	0.09	1.53	0.10	1.77	0.81	1.51	0.71
1.84	0.07	1.49	0.07	1.83	0.07	1.57	0.09	1.81	0.84	1.55	0.75
1.88	0.06	1.53	0.06	1.87	0.06	1.60	0.09	1.85	0.87	1.59	0.80
1.93	0.05	1.56	0.05	1.92	0.05	1.64	0.08	1.90	0.90	1.62	0.83
1.97	0.04	1.60	0.04	1.96	0.05	1.68	0.07	1.94	0.92	1.66	0.85
2.01	0.03	1.63	0.03	2.00	0.04	1.71	0.06	1.98	0.93	1.70	0.87
2.06	0.03	1.66	0.03	2.04	0.03	1.75	0.05	2.02	0.95	1.73	0.89
2.10	0.02	1.70	0.02	2.09	0.02	1.79	0.04	2.07	0.96	1.77	0.91
2.14	0.02	1.73	0.02	2.13	0.02	1.82	0.04	2.11	0.97	1.80	0.92
2.19	0.01	1.77	0.01	2.17	0.01	1.86	0.03	2.15	0.98	1.84	0.94
2.23	0.01	1.80	0.01	2.22	0.01	1.90	0.02	2.19	0.98	1.88	0.95
2.27	0.01	1.83	0.01	2.26	0.01	1.93	0.02	2.24	0.98	1.91	0.96
2.32	0.01	1.87	0.01	2.30	0.01	1.97	0.02	2.28	0.99	1.95	0.97
2.36	0.00	1.90	0.00	2.34	0.00	2.01	0.01	2.32	0.99	1.99	0.98
2.40	0.00	1.94	0.00	2.39	0.00	2.04	0.01	2.36	0.99	2.02	0.98
2.44	0.00	1.97	0.00	2.43	0.00	2.08	0.01	2.41	1.00	2.06	0.98
2.49	0.00	2.00	0.00	2.47	0.00	2.12	0.01	2.45	1.00	2.10	0.99
2.53	0.00	2.04	0.00	2.51	0.00	2.15	0.00	2.49	1.00	2.13	0.99
2.57	0.00	2.07	0.00	2.56	0.00	2.19	0.00	2.53	1.00	2.17	0.99
2.62	0.00	2.11	0.00	2.60	0.00	2.23	0.00	2.58	1.00	2.21	1.00
2.66	0.00	2.14	0.00	2.64	0.00	2.26	0.00	2.62	1.00	2.24	1.00

Pseudo –static probabilistic analyses data - PDF -Beach width ratio –criteria UTSF

L/H=4						L/H=6					
Kh=0.038		Kh=0.05		Kh=0.1		Kh=0.038		Kh=0.05		Kh=0.1	
μFOS	1.16	**μFOS**	1.11	**μFOS**	0.95	**μFOS**	1.28	**μFOS**	1.23	**μFOS**	1.05
σFOS	0.26	**σFOS**	0.25	**σFOS**	0.21	**σFOS**	0.28	**σFOS**	0.27	**σFOS**	0.22
σ²FOS	**0.07**	**σ²FOS**	**0.06**	**σ²FOS**	**0.04**	**σ²FOS**	**0.08**	**σ²FOS**	**0.07**	**σ²FOS**	**0.05**
FOS_i	**f_{FOS}**	**FOS_i**	**f_{FOS}**	**FOS_i**	**f_{FOS}**	**FOS_i**	**f_{FOS}**	**FOS_i**	**f_{FOS}**	**FOS_i**	**f_{FOS}**
0.37	0.00	0.36	0.00	0.30	0.00	0.48	0.00	0.48	0.00	0.42	0.00
0.40	0.00	0.39	0.00	0.32	0.00	0.52	0.00	0.51	0.00	0.44	0.00
0.43	0.00	0.42	0.00	0.35	0.00	0.55	0.00	0.54	0.00	0.47	0.00
0.46	0.00	0.45	0.00	0.37	0.00	0.59	0.01	0.58	0.01	0.50	0.00
0.49	0.00	0.48	0.00	0.40	0.00	0.62	0.01	0.61	0.01	0.52	0.01
0.52	0.00	0.51	0.00	0.42	0.00	0.66	0.01	0.64	0.01	0.55	0.01
0.56	0.01	0.54	0.01	0.45	0.01	0.70	0.01	0.68	0.01	0.58	0.01
0.59	0.01	0.57	0.01	0.48	0.01	0.73	0.02	0.71	0.02	0.61	0.01
0.62	0.01	0.60	0.01	0.50	0.01	0.77	0.02	0.75	0.02	0.63	0.02
0.65	0.01	0.63	0.01	0.53	0.01	0.80	0.03	0.78	0.03	0.66	0.02
0.68	0.02	0.66	0.02	0.55	0.02	0.84	0.03	0.81	0.03	0.69	0.02
0.71	0.02	0.69	0.02	0.58	0.02	0.87	0.04	0.85	0.04	0.71	0.03
0.74	0.03	0.72	0.03	0.60	0.02	0.91	0.05	0.88	0.05	0.74	0.03
0.77	0.03	0.75	0.03	0.63	0.03	0.95	0.06	0.92	0.05	0.77	0.04
0.80	0.04	0.78	0.04	0.65	0.03	0.98	0.06	0.95	0.06	0.80	0.05
0.83	0.04	0.81	0.05	0.68	0.04	1.02	0.07	0.98	0.07	0.82	0.05
0.86	0.05	0.84	0.05	0.71	0.04	1.05	0.08	1.02	0.08	0.85	0.06
0.89	0.06	0.87	0.06	0.73	0.05	1.09	0.09	1.05	0.09	0.88	0.07
0.92	0.07	0.90	0.07	0.76	0.06	1.13	0.10	1.08	0.09	0.90	0.07
0.95	0.07	0.93	0.07	0.78	0.06	1.16	0.10	1.12	0.10	0.93	0.08
0.98	0.08	0.96	0.08	0.81	0.07	1.20	0.11	1.15	0.10	0.96	0.08
1.02	0.09	0.99	0.09	0.83	0.07	1.23	0.11	1.19	0.11	0.99	0.08
1.05	0.09	1.01	0.09	0.86	0.08	1.27	0.11	1.22	0.11	1.01	0.09
1.08	0.10	1.04	0.10	0.88	0.08	1.30	0.11	1.25	0.11	1.04	0.09
1.11	0.10	1.07	0.10	0.91	0.08	1.34	0.11	1.29	0.11	1.07	0.09
1.14	0.10	1.10	0.10	0.94	0.08	1.38	0.11	1.32	0.10	1.10	0.09
1.17	0.10	1.13	0.10	0.96	0.08	1.41	0.10	1.36	0.10	1.12	0.08
1.20	0.10	1.16	0.10	0.99	0.08	1.45	0.10	1.39	0.09	1.15	0.08
1.23	0.10	1.19	0.09	1.01	0.08	1.48	0.09	1.42	0.08	1.18	0.07
1.26	0.10	1.22	0.09	1.04	0.08	1.52	0.08	1.46	0.08	1.20	0.07
1.29	0.09	1.25	0.08	1.06	0.07	1.55	0.07	1.49	0.07	1.23	0.06
1.32	0.09	1.28	0.08	1.09	0.07	1.59	0.06	1.52	0.06	1.26	0.06
1.35	0.08	1.31	0.07	1.12	0.06	1.63	0.05	1.56	0.05	1.29	0.05
1.38	0.07	1.34	0.06	1.14	0.06	1.66	0.05	1.59	0.04	1.31	0.04
1.41	0.06	1.37	0.06	1.17	0.05	1.70	0.04	1.63	0.04	1.34	0.04
1.44	0.06	1.40	0.05	1.19	0.04	1.73	0.03	1.66	0.03	1.37	0.03
1.48	0.05	1.43	0.04	1.22	0.04	1.77	0.03	1.69	0.03	1.39	0.03
1.51	0.04	1.46	0.04	1.24	0.03	1.80	0.02	1.73	0.02	1.42	0.02
1.54	0.04	1.49	0.03	1.27	0.03	1.84	0.02	1.76	0.02	1.45	0.02
1.57	0.03	1.52	0.03	1.29	0.02	1.88	0.01	1.80	0.01	1.48	0.01
1.60	0.02	1.55	0.02	1.32	0.02	1.91	0.01	1.83	0.01	1.50	0.01
1.63	0.02	1.58	0.02	1.35	0.01	1.95	0.01	1.86	0.01	1.53	0.01
1.66	0.02	1.61	0.01	1.37	0.01	1.98	0.01	1.90	0.01	1.56	0.01
1.69	0.01	1.64	0.01	1.40	0.01	2.02	0.00	1.93	0.00	1.58	0.00
1.72	0.01	1.67	0.01	1.42	0.01	2.05	0.00	1.97	0.00	1.61	0.00
1.75	0.01	1.70	0.01	1.45	0.01	2.09	0.00	2.00	0.00	1.64	0.00
1.78	0.01	1.73	0.00	1.47	0.00	2.13	0.00	2.03	0.00	1.67	0.00
1.81	0.00	1.76	0.00	1.50	0.00	2.16	0.00	2.07	0.00	1.69	0.00
1.84	0.00	1.79	0.00	1.52	0.00	2.20	0.00	2.10	0.00	1.72	0.00
1.87	0.00	1.82	0.00	1.55	0.00	2.23	0.00	2.13	0.00	1.75	0.00
1.90	0.00	1.85	0.00	1.58	0.00	2.27	0.00	2.17	0.00	1.77	0.00

Probabilistic analyses data – PDF and CDF –WRTD different stability criteria

PDF -FOS- WRTD- Ultimate Height				ks/kc=10000		ks/kc=100		ks/kc=10000		ks/kc=100	
S		PS		PDF-MP LEM -S		PDF-MP LEM-PS		CDF -S		CDF-PS	
μFOS	1.59	**μFOS**	1.34	**μFOS**	1.59	**μFOS**	1.56	**μFOS**	1.59	**μFOS**	1.56
σFOS	0.21	**σFOS**	0.17	**σFOS**	0.21	**σFOS**	0.21	**σFOS**	0.21	**σFOS**	0.21
σ²FOS	**0.04**	**σ²FOS**	**0.03**	**σ²FOS**	**0.04**	**σ²FOS**	**0.04**	**σ²FOS**	**0.04**	**σ²FOS**	**0.04**
1.02	0.00	0.84	0.00	1.02	0.00	0.99	0.00	1.01	0.00	0.98	0.00
1.05	0.00	0.86	0.00	1.05	0.00	1.01	0.00	1.04	0.00	1.00	0.00
1.07	0.00	0.89	0.00	1.07	0.00	1.04	0.00	1.06	0.00	1.02	0.00
1.10	0.01	0.91	0.00	1.10	0.01	1.06	0.00	1.09	0.01	1.05	0.00
1.12	0.01	0.93	0.00	1.12	0.01	1.09	0.01	1.11	0.01	1.07	0.01
1.15	0.01	0.95	0.01	1.15	0.01	1.11	0.01	1.14	0.01	1.10	0.01
1.17	0.01	0.97	0.01	1.17	0.01	1.14	0.01	1.16	0.02	1.12	0.01
1.20	0.01	0.99	0.01	1.20	0.01	1.16	0.01	1.19	0.02	1.15	0.02
1.22	0.02	1.01	0.01	1.22	0.02	1.19	0.02	1.21	0.03	1.17	0.03
1.25	0.02	1.03	0.01	1.25	0.02	1.21	0.02	1.24	0.04	1.20	0.03
1.27	0.03	1.05	0.02	1.27	0.03	1.23	0.02	1.26	0.05	1.22	0.04
1.30	0.03	1.07	0.02	1.30	0.03	1.26	0.03	1.28	0.06	1.25	0.06
1.32	0.04	1.09	0.03	1.32	0.04	1.28	0.03	1.31	0.08	1.27	0.07
1.35	0.04	1.11	0.03	1.35	0.04	1.31	0.04	1.33	0.11	1.30	0.10
1.37	0.05	1.14	0.03	1.37	0.05	1.33	0.05	1.36	0.13	1.32	0.12
1.40	0.05	1.16	0.04	1.40	0.05	1.36	0.05	1.38	0.16	1.35	0.16
1.42	0.06	1.18	0.04	1.42	0.06	1.38	0.06	1.41	0.19	1.37	0.17
1.45	0.07	1.20	0.05	1.45	0.07	1.41	0.06	1.43	0.23	1.40	0.21
1.47	0.07	1.22	0.05	1.47	0.07	1.43	0.07	1.46	0.27	1.42	0.25
1.50	0.07	1.24	0.06	1.50	0.08	1.46	0.07	1.48	0.31	1.44	0.30
1.52	0.08	1.26	0.06	1.52	0.08	1.48	0.08	1.51	0.35	1.47	0.33
1.55	0.08	1.28	0.07	1.55	0.08	1.51	0.08	1.53	0.41	1.49	0.38
1.57	0.08	1.30	0.07	1.57	0.08	1.53	0.08	1.56	0.45	1.52	0.43
1.59	0.08	1.32	0.07	1.59	0.08	1.56	0.08	1.58	0.50	1.54	0.48
1.62	0.08	1.34	0.07	1.62	0.08	1.58	0.08	1.61	0.56	1.57	0.53
1.64	0.08	1.37	0.07	1.64	0.08	1.61	0.08	1.63	0.60	1.59	0.58
1.67	0.08	1.39	0.07	1.67	0.08	1.63	0.08	1.66	0.64	1.62	0.62
1.69	0.07	1.41	0.06	1.69	0.07	1.65	0.08	1.68	0.67	1.64	0.66
1.72	0.07	1.43	0.06	1.72	0.07	1.68	0.07	1.71	0.71	1.67	0.70
1.74	0.06	1.45	0.06	1.74	0.06	1.70	0.07	1.73	0.75	1.69	0.73
1.77	0.06	1.47	0.05	1.77	0.06	1.73	0.06	1.76	0.78	1.72	0.78
1.79	0.05	1.49	0.05	1.79	0.05	1.75	0.05	1.78	0.82	1.74	0.80
1.82	0.05	1.51	0.04	1.82	0.05	1.78	0.05	1.81	0.85	1.77	0.84
1.84	0.04	1.53	0.04	1.84	0.04	1.80	0.04	1.83	0.87	1.79	0.86
1.87	0.03	1.55	0.03	1.87	0.03	1.83	0.04	1.86	0.89	1.81	0.88
1.89	0.03	1.57	0.03	1.89	0.03	1.85	0.03	1.88	0.91	1.84	0.90
1.92	0.02	1.60	0.02	1.92	0.02	1.88	0.03	1.90	0.92	1.86	0.92
1.94	0.02	1.62	0.02	1.94	0.02	1.90	0.02	1.93	0.95	1.89	0.94
1.97	0.02	1.64	0.02	1.97	0.02	1.93	0.02	1.95	0.95	1.91	0.95
1.99	0.01	1.66	0.01	1.99	0.01	1.95	0.01	1.98	0.96	1.94	0.96
2.02	0.01	1.68	0.01	2.02	0.01	1.98	0.01	2.00	0.97	1.96	0.97
2.04	0.01	1.70	0.01	2.04	0.01	2.00	0.01	2.03	0.98	1.99	0.98
2.07	0.01	1.72	0.01	2.07	0.01	2.02	0.01	2.05	0.99	2.01	0.98
2.09	0.00	1.74	0.00	2.09	0.00	2.05	0.01	2.08	0.99	2.04	0.99
2.12	0.00	1.76	0.00	2.12	0.00	2.07	0.00	2.10	0.99	2.06	0.99
2.14	0.00	1.78	0.00	2.14	0.00	2.10	0.00	2.13	1.00	2.09	0.99
2.16	0.00	1.80	0.00	2.16	0.00	2.12	0.00	2.15	1.00	2.11	1.00
2.19	0.00	1.83	0.00	2.19	0.00	2.15	0.00	2.18	1.00	2.14	1.00
2.21	0.00	1.85	0.00	2.21	0.00	2.17	0.00	2.20	1.00	2.16	1.00
2.24	0.00	1.87	0.00	2.24	0.00	2.20	0.00	2.23	1.00	2.19	1.00
2.24	0.00	1.89	0.00	2.24	0.00	2.22	0.00	2.25	1.00	2.21	1.00
2.24	0.00	1.91	0.00	2.24	0.00	2.25	0.00	2.28	1.00	2.23	1.00

Pseudo –static probabilistic analyses data - PDF -permeability ratio criteria-WRTD

PDF Ks/kc=100						PDF Ks/kc=10000					
Kh=0.038		Kh=0.05		Kh=0.1		Kh=0.038		Kh=0.05		Kh=0.1	
μFOS	1.36	**μFOS**	1.31	**μFOS**	1.12	**μFOS**	1.39	**μFOS**	1.34	**μFOS**	1.15
σFOS	0.18	**σFOS**	0.17	**σFOS**	0.15	**σFOS**	0.18	**σFOS**	0.17	**σFOS**	0.15
σ²FOS	**0.03**	**σ²FOS**	**0.03**	**σ²FOS**	**0.02**	**σ²FOS**	**0.03**	**σ²FOS**	**0.03**	**σ²FOS**	**0.02**
FOS_i	f_{FOS}	**FOS_i**	f_{FOS}	**FOS_i**	f_{FOS}	**FOS_i**	f_{FOS}	**FOS_i**	f_{FOS}	**FOS_i**	f_{FOS}
0.84	0.00	0.80	0.00	0.69	0.00	0.88	0.00	0.84	0.00	0.72	0.00
0.86	0.00	0.82	0.00	0.71	0.00	0.90	0.00	0.86	0.00	0.74	0.00
0.88	0.00	0.84	0.00	0.73	0.00	0.92	0.00	0.89	0.00	0.76	0.00
0.90	0.00	0.86	0.00	0.74	0.00	0.95	0.00	0.91	0.00	0.78	0.00
0.92	0.00	0.89	0.00	0.76	0.00	0.97	0.00	0.93	0.00	0.79	0.00
0.95	0.00	0.91	0.00	0.78	0.00	0.99	0.01	0.95	0.01	0.81	0.00
0.97	0.01	0.93	0.01	0.80	0.00	1.01	0.01	0.97	0.01	0.83	0.01
0.99	0.01	0.95	0.01	0.81	0.01	1.03	0.01	0.99	0.01	0.85	0.01
1.01	0.01	0.97	0.01	0.83	0.01	1.05	0.01	1.01	0.01	0.87	0.01
1.03	0.01	0.99	0.01	0.85	0.01	1.08	0.02	1.03	0.01	0.88	0.01
1.05	0.02	1.01	0.02	0.87	0.01	1.10	0.02	1.05	0.02	0.90	0.01
1.08	0.02	1.03	0.02	0.88	0.02	1.12	0.02	1.07	0.02	0.92	0.02
1.10	0.02	1.05	0.02	0.90	0.02	1.14	0.03	1.09	0.02	0.94	0.02
1.12	0.03	1.07	0.03	0.92	0.02	1.16	0.03	1.11	0.03	0.96	0.03
1.14	0.03	1.09	0.03	0.94	0.03	1.18	0.04	1.14	0.03	0.97	0.03
1.16	0.04	1.11	0.04	0.96	0.03	1.21	0.04	1.16	0.04	0.99	0.03
1.18	0.04	1.14	0.04	0.97	0.04	1.23	0.05	1.18	0.04	1.01	0.04
1.21	0.05	1.16	0.05	0.99	0.04	1.25	0.05	1.20	0.05	1.03	0.04
1.23	0.05	1.18	0.05	1.01	0.04	1.27	0.06	1.22	0.05	1.04	0.05
1.25	0.06	1.20	0.06	1.03	0.05	1.29	0.06	1.24	0.06	1.06	0.05
1.27	0.06	1.22	0.06	1.04	0.05	1.31	0.07	1.26	0.06	1.08	0.05
1.29	0.07	1.24	0.06	1.06	0.06	1.34	0.07	1.28	0.06	1.10	0.06
1.31	0.07	1.26	0.07	1.08	0.06	1.36	0.07	1.30	0.07	1.12	0.06
1.34	0.07	1.28	0.07	1.10	0.06	1.38	0.07	1.32	0.07	1.13	0.06
1.36	0.07	1.30	0.07	1.12	0.06	1.40	0.07	1.34	0.07	1.15	0.06
1.38	0.07	1.32	0.07	1.13	0.06	1.42	0.07	1.37	0.07	1.17	0.06
1.40	0.07	1.34	0.07	1.15	0.06	1.44	0.07	1.39	0.07	1.19	0.06
1.42	0.07	1.36	0.06	1.17	0.06	1.47	0.07	1.41	0.06	1.21	0.06
1.44	0.06	1.39	0.06	1.19	0.05	1.49	0.06	1.43	0.06	1.22	0.05
1.46	0.06	1.41	0.06	1.20	0.05	1.51	0.06	1.45	0.06	1.24	0.05
1.49	0.06	1.43	0.05	1.22	0.05	1.53	0.05	1.47	0.05	1.26	0.05
1.51	0.05	1.45	0.05	1.24	0.04	1.55	0.05	1.49	0.05	1.28	0.04
1.53	0.05	1.47	0.04	1.26	0.04	1.58	0.04	1.51	0.04	1.30	0.04
1.55	0.04	1.49	0.04	1.27	0.03	1.60	0.04	1.53	0.04	1.31	0.03
1.57	0.04	1.51	0.03	1.29	0.03	1.62	0.03	1.55	0.03	1.33	0.03
1.59	0.03	1.53	0.03	1.31	0.03	1.64	0.03	1.57	0.03	1.35	0.02
1.62	0.03	1.55	0.03	1.33	0.02	1.66	0.02	1.60	0.02	1.37	0.02
1.64	0.02	1.57	0.02	1.35	0.02	1.68	0.02	1.62	0.02	1.38	0.02
1.66	0.02	1.59	0.02	1.36	0.01	1.71	0.02	1.64	0.02	1.40	0.01
1.68	0.01	1.61	0.01	1.38	0.01	1.73	0.01	1.66	0.01	1.42	0.01
1.70	0.01	1.64	0.01	1.40	0.01	1.75	0.01	1.68	0.01	1.44	0.01
1.72	0.01	1.66	0.01	1.42	0.01	1.77	0.01	1.70	0.01	1.46	0.01
1.75	0.01	1.68	0.01	1.43	0.01	1.79	0.01	1.72	0.01	1.47	0.01
1.77	0.01	1.70	0.01	1.45	0.00	1.81	0.00	1.74	0.00	1.49	0.00
1.79	0.00	1.72	0.00	1.47	0.00	1.84	0.00	1.76	0.00	1.51	0.00
1.81	0.00	1.74	0.00	1.49	0.00	1.86	0.00	1.78	0.00	1.53	0.00
1.83	0.00	1.76	0.00	1.51	0.00	1.88	0.00	1.80	0.00	1.55	0.00
1.85	0.00	1.78	0.00	1.52	0.00	1.90	0.00	1.83	0.00	1.56	0.00
1.88	0.00	1.80	0.00	1.54	0.00	1.92	0.00	1.85	0.00	1.58	0.00
1.90	0.00	1.82	0.00	1.56	0.00	1.94	0.00	1.87	0.00	1.60	0.00
1.92	0.00	1.84	0.00	1.58	0.00	1.97	0.00	1.89	0.00	1.62	0.00
1.94	0.00	1.86	0.00	1.59	0.00	1.99	0.00	1.91	0.00	1.64	0.00